

**HEAT TRANSFER DURING ACID
MINE DRAINAGE PRODUCTION IN
A WASTE ROCK DUMP,
LA MINE DOYON (QUÉBEC)**

MEND Report 1.14.2c

This work was done on behalf of MEND and sponsored by
Cambior Incorporated,
Lac Minerals, and
the Province of Québec and the
Canada Centre for Mineral and Energy Technology (CANMET)
through the CANADA/Québec Mineral Development Agreement

**March 1994
Revised: August 1997**

**GROUPE de RECHERCHE en
GÉOLOGIE de L'INGÉNIEUR**

Rapport GREGI 93-03

**Heat Transfer During Acid Mine Drainage Production
in a Waste Rock Dump, La Mine Doyon (Québec)**

FINAL REPORT

By

René Lefebvre, Pierre Gélinas and Denis Isabel

**DÉPARTEMENT DE GÉNIE GÉOLOGIQUE
Faculté des sciences et de génie
Université Laval
Québec**

March 1993

Abstract

Acid mine drainage (AMD) resulting from pyrite oxidation is produced in two large waste rock dumps at La Mine Doyon located in Northwestern Quebec. A monitoring program for the South Dump is designed to characterize the physical and geochemical conditions prevailing during AMD production within this coarse unsaturated material. Pyrite oxidation generates heat so, among other instrumentation, the program includes 6 wells drilled through the wastes equipped with thermistor strings reaching the underlying soil and bedrock. Measured temperatures reach up to 65°C halfway through the 30 m thick waste rock dump. We report here on the analysis of the thermal data gathered weekly for two years at the site.

We consider heat transfer within the dump by conduction through the bulk of the material (rocks and water) and by advection due to fluid (mainly air) movement in the pores. Seasonal air temperature variations induce cyclic temperature variations within the dump. Fourier analysis is used to characterize these variations and provide the amplitude and phase of the cyclic variations at each measured point. These parameters allow for the evaluation of the bulk thermal properties of waste rocks. The relationship between attenuation and phase shift also provides an estimate of the magnitude and direction of advection. Air convection is driven by the steep temperature gradients within the wastes which affect air density. The analysis also reveals that the average heat stored within the dump has decreased significantly during the monitoring period.

Once the thermal properties of the wastes are known, the heat generation rate is calculated from the mean temperature profiles. Assuming most of the heat production results from pyrite oxidation, the oxidation rate may be evaluated from the thermal data independently of any AMD production model. The oxygen required for pyrite oxidation could be supplied by diffusion or air convection in the wastes. The estimated oxidation rate is actually too high to be sustained by oxygen diffusion alone and air advection is seen to be the dominant oxygen supply mechanism. The thermal data provides strong evidence for the presence of convection cells within the dump. This is confirmed by thermographic surveys and by the oxygen concentrations measured within the dump. A conceptual model of air convection patterns within the dump is proposed based on the available monitoring data. Since air convection seems to be the main mechanism responsible for the high AMD production rate in these waste rocks, control measures aiming at a reduction in AMD should focus on means of reducing air convection.

Résumé

L'oxydation de la pyrite produit un drainage minier acide (DMA) à deux vastes haldes de stériles à la mine Doyon, qui est située dans le nord-ouest du Québec. Un programme de surveillance de la halde sud a été conçu pour caractériser les conditions physiques et géochimiques qui prévalent durant la production de DMA à l'intérieur de ce matériau non saturé grossier. Comme l'oxydation de la pyrite produit de la chaleur, le programme comprend, entre autres instruments, 6 puits forés à travers les stériles. Ils sont munis de chaînes de thermistances descendus jusqu'au sol et au socle sous-jacents. Les températures mesurées atteignent 65 °C à mi-distance de la profondeur totale (30 m) de la halde de stériles. L'analyse des données thermiques recueillies hebdomadairement pendant deux ans est présentée dans ce rapport.

Le transfert de chaleur au sein de la halde s'effectue par conduction à travers l'ensemble du matériau (roches et eau) et par advection causée par le déplacement des fluides (principalement air) dans les pores. Les variations saisonnières de température de l'air provoquent des variations cycliques de la température dans la halde. L'analyse de Fourier est utilisée pour caractériser ces variations et établir l'amplitude et la phase des variations cycliques à chaque point de mesure. Ces paramètres permettent d'évaluer les propriétés thermiques globales des stériles. Le lien qui existe entre l'atténuation et le changement de phase permet une estimation de l'importance et de la direction de l'advection. La convection de l'air est dirigée par les gradients de température abrupts dans les stériles, ce qui a pour effet de modifier la densité de l'air. L'analyse révèle également que la chaleur moyenne stockée dans la halde a diminué significativement durant la période de surveillance.

Lorsque les propriétés thermiques des stériles sont connues, le taux de production de chaleur est calculé à partir des profils de températures moyennes. En supposant que la grande partie de la production de chaleur est causée par l'oxydation de la pyrite, le taux d'oxydation peut être évalué à partir des données thermiques quel que soit le modèle de production de DMA utilisé. L'oxygène requis pour oxyder la pyrite pourrait provenir de la diffusion ou de la convection de l'air dans les stériles . Le taux d'oxydation estimé est en réalité trop élevé pour être maintenu par la seule diffusion de l'oxygène et l'advection de l'air semble être le principal mécanisme d'approvisionnement en oxygène. Les données thermiques fournissent des indices importants de la présence de cellules de convection dans la halde. Ces indices sont confirmés par des levés thermographiques et les concentrations d'oxygène mesurées dans la halde. Un modèle conceptuel des configurations de convection d'air dans la halde, basé sur les données de surveillance disponibles est proposé. Comme la convection de l'air semble être le principal mécanisme à l'origine du taux élevé de DMA dans les stériles, les mesures visant à réduire le DMA devraient être axées sur les moyens de réduction de la convection de l'air.

Table of contents

List of tables	iv
List of figures	v
1 - Introduction	1
2 - Heat transfer during acid mine drainage	4
2.1 - Acid mine drainage production mechanisms	4
2.2 - Heat transfer mechanisms	6
3 - Interpretation of cyclic temperature variations	10
3.1 - Fourier analysis of cyclic temperature variations	11
3.2 - Heat stored within the dump	13
3.3 - Evaluation of the thermal properties of waste rocks	16
4 - Heat production in waste rocks	21
4.1 - Simple conduction model	21
4.2 - Conduction and advection model	22
4.3 - Air convection conceptual model	24
5 - Conclusion	27
6 - References	28

Appendix

- A - Fourier analysis of cyclic temperature changes
- B - Heat transfer with a periodic surface temperature variation
- C - Heat transfer by conduction and advection with a heat source
- D - Calculation of the heat stored within the dump
- E - Temperature data

List of tables

1 - Properties of the South Dump and waste rocks	30
2 - Thermal conductivity and fluid flux from Stallman's solution	30
3 - Parameters and heat production for the conduction-advection model	31

List of figures

1 -	South Dump instrumentation	32
2 -	Monitoring well instrumentation example	33
3 -	Physical mechanisms operating in waste rock dumps	34
4 -	Mid-month temperature profiles for the first monitoring year	35
5 -	Air temperature compared with surface temperature	36
6 -	Cyclic temperature variations for monitoring well #5	37
7 -	Cyclic temperature variation analysis for well #6 (1,0 m)	38
8 -	Amplitude and phase as a function of depth for all wells	39
9 -	Mean temperature profiles for all wells	40
10 -	Initial and final temperature profiles	41
11 -	Change in heat stored during the monitoring period	43
12 -	Relationship between attenuation and phase for all wells	43
13 -	a) Polynomial temperature correlation with depth	44
13 -	b) Heat flux and production from the conduction model	44
14 -	a) Temperature computed from the advection model (well #1)	45
14 -	b) Heat flux and production from the advection model (well #1)	45
15 -	a) Temperature computed from the advection model (well #5)	46
15 -	b) Heat flux and production from the advection model (well #5)	46
16 -	Thermographic survey measured at the dump surface	47

17 - Schematic diagram of air convection patterns	48
---	----

1 - Introduction

Acid mine drainage (AMD) is the most important environmental problem facing the mining industry. Acidity is produced by oxidation of the sulfides present in mine wastes, and the resulting acidic conditions favor heavy metals solubilization. The reaction is catalyzed by iron-oxidizing bacteria. AMD production occurs in different types of mine wastes. Tailings are a by-product of ore treatment and are composed of fine particles (sand and silt size). Waste rocks are barren material removed from open pits to access the ore. Waste rocks have a wide range of sizes (mm to m) depending on the blasting pattern and the mechanical properties of the rocks.

AMD production in waste rocks differs significantly from that in tailings. Waste rock piles generally have a thick unsaturated zone (several meters) and are very permeable due to the coarse nature of the material. The great thickness of waste rock piles allows them to reach high temperatures caused by the exothermic pyrite oxidation beyond the zone influenced by cyclic surface temperature variations. When the wastes are permeable enough, these high temperatures induce density-driven air convection currents within the piles providing oxygen for pyrite oxidation. Oxygen supply by advection is more efficient than diffusion which is the main mechanism for oxygen supply in tailings. Tailings have been well characterized and the mechanisms responsible for AMD production in them are relatively well understood. However, very few complete monitoring programs have been done on waste rock dumps.

One of the objectives of the project undertaken at the Doyon mine is to provide data on the physico-chemical conditions prevailing in waste rock dumps undergoing AMD production. We are especially concerned with obtaining data which could be used to determine water (hydrology), energy (heat transfer) and mass (geochemistry) balances for the dump. This data will be used to characterize the dump and model the physical and geochemical processes responsible for AMD production. Once validated and calibrated, those models could be used to predict the long term behavior of the dump if it is subjected or not to AMD control measures. Figure 1 shows the South Waste Dump at the Doyon mine which has been instrumented.

The monitoring program includes different installations. Trenches were dug in the dump to allow for sampling. There is a network of leachate collection ditches around the dump, and weir stations allow sampling and flow rate measurements. Two lysimeter groups were installed to measure and collect infiltrating water at the surface of the dump. There is a ring of observation wells around the

dump but we are interested in the wells which were drilled through the wastes. More details on the site and the monitoring program are provided elsewhere (Gélinas et al., 1992).

The South Dump contains an estimated 20,7 million tones of waste rocks and covers roughly a 500 m by 900 m area with an average thickness of more than 30 m. The pyrite concentration varies from 1,5% to 7% depending on the rock type. The dump is subdivided in three zones containing different proportions of the lithologies extracted from the main pit. Sericite schists dominate the zone containing the bulk of the waste from the main pit: this lithology is responsible for the strong AMD production of the dump. Sericite schists are very friable and allow easy access of water and oxygen to the pyrite contained in the blocks. A very low grade ore pile contains less schists and more acid volcaniclastites and mafic rocks which are less prone to AMD production. A third zone only contains mafic rocks which do not represent a significant AMD production problem. The leachate is characterized by a pH near 2.0 and an average sulfate content of 60 000 mg/l, and it is treated at a high density sludge plant. The South Waste Dump received reactive waste rocks from an open pit gold mine from 1983 to 1987. From 1987 to 1989, only non reactive "green rocks" were placed in a separate area of the dump. AMD production was first noticed in 1985 and reached a relatively stable level in 1988.

Characterization of the dump and waste rocks is an essential part of the study. Due to the coarse nature of the material, standard techniques are not always applicable to the evaluation of the key properties required for modeling. Actually, another objective of the project is to adapt or develop field methods to characterize waste rock dump. For example, wet bulk density of the entire dump was determined from a gravity survey. Details about the determination of this and other properties are provided by Lefebvre (1992). Table 1 summarizes some of the properties of the dump and waste rocks.

This report focuses on the temperature data acquired during almost two years of monitoring (from March 1991 until December 1992). This data is interpreted to determine the thermal properties of the wastes, to evaluate the importance of the different heat transfer mechanisms, to calculate the heat production rate and relate it to the AMD production rate, and to asses the impact of heat transfer on the oxygen supply. Figure 2 shows an example of an instrumented monitoring well within the waste rock dump. Temperature measurements are taken with thermistors at three (3) levels at depths of about 0.3, 0.5 and 1.0 m in a shallow hole (not shown) and generally at eight (8) levels (9 in well #1 and 7 in well #5) at depths of about 1.5, 2, 3, 5, 10, 15, 20 and 30 m. Measurements were made weekly for two years and are still on-going. These holes also allow gas sampling at the same levels as temperature

measurements and leachate sampling at the base of the wastes and in the underlying bedrock. These measurements will not be discussed here.

After a brief discussion of AMD production mechanisms in waste rock dumps, with an emphasis on heat transfer, we will present the interpretation of the cyclic temperature variations from which the thermal properties of the waste rocks are derived. This analysis also provides information on the magnitude of heat transfer by advection and on the amount of heat stored within the dump. The next section presents an estimate of heat generation rates from temperature profiles. These rates are related to the pyrite oxidation rates and the oxygen supply required. Finally, the relationship between heat generation and air flow is discussed. The analysis presented in this report is based on analytical solutions and was meant as a guide for numerical modeling which is now underway. However, the study is necessary because it provides information on material properties and indications of the important physical mechanisms involved in AMD production which will have to be modeled numerically.

2 - Heat transfer during acid mine drainage

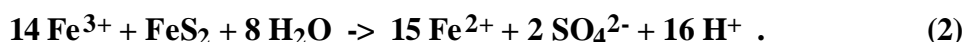
2.1 - Acid mine drainage production mechanisms

Two mechanisms are responsible for pyrite oxidation (Nordstrom, 1977; Hiskey et Schlitt, 1981, Lowson, 1982; Jaynes et al., 1983):

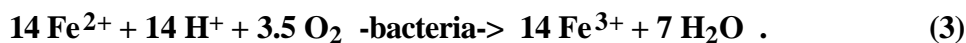
- 1) Direct reaction of pyrite with oxygen and water:



- 2) Pyrite oxidation by ferric iron:



In order for the second mechanism to operate, ferric iron must be present. At the low pH characteristic of AMD, the ferrous iron (Fe^{2+}) transformation to ferric iron (Fe^{3+}) is facing very slow chemical kinetic rates. However, certain types of bacteria (such as *Thiobacillus ferrooxidans*) use the ferrous-ferric oxidation as an energy source. The second mechanism is then catalyzed by ferric iron-producing bacteria:



The sum of reactions (2) and (3) gives reaction (1) so that, whatever the mechanism, at the sites of pyrite oxidation, 2 moles of H^+ (responsible for acidity) are produced for every 3,5 moles of O_2 consumed. To obtain significant oxidation rates, high oxygen concentrations in the gas phase must be present because of the slow oxygen diffusion rates through water. Pyrite oxidation at significant rates will then be restricted to the non saturated portion of mine wastes. Pyrite oxidation is a strongly exothermic reaction producing 1409 kJ of heat for every mole of pyrite oxidized. This reaction may then be detected by the temperature increase resulting from the release of heat. The chemical process of pyrite oxidation during AMD production is thus linked to physical mechanisms: heat production, oxygen supply and water infiltration. The relationships between these processes will be discussed briefly.

Figure 3 is a conceptual model of the physical mechanisms operating in AMD-producing waste rock dumps based on the data acquired during the monitoring program at the Doyon mine. AMD production in waste rocks is dependent on the coupled physical mechanisms of oxygen supply, heat production and transfer, as well as water infiltration. These processes are driven mainly by heat production in the following cycle: 1) pyrite oxidation releases heat which is dissipated at the surface and base of the dump, 2) temperature gradients occurring during heat transfer induce air density gradients which are responsible for air convection in the dump, 3) air convection brings oxygen within the dump which is used, directly or indirectly, for pyrite oxidation which again releases heat and the cycle is completed. Water infiltration is also tied, although not as closely, to heat transfer because water evaporates and condenses as air moves through regions having different temperatures. The system is "regulated" by the increasing or decreasing activity of bacteria in response to the conditions present in different parts of the dump. For example, bacterial activity will decrease as temperature increases beyond the optimal conditions for their development thus preventing temperature from reaching higher levels.

Conceptual and numerical models have been developed to describe the interaction between some of those physical mechanisms as well as the related geochemical processes (Cathles and Schlitt, 1980; Jaynes et al., 1984; Davis and Ritchie, 1986; Pantelis and Ritchie, 1991; Hart et al., 1991). Most of these models have led to the conclusion that oxygen supply is the key mechanism controlling the AMD production rate. Unfortunately, there is a lack of complete monitoring data sets in waste rock piles to validate and calibrate those models which have thus far only generated theoretical results.

To our knowledge, no site has ever been the subject of a modeling effort in which monitoring data has formed the basis for the calibration and validation of a model. Consequently, our aim is not to devise a new model but rather to fully characterize a waste rock dump, determine its transfer properties through the analytical and numerical interpretation of monitoring data, and finally to model numerically the main processes responsible for AMD production. The present report serves as a first step in the interpretation of the monitoring data, mainly the temperature data, and provides methods to derive the thermal properties of waste rocks, estimate the AMD production rate and also identify key AMD production mechanisms.

2.2 - Heat transfer mechanisms

Thermal properties of mine wastes control the effect of heat generation by pyrite oxidation as well as the impact of seasonal surface temperature changes. Due to the very coarse nature of waste rocks, those properties could hardly be measured in the laboratory and thus have to be derived instead from the interpretation of thermal monitoring data.

Thermal conductivity (k_t , W/m °C) is the capacity of a medium to transfer heat. This property is defined by the empirical Fourier law of heat conduction. This law states that the heat flux q (W/m²) through a medium is proportional to the temperature gradient across the medium dT/dx (°C/m). Thermal conductivity is the proportionality constant. When only one dimension x (m) is considered, we have:

$$q = -k_t \frac{dT}{dx} . \quad (4)$$

Heat capacity is the property of a medium to store heat (per unit of volume or mass) when it is subjected to a unit temperature change. Volumetric heat capacity C_v of a non saturated porous medium may be computed from mass heat capacity C_m (J/kg °C) and densities r (kg/m³) of water and solids for a given value of residual water saturation S_{wr} and porosity n of the material:

$$C_v = C_{m_{solids}} \cdot r_{solids} \cdot (1 - n) + C_{m_{water}} \cdot r_{water} \cdot n \cdot S_{wr} . \quad (5)$$

The above relationship neglects the heat capacity of the gas phase which may become significant in certain cases. Since the densities and mass heat capacities of solids and water are generally well known and do not vary much, C_v may generally be calculated with little uncertainty. If we use the properties of the wastes listed in table 1 and the known average properties of water and solids, we have:

$$C_v = 837 \cdot 2740 \cdot (1 - 0.33) + 4184 \cdot 1000 \cdot 0.33 = 1.98 \text{ MJ}/\text{°C m}^3 .$$

Heat diffusivity \tilde{N} (m²/s) is the ability of a medium to change temperature: it is the ratio of heat conductivity k_t and volumetric heat capacity C_v :

$$\tilde{N} = \frac{k_t}{C_v} . \quad (6)$$

Heat transfer by conduction in one dimension in a system where there is an internal source of heat production may be expressed by the following differential equation:

$$C_v \frac{\partial T}{\partial t} = \frac{\partial q}{\partial x} + Q(x), \text{ where } q = -k_t \frac{\partial T}{\partial x} \quad (7)$$

C_v :	volumetric heat capacity ($\text{J/m}^3 \text{ } ^\circ\text{C}$),	T :	temperature ($^\circ\text{C}$),
t :	time (s),	q :	heat flux (J/s m^2 , or W/m^2),
x :	distance (m),	$Q(x)$:	heat generation rate (J/sm^3 or (W/m^3)).
k_t :	thermal conductivity ($\text{J/s m } ^\circ\text{C}$, or $\text{W/m } ^\circ\text{C}$),		

The differential equation represents the continuity equation for the conservation of heat. The equation states that there must be an equilibrium between the rates of heat getting in and out of the system ($\partial q/\partial x$), the internal heat generation rate (Q), and the change in heat storage with time in the system ($C_v \partial T/\partial t$). This equation may represent heat dissipation by conduction towards the base or the surface of mine wastes in which there is heat produced by pyrite oxidation.

AMD production in mine wastes takes place over extended time periods (up to hundreds of years). Consequently, in the short term when such an AMD-generating system is observed, it may be considered in a pseudo steady state ($\partial T/\partial t = 0$). This means that temperature profiles have reached an equilibrium position which does not vary with time (not notwithstanding superficial cyclic variations). The differential equation for heat conduction may then be expressed as follows:

$$Q(x) = -k_t \frac{d^2 T}{dx^2}. \quad (8)$$

Heat production by pyrite oxidation may then be derived from temperature profiles if heat conductivity is known (measured in the lab or the field). The interest of this estimate is that pyrite oxidation and AMD production rates may be globally estimated by this energy balance exercise without the need for any model of the actual heat production phenomenon.

The foregoing discussion supposed that heat conduction was the only heat transfer mechanism. Actually, heat may also be transferred by fluid (water or air) in movement (termed convection or advection) in the porous media. The convective heat flux \mathbf{q} (W/m^2) is expressed as follows:

$$\mathbf{q} = \mathbf{v} \mathbf{c}_0 \mathbf{r}_0 \mathbf{T}, \quad (9)$$

and depends on the fluid flux \mathbf{v} (m/s), the volumetric heat capacity of the fluid $\mathbf{c}_0 \mathbf{r}_0$ ($\text{J/m}^3 \text{ }^\circ\text{C}$) and the temperature \mathbf{T} ($^\circ\text{C}$). With dry air at a low temperature and a small fluid flux, the convective heat flux will be negligible. However, when the temperature is high, air contains much more water vapor at saturation and can carry a significant amount of heat.

In order to completely describe heat transfer in waste rocks, we then have to consider conduction and advection, and the presence of a heat source. The following differential equation (in one dimension x) then describes the full process:

$$k_t \frac{\partial^2 T}{\partial x^2} - v c_o r_o \frac{\partial T}{\partial x} + Q(x) = c r \frac{\partial T}{\partial t}, \quad (10)$$

where,

k_t :	thermal conductivity ($\text{W/ m }^\circ\text{C}$),	Q :	heat source (W/m^3),
T :	temperature ($^\circ\text{C}$),	x :	distance (m),
v :	fluid flux (m/s),	c_o :	fluid heat capacity ($\text{J/kg }^\circ\text{C}$)
r_o :	fluid density (kg/m^3),	c :	medium heat capacity ($\text{J/kg }^\circ\text{C}$)
r :	medium density (kg/m^3),	t :	time (s).

Heat conduction, represented by the first term, occurs through the whole porous medium (solids and fluids) whereas advection (second term) is caused by fluid movement. In an unsaturated medium such as a waste rock dump, both water and air may contribute to advective heat transfer. The flow of water and air is described by Darcy's law. In the case of infiltrating water, the fluid potential causes a downward flow. However, in the case of air, the flow is mainly controlled by density gradients in this non-isothermal system and flow may be upward as well as downward. The changes in temperature occur very slowly in a waste rock dump except for the diurnal or annual cyclic changes in surface temperature.

In order to provide relationships useful for the analysis of the thermal data, equation 10 will have to be solved for different boundary conditions. First, we will present an analysis of cyclic temperature variations from which thermal properties of the waste rocks are derived and the effect of advection is detected. Then, the temperature profiles will be used to calculate the heat generation rate in the dump.

Harries and Ritchie (1985) report on a similar use of temperature profiles to determine heat production rates. As mentioned before, those rates are directly related to the pyrite oxidation rate without the need for a model of the actual phenomenon producing the heat. For this reason, temperature profile measurements represent the best available calibration method for AMD production models where either thick pyrite oxidation zones are present or where cyclic surface temperature changes are not significant.

3 - Interpretation of cyclic temperature variations

Waste rock dumps are submitted to cyclic annual or diurnal atmospheric temperature variations at their surface, especially under northern climates. These cyclic variations undergo a reduction in amplitude and a shift in phase as they propagate through the wastes. The magnitude of the amplitude and phase changes depends on the thermal properties of the wastes. Consequently, the measurement of the amplitude and phase of cyclic temperature variations at different depths allows the computation of the thermal properties of the wastes.

At the Doyon mine site, temperature measurements were made with thermistors in six (6) wells at 11 different levels (figure 2). Weekly temperature measurements are now available for a two year period. Figure 4 shows selected temperature profiles measured in the middle of each month during the first monitoring year. The profiles are all plotted from -10 to 70 °C and show major temperature increases (up to 65°C) above the mean surface air temperature which is 2°C in this area. Temperature increases from the surface to reach a maximum value in the upper half or middle of the waste pile and then decreases toward the base. The temperature profiles show important fluctuations near the surface which are induced by cyclic seasonal surface temperature variations. These cyclic temperature changes do not have much influence beyond the 10 m depth.

Figure 5 shows the relationship between air temperature and the measurements in the six wells near the surface of the dump. The air temperature is a filtered average of daily mean temperature measurements from three weather stations in the mine area in 1991. We see that surface temperature measurements generally follow the air temperature changes but show less variability, especially during the winter. However, the temperatures recorded within the dump are higher than the air temperature, and more so in the wells in which the temperature is hotter. This may be explained by the heat provided by the dump which is transferred from the hot inner region to the colder surface. The larger spread in temperature during the cold winter days may be partly attributed to the presence of an insulating snow cover at the surface of the dump.

Figure 6 provides another view of the temperature data which emphasizes the time variations of this parameter: it shows, against time, all the weekly temperature measurements made during the first monitoring year at each measure point in well #5. The points are the measurements whereas the lines are best fit sinusoidal curves adjusted to the data. This figure shows one annual cycle of temperature changes within the waste dump. Seasonal surface temperature variations have a high amplitude (about ±15 °C) and influence the temperature within the wastes down to at least 10 m. The mean temperature

increases from the surface to the center of the waste (this well does not have temperature measurements in the lower half of the dump).

The near surface measurements show more variability because they are influenced by daily cycles and short term weather changes. However, those short term temperature changes do not seem to affect measurements beyond 2 m depth. The amplitude of the temperature changes is reduced as we get deeper within the wastes. Also, there is a shift in the phase of the cyclic variations as it penetrates the dump: the temperature maxima and minima occur at a later time at depth than at the surface. For example, at 0,3 m the temperature change has a 15°C amplitude and the maximum is recorded in July whereas at a depth of 5 m the amplitude is reduced to less than 5°C and the maximum occurs in September. As we will show, the change in amplitude and phase with depth of the temperature variations may be used to derive the thermal properties of the waste rocks as well as indicate the magnitude and direction of advection within the dump. The first step, discussed in the next section, is to evaluate the amplitude and phase of the temperature changes at each measure point.

3.1 - Fourier analysis of cyclic temperature variations

The cyclic nature of the temperature measurements has to be characterized in order to reduce the results of two years of temperature monitoring to a few parameters. Figure 7 provides a representative example of the temperature data collected during two years at each measure point. It is apparent that the temperature measurements show a cyclic variation but also exhibit a reduction in mean value during the monitoring period. Fourier analysis is then used to translate the temperature measurements in terms of a linear trend added to a cyclic sinusoidal variation. As seen in figure 7, this type of model is a good representation of the data. The problem is then to find the parameters which allow the best fit of the data with this model.

Mathematically, the two components of the model, the linear trend and the cyclic change, are expressed as follows. The linear trend in average temperature $T_a(t)$ (°C) is represented by an initial temperature value T_0 (°C) at time t (day) zero and the slope of the linear change m (°C/d):

$$T_a = T_0 + m t . \quad (11)$$

The cyclic temperature variation with time $DT(t)$ may be expressed as the first harmonic of the Fourier series, with a one year period, representing this variation (Davis, 1973; Burden and Faires, 1989):

$$DT(t) = a \cos 2\pi t + b \sin 2\pi t = a C + b S , \quad (12)$$

	t	t	
where,	t : time (days),		a : cosine coefficient,
	b : sine coefficient,	t :	variation period (365 days),
	C : $\cos(2\pi t/\tau)$,		S : $\sin(2\pi t/\tau)$.

The change in temperature with time $T(t)$ will then be the sum of the contributions of the linear trend $T_a(t)$ added to the cyclic trend $\Delta T(t)$:

$$T(t) = T_a(t) + \Delta T(t) = T_0 + m t + a C + b S . \quad (13)$$

The four parameters T_0 , m , a and b defining the change in temperature with time may be computed from the temperature measurements as a function of time at different depths. The method of least squares is used to determine the parameters which allow the best description of the observed temperature as equation 13 (details in appendix A). Once coefficients T_0 , m , a and b are determined, cyclic temperature variations may also be expressed in terms of the amplitude ΔT and phase P of a sinusoidal wave using the following transformation:

$$\Delta T(t) = a \cos x + b \sin x = \Delta T \sin(x - P) , \quad (14)$$

where,

$$\Delta T = (a^2 + b^2)^{(1/2)} \text{ and } \tan P = -\frac{a}{b} . \quad (15)$$

The transformation presented in equation 15 is for the case where parameters a and b are both positive (appendix A). Fourier analysis results are presented in appendix A. Calculations were carried by arbitrarily using January 1st 1991 as day zero. The determination coefficients R^2 calculated are generally above 0,9 and indicate that most of the measured temperatures are well represented by equation 13.

Figures 8a and 8b show respectively the amplitude and phase derived from the Fourier analysis for all temperature measure points as a function of depth (the results for each individual well are presented in appendix A) . There is an exponential decline in amplitude with depth whereas the phase increases linearly with depth. This behavior is expected from theory (see section 3.3) and allows an evaluation of the thermal properties of the waste rocks. However, the data below 5-10 meters show much more variability and follows a different trend in amplitude and phase with depth. This behavior may partly be attributed to the larger relative error in the measurements at these levels. Also, the fact that temperature does not follow a cyclic variation pattern at these levels but instead may increase or decrease steadily accounts for the erratic behavior of the amplitude and

phase estimates. A different air convection regime in the lower half of the dump could also be responsible for the different trends. Consequently, only the near surface measurements will be used to derive the thermal properties of the wastes using the analytical method described in section 3.3.

3.2 - Heat stored within the dump

Fourier analysis provides us with the linear trend in average temperature $T_a(t)$ within the dump during the monitoring period. This trend is expressed as an initial temperature value T_0 at time t zero (January 1, 1991) and the slope of the linear change m which may be used to calculate the mean T_m (at February 1, 1992) and final average temperature T_f (at January 1, 1993). The results are presented in appendix D.

Figure 9 shows the mean temperature profiles for all wells. The near surface temperature tends toward the mean air temperature which is 2 °C in that area. Temperature increases rapidly in the top five meters to reach between 25 and 60 °C except for well #3 which exhibits a much smaller temperature increase and only reaches about 14 °C. Maximum temperature is located between 10 and 20 m and varies between 40 and 65 °C (except again for #3). Temperature slowly decreases from the maximum to values between 20 and 45 °C at the base of the dump. Temperature measurements in the saturated zone at the base of the piezometers have shown that temperature gradients remain about constant below the unsaturated zone (not presented in this report). The temperature close to the surface is different for each well. As mentioned before, the wells with the highest temperature within the dump tend to also have the highest temperature at the surface.

Figure 10 shows a comparison between average initial and final temperature profiles for all wells. All wells but #3 show a significant decrease in average temperature during the monitoring period. The larger temperature decrease in well #4 can be explained by the approximately 10 m deep excavation of waste rocks only 15 m north of the well. These operations were done in the spring and summer of 1992 to obtain backfill material for the mine. By comparing the temperature data before and after the excavation, we determined that this new exposed vertical face near well #4 not only caused heat loss but also changed the air circulation pattern in this area (compare results with Lefebvre et al., 1992). These average temperature profiles may be used to calculate the average heat stored within the dump at the beginning and end of the monitoring period.

The average volumetric heat stored within the dump H (MJ/m^3) is obtained from the average temperature profiles and the relationship:

$$\mathbf{H} = \mathbf{C}_v \cdot (\mathbf{T}_{mes} - \mathbf{T}_{base}) , \quad (16)$$

where \mathbf{T}_{mes} and \mathbf{T}_{base} are respectively the measured and base temperatures ($^{\circ}\text{C}$) and the volumetric heat capacity \mathbf{C}_v ($\text{MJ}/^{\circ}\text{C m}^3$) of the wastes obtained from equation 5. The base temperature is taken as $5\ ^{\circ}\text{C}$ which is slightly higher than the average air temperature in the area. This rounded temperature value is closer to the dump surface temperature which is higher than the normal air temperature. The rounded number is actually a better limit condition. Results are presented in figure 11 whereas detailed calculations and other figures are included in appendix D. For a given well, the total heat stored within the dump per unit area \mathbf{H}_t (MJ/m^2) is obtained by integrating the values of \mathbf{H} with depth. Numerically, the integration is carried by summing the total heat stored between n adjacent temperature measurements using the trapezoidal rule:

$$H_t = \sum_{i=1}^{n-1} 0.5 |z_{i+1} - z_i| \Delta H_i + \Delta H_i C \quad (17)$$

The change in volumetric \mathbf{H} and total \mathbf{H}_t heat stored within the dump during the monitoring period is simply derived from the difference in the values calculated for the initial and final average temperature profiles (figure 11). The heat stored within the dump has decreased during the two year monitoring period by a factor of 10 to 20% and is now at about 1 300 to 2 700 MJ/m^2 . Note that only wells #1, #2 and #6 are considered giving representative values since well #3 has much lower temperatures than other wells, well #5 does not reach the base of the dump, and well #4 is affected by the recent removal of waste rocks near this well.

In order to evaluate whether those changes in heat storage are significant, the variation in heat stored caused by seasonal cyclic temperature changes were also calculated. As described in the next section, the cyclic temperature variation $\Delta T(t,z)$ with respect to time and depth is described by the following relationship:

$$\Delta T(t,z) = \Delta T_0 e^{-az} \sin(2\pi t/T - bz) , \quad (18)$$

where ΔT_0 is the amplitude of the temperature change at the surface of the dump whereas a and b are parameters describing respectively the amount of attenuation and phase change of the temperature variation occurring with depth. The exponential term in 18 describes the "envelope" of the temperature change with depth. We can thus derive the total annual change in heat stored per unit dump area ΔH_c (MJ/m^2) caused by cyclic temperature variations from the product of volumetric heat capacity \mathbf{C}_v and the integral (sum) of the envelope of the temperature variation with depth:

$$DH_c(t) = \int_0^L C_v \Delta T(z, t) dz \quad (19a)$$

Replacing $T(z, t)$ with $T_o e^{-az} \sin(2\pi t / -bz)$, integrating the above expression while treating t as a constant, we obtain

$$\begin{aligned} \Delta H_c(t) &= C_v T_o \int_0^L e^{-az} \sin(2\pi t / t - bz) dz \\ \Delta H_c(t) &= C_v \Delta T_o \left[\frac{e^{-az}}{a^2 + b^2} (b \cos(2\pi t / t - bz) - a \sin(2\pi t / t)) \right] \end{aligned}$$

When $z=L$, e^{-az} is very small and can be neglected, thus

$$\Delta H_c(t) = C_v \Delta T_o \frac{e^{-az}}{a^2 + b^2} [a \sin(2\pi t / t) - b \cos(2\pi t / t)] \quad (19b)$$

To obtain the maximum of $H_c(t)$ with respect to time t , take its first derivative and let it be zero,

$$\frac{d\Delta H_c(t)}{dt} = 0$$

and solve for t , we obtain

$$\frac{2pt}{t} = \text{atan}\left(-\frac{a}{b}\right),$$

$$\tan\left(\frac{2pt}{t}\right) = -\frac{a}{b}, \text{ and}$$

$$t = \frac{t}{2p} \text{atan}\left(-\frac{a}{b}\right). \quad (19c)$$

The results, presented in appendix D, show that seasonal cyclic temperature changes are responsible for ± 3 to 9 % variations in the heat stored within the dump. The reduction in heat storage during the monitoring period, which is about twice these values, may then be considered significant. This reduction in heat storage could equally be attributed to an increased heat loss caused by a cooler than usual summer in 1992 or by a reduction in heat production related to the slowing down of AMD production. The impact of both processes will be evaluated in the next phase of the project by

numerical modeling. At this time, we can still conclude that thermal data indicates that the AMD production rate in the South Dump is no longer increasing.

3.3 - Evaluation of the thermal properties of waste rocks

The problem of heat transfer by conduction and advection in one dimension in a system subjected to a cyclic surface temperature was solved analytically by Stallman (1965). Heat transfer by conduction and advection is described by the following differential equation:

$$k_t \frac{\partial^2 T}{\partial z^2} - qc_o r_o \frac{\partial T}{\partial z} = cr \frac{\partial T}{\partial t}, \quad (20)$$

where:

k_t :	medium thermal conductivity (solid and water) (W/m °C),
T :	temperature (°C),
v :	fluid flux (m/s),
r_o :	fluid density (kg/m^3),
r :	medium density (kg/m^3),
z :	<u>positive downward</u> depth (m),
c_o :	fluid heat capacity ($\text{J}/\text{kg}^\circ\text{C}$),
c :	medium heat capacity ($\text{J}/\text{kg}^\circ\text{C}$),
t :	time (s).

To solve equation 20, we take as a first boundary condition that the surface is undergoing a cyclic temperature variation of period t (s):

$$T_o = T_{mo} + DT_o \sin 2\pi t/t, \quad (21)$$

where,

T_o :	surface temperature (°C),	T_{mo} :	mean surface temperature (°C),
DT_o :	surface temperature variation amplitude (°C).		

The second boundary condition is that, as depth tend toward infinity, the temperature reaches the mean temperature at that level T_{mz} . The solution for the temperature variation $T(t,z)$ (°C) as a function of time t (s) for a depth z (m) is given by (detailed derivation in appendix B):

$$T(t,z) = T_{mz} + DT e^{-az} \sin(2\pi t/t - bz), \quad (22)$$

where,

T_{mz} :	mean temperature at depth z (°C),	t :	variation period (s),
DT :	surface temperature variation amplitude (°C).		

Parameters a and b are defined as follows:

$$\mathbf{a} = [(\mathbf{K}^2 + \mathbf{V}^4/4)^{1/2} + \mathbf{V}^2/2]^{1/2} - \mathbf{V} , \quad (23)$$

$$\mathbf{b} = [(\mathbf{K}^2 + \mathbf{V}^4/4)^{1/2} - \mathbf{V}^2/2]^{1/2} , \quad (24)$$

where,

$$K = \frac{\mathbf{pcr}}{k_t t} \quad \text{and} \quad V = \frac{qc_o r_o}{2k_t} . \quad (25)$$

Relationships 23 and 24 define a system with two unknowns \mathbf{K} and \mathbf{V} . Stallman (1965) presents a solution method using the ratio of parameters \mathbf{a} and \mathbf{b} . However, this method is cumbersome and does not allow the determination of \mathbf{V} in the case where fluid advection is upward (\mathbf{q} is negative). The system may be solved more simply by defining the unknowns \mathbf{K} and \mathbf{V} directly as functions of parameters \mathbf{a} and \mathbf{b} (see appendix B for details):

$$\mathbf{V} = \frac{\mathbf{b}^2 - \mathbf{a}^2}{2\mathbf{a}} , \quad (26)$$

and

$$\mathbf{K} = \mathbf{ab} + \mathbf{bV} , \quad (27a)$$

or, in terms of \mathbf{a} and \mathbf{b} :

$$\mathbf{K} = \mathbf{ab} + \mathbf{b} \frac{\mathbf{b}^2 - \mathbf{a}^2}{2\mathbf{a}} . \quad (27b)$$

The solution method then consists of determining parameters \mathbf{a} and \mathbf{b} graphically from the temperature data, evaluating \mathbf{V} and \mathbf{K} from relationships 26 and 27, and, finally, calculating k_t and \mathbf{q} by transforming relationship 25:

$$k_t = \frac{\mathbf{pcr}}{Kt} \quad \text{and} \quad q = \frac{V2k_t}{c_o r_o} . \quad (28)$$

When heat transfer is only occurring by conduction ($\mathbf{q}=0$), parameters \mathbf{a} and \mathbf{b} are equal and given by the following expression from which thermal conductivity k_t may be derived:

$$a = b = \sqrt{\frac{\mathbf{pcr}}{k_t t}} . \quad (29)$$

Parameters \mathbf{a} and \mathbf{b} are derived respectively from plots of attenuation \mathbf{A} and phase difference $\Delta\mathbf{P}$ with depth \mathbf{z} , since from equation 22 we have:

$$A = \ln \frac{\dot{e}^? T_z}{\dot{e}^? T_{o\dot{u}}} = -a z , \quad (30)$$

where ΔT_z and ΔT_o are respectively the amplitudes of the cyclic temperature variations at depth z and at the surface, and

$$DP = P(z) - Po = \frac{2p?t}{t} = b z , \quad (31)$$

where $P(z)$ and Po are the phases at depth z and at the surface ($z=0$), and Dt is the time difference between the peaks (or other characteristic points) of the sine waves representing the cyclic temperature variations at z and at the surface. The determination of parameters a and b from plots using relationships 30 and 31 requires the prior knowledge of ΔT_o and Po . a and b may also be respectively derived from plots of $\log DT_z$ (or $\ln DT_z$) and $P(z)$ with depth z :

$$\ln DT_z = \ln DT_o - a z \text{ or } \log DT_z = \log DT_o - \frac{a z}{2.3} , \quad (32)$$

and

$$P(z) = Po + b z . \quad (33)$$

From these plots, a and b are derived as well as the values of amplitude ΔT_o and phase Po at the surface from the extension of the regression curve on the dependent variable axis.

Regressions of amplitude and phase with depth for the near-surface data were made for each individual well (not shown). Table 2 presents the values of parameters a and b derived from those plots and the computed values of thermal conductivity k_t , and advection fluid flux if the fluid considered is water or air.

Even if, as mentioned before, the heat capacity of gases is low, heat transfer by gas convection may be important when temperature gradients are high. Cathles and Apps (1975) give a relationship for volumetric heat capacity of water vapor saturated air $r_g c_g$ (MJ/m³ °C) which includes the effect of the latent heat of vaporization of water:

$$r_g c_g = 5.4 \times 10^{-3} (0.126 + 0.0283 T) , \quad (34)$$

where temperature T is in °C. At 25 °C, volumetric heat capacity of air is 0.005 MJ/m³ °C.

The net advective heat flux results from the simultaneous flow of water and air. Water infiltration in the unsaturated zone is always vertically downward whereas air flow is driven by density gradients generated by temperature differences in the waste rock pile. Air flow is also controlled by the creation of convection cells. In the upper half of the dump, temperature increases rapidly with depth and air flow is generally upward. The advective heat flux ($q_{c_0 r_0}$, J/m² s) will then be the sum of the water advective flux $q_w c_w r_w$ and the air advective flux $q_g c_g r_g$ which may have opposite directions (q positive downward):

$$q c_0 r_0 = q_w c_w r_w + q_g c_g r_g . \quad (35)$$

Fluid fluxes in table 2 were calculated for water and air if either fluid were the only one contributing to advective heat transfer. Negative signs indicate upward fluxes. If water is vaporized in the hotter regions of the dump and water vapour rises to the colder regions of the dump and then condenses there, significant heat can be transferred from the hotter to the colder regions by absorbing vaporization heat, by releasing condensation heat, and by convection heat transfer to the vapour. Also, such internal circulation of water can increase the downward water flux through a certain plane to well above that accounted for by the annual infiltration flux of 0.5m. Hydrographs from weir stations and the lysimeter data should provide us with a good estimate of infiltration in 1993. In any case, infiltration cannot exceed precipitations, so water flow cannot be the main contribution to advective heat transfer. Furthermore, important water infiltration is restricted mainly to a few weeks in the spring during snow melt. Advective heat transfer, especially upward, may thus only be explained by air convection at a few meters per day.

The thermal conductivity k_t computed using Stallman's solution are generally in a normal range and close to the values used by Cathles and Apps (1975). However, the values obtained for wells #2 and #6 which have higher advection rates are very different and may not represent the true medium properties. If we exclude these two wells, the average thermal conductivity obtained is 2.52 W/m °C. This value will be used in the following section to calculate the heat production rate.

The difference between the values of parameters **a** and **b** is an indication of the magnitude and direction of advective heat transfer. Figure 12 shows that the relationship between attenuation and phase for near-surface data is different for each well and is indicative of advection direction. The direction of advective heat transfer can be determined from the ratio of parameters **a** and **b**. A ratio **a/b** of one indicates no significant advective heat transfer whereas a ratio above one indicates an upward net advective heat transfer and a ratio below one indicates a downward net advective heat transfer.

Advection direction also affects the shape of temperature profiles. Wells where advective heat transfer is upward (#1 and #6) have steeper near surface temperature gradients and reach their maximum temperature values at shallower depths than well in which advective heat transfer is downward (#2, #3 and #5). Well #3 does not have high temperature gradients to generate important air flow. Well #5 has a fine grained overburden material within the waste rock which may prevent upward air movements. Well #2 may be within a downward circulating convection current. These suppositions generally agree with an infrared thermographic survey even though more work will have to be done to explain the behavior of each individual well. This matter is further discussed in the last section.

It is important to note that thermal conductivities and fluid fluxes derived from this analysis are effective properties affected by the near-surface temperature gradients. In wells where high temperature gradients prevail, the effective thermal conductivity will be higher than would be the case in an isothermal system. Numerical modeling is needed to better evaluate the effect of upward heat conduction and advection when the system is submitted to cyclic temperature variations and to asses the effect of water evaporation and condensation. However, the analysis does show the importance of advection in the transfer of heat in the system.

4 - Heat production in waste rocks

As mentioned before, heat production in waste rocks undergoing AMD production may be related directly to pyrite (or another sulfide) oxidation. If heat production rates can be evaluated, the rate of pyrite oxidation can be derived as well as the rate of oxygen consumption. Two methods were used to derive the heat production rate from the mean temperature profiles. A simple conduction model is first used, followed next by an analytical solution also taking into account advection and oxygen supply. Neither model can fully describe all the mechanisms of heat transfer in a waste rock dump but they do provide simple means of estimating the heat production rate.

4.1 - Simple conduction model

In a steady state system in which conduction is the dominant heat transfer mechanism, the heat production rate may be calculated simply from equation 8 presented earlier. This relationship requires the knowledge of thermal conductivity k_t and the temperature gradient variation d^2T/dx^2 . k_t was derived in the previous section and we may use a value of 2.5 W/m°C as representative of the waste rocks. d^2T/dx^2 may be derived from a correlation of temperature measurements with depth. Wells #1, #2, #4, and #5 have a similar temperature profile and are judged representative of the general thermal regime in the waste dump. Figure 13a shows a fair agreement for a third order polynomial regression of the mean temperatures with depth for these wells.

The heat flux by conduction q (W/m²) is given by Fourier's law (equation 4) and is derived from the derivative of temperature with depth dT/dx . Figure 13b shows the heat flux q and the heat production rate Q derived from the correlation in figure 13a. Negative values of q indicate an upward flux whereas positive values are for downward flux. The use of a third order polynomial implies a linear decrease of heat production Q with depth since the second derivative of temperature with depth will be linear. The correlation would also indicate that no more heat production occurs below 22 m depth. The negative values of Q are an artifact of the regression and the temperature gradient is known to remain relatively constant below the base of the waste rock pile. The total heat production per unit area in the dump is then obtained from the difference in heat fluxes at the top of the pile and at 22 m depth. The value so derived is 20 W/m² and represents a pyrite oxidation rate of 55 kg/year for every m² of dump surface and thus represents a very important mass of pyrite oxidized.

4.2 - Conduction and advection model

An analytical model of steady state heat transfer by conduction and advection in a medium where heat is being generated may be derived based on equation 10 (see details in appendix C). The solution provides the temperature as a function of depth $T(x)$ ($^{\circ}\text{C}$) above the normal temperature of the medium T_m ($^{\circ}\text{C}$):

$$T(x) - T_m = \frac{\dot{e}}{\dot{e}Ae^{Ab}} \cdot \frac{B}{EA+A^2} e^{-(E+A)b\frac{x}{u}} (e^{Ax}-1) + \frac{B}{E^2+AE} (1-e^{-Ex}) , \quad (36)$$

where,

$$A = \frac{qc_o r_o}{k_t} \quad B = \frac{FC_o K_{Ox}}{k_t} \quad E = \sqrt{\frac{K_{Ox}}{D_e}}$$

- | | | | |
|------------------------|--|------------------------|--|
| F: | conversion factor (0,4 MJ/mol), | K_{Ox}: | kinetic rate constant (s^{-1}), |
| D_e: | effective diffusion coefficient (m^2/s), | C_o: | surface oxygen conc. (9,4 mol/ m^3). |
| T'_b: | temperature gradient at the base of
the dump ($^{\circ}\text{C}/\text{m}$). | B: | depth of base, |

The model supposes pyrite oxidation has first order kinetics with respect to the oxygen concentration and that the oxygen supply is by diffusion. These assumptions are equivalent to supposing an exponential decline in heat production from the surface. So, even though air convection is an important mean of oxygen supply, the model can still be used to represent heat production and transfer. One further limitation of the model is the use of a unique value for fluid flux. Since air flow is actually dependent on temperature gradients, it would not be constant throughout the dump. The potential controlling air flow would even be in opposite direction in the upper and lower half of the waste pile since the temperature gradient changes direction about midway through the pile.

The model was applied to all wells and the mean temperature profiles were used to identify representative parameters to fit the model to the data (table 3). Since the model requires a few parameters as input, most of these were kept the same for all wells. Only the ease of oxygen supply through the wastes (represented by D_e) and the magnitude and direction of advection (represented by the fluid flux) were modified from one well to the next. The magnitude of advection as indicated by table 2 could not be used directly since the model does not represent the same phenomena as the analytical solution. However, the direction of advection was respected for all wells but #4. In that case, the advection direction was recently changed by excavation near the well so that, in the middle of the monitoring period, advection was still upward for that well.

We will present the results of the model for two wells with opposite advection directions to illustrate how it affects the shape of the temperature profiles. Figure 14 shows the temperature profile, heat flux and heat production for well #1 derived using an upward adective flux. These results do not necessarily represent an optimal solution but one representative of the measured temperature. Figure 15 shows the same parameters derived for well #5 where downward heat transfer by convection is considered. For similar heat production profiles, the temperature distribution is very different.

The wells for which the cyclic temperature data indicated significant upward adective heat transfer (wells #1, #6 and #4 for the mean profile) are the ones showing steep near surface temperature gradients and a maximum temperature in the upper half of the dump. The other wells (#2, #3, #5 and the final temperature for #4), which did not have indications of upward adective heat transfer, show more gradual temperature increases and reach a maximum temperature in the lower half of the dump.

The total heat production per unit dump surface area Q_t (W/m^2) is obtained by integration of the heat production curve generated from the model. If we except well #3 with 7.6 W/m^2 , the other wells have total heat production ranging from 15.4 to 20.9 W/m^2 . These values are in the same range as the results from the simple conduction model. It is interesting to compare this production rate with the heat stored in the dump which was derived earlier. The total heat production rate calculated would generate between about 490 and 660 MJ of heat per year. This means there is an amount of heat stored in the dump equivalent to between 2.5 and 4 years of heat production at the present rate.

This estimate has very practical importance, especially when compared with similar evaluations on water and acidity stored within the dump which come out with about the same magnitude of accumulation relative to the annual production (not discussed in this report). This stored "potential" implies that whatever is done to control AMD production in the dump, it will take some time before the results are felt because of the high "inertia" of the system.

4.3 - Air convection conceptual model

Several lines of evidence indicate the importance of air convection in the South Dump. These evidences are the visual observations on the dump surface, the temperature profiles, the air composition within the dump, the oxygen requirements to sustain the observed heat production rate, and especially the thermographic surveys of the dump surface. These evidences allow the development of a conceptual model on the patterns of air convection within the dump.

The occurrence of air flow within the dump is more easily observed at the surface of the dump late during the fall or in the winter. Zones through which hot air flows out at the surface of the dump have an area of just a few square meters and are characterized by either the presence of steam (especially on cold fall mornings), a hot surface, the absence of snow or unfrozen ground during winter. The exit of hot air was noted especially at the southern rim of the dump where temperatures exceeding 20 °C were measured between blocks a few centimeters from the surface in the middle of winter.

Quantitative evidences of air convection are provided by the temperature profiles. The relationship between attenuation and phase derived from the cyclic temperature variations indicate the presence of important upward and downward air flow in different parts of the dump. The air movement also affects the shape of the temperature profiles which are also diagnostic of the advection direction. The analytical advection model developed confirmed the effect of air advection direction on the shape of the temperature profiles. The two types of temperature profiles illustrated in figures 14 and 15 would be generated by convection cells in which regions of upward and downward air movement would be present.

The best evidences of air convection were provided by infrared thermographic surveys of the dump surface. These surveys will not be discussed in details here but the main conclusions drawn from these measurements will be mentioned. Two types of thermographic surveys were done on the dump surface. An airborne survey was first done in the fall of 1991 and provided a video of the temperature patterns at the surface of the dump. A second survey was done at the end of summer 1992 with a portable instrument and measurements were made on the dump surface in a grid and on a section across the dump. The aim of the second survey was to confirm the presence of the temperature anomalies detected the previous year and verify if the patterns previously detected were stable in time.

Thermographic surveys allow the identification of relatively hot or cold surfaces on the dump. These are interpreted as representing respectively areas of hot air exit from the dump and areas of cold atmospheric air entry in the dump. The airborne survey indicated that important air entry occurs at the base of the dump and hot air exits at the upper rim all around the dump. Within the dump, irregular patterns emerge indicating the presence of areas of air entry and air exit arranged in irregular convection cells. As an example, figure 16 shows a thermographic section measured at the dump surface showing alternating hot and cold areas spaced 10 to 15 m apart. These features are interpreted as evidences for the general size of convection cells within the dump.

If convection cells are supposed having about the same dimensions vertically as the ones observed horizontally, figure 16 would then indicate that the convection cells are restricted to the upper half of the dump. Actually, there are other evidences for the presence of two sets of convection cells in the upper and lower half of the dump. First, air convection is driven by differences in air density controlled by temperature gradients. Since temperature reaches a maximum at about the center of the dump, air should generally have opposite direction in the upper and lower half of the dump. Furthermore, the observed air composition in the dump shows relatively high oxygen concentration in the upper half of the dump whereas the lower half is depleted in oxygen.

These evidences would indicate that two different convection regimes exist in the dump: 1) rapid convection in the upper half driven by steep temperature gradients bringing in oxygen from the surface and 2) slow air movement (or even stagnant air) in the lower half of the dump due to the slowly upward increasing temperature gradients. The air in the lower half of the dump is not in contact with atmospheric oxygen and could actually be trapped thus explaining the very low oxygen concentration in this zone. Trapping is further supported by the high CO₂ buildup (to more than 5% in places) in the lower half of the dump which is likely the result of partial leachate neutralization by carbonates. Also, the convection patterns seem to be quite stable in time since the surface survey found similar temperature patterns as the ones observed the preceding year by the airborne survey. The stability of the patterns is also indicated by the gas composition within the dump which shows little variation in time for a given well.

Figure 17 schematically summarizes our present view of the air convection patterns within the dump based on the monitoring data presently available. The dump is believed to have two convection zones: a fast convection zone at the edge and the upper half of the dump and a slow convection (or stagnant air) zone in the lower half of the dump. Zones of upward and downward air movement show different temperature and oxygen concentration profiles. In zones of downward air movement, the temperature profiles have a relatively low near surface temperature gradient and maximum temperature is reached in the lower half of the dump. In these zones, oxygen concentration is near atmospheric values in the upper half of the dump but remains near 5% below the middle of the dump. In zones of upward air movement, temperature profiles show steep near surface temperature gradients and reach a maximum value in the upper half of the dump. In these zones, the oxygen concentration in the upper half of the dump is lower than atmospheric values, probably because some oxygen is consumed as air circulates down through the dump before moving back up.

An important aspect to mention is that heat production, and thus AMD production, is higher near the surface of the dump than below despite the fact that temperature reaches a maximum value in

the middle of the dump. The reason why temperature is not also at its highest value where heat production is at its peak is simply that more heat is lost near the surface of the dump than in the middle which is far from heat loss surfaces. Trenches and lysimeters provide evidence for high oxidation rates near the surface. High concentration leachate is recovered from the lysimeters even near the surface. Also, new minerals (mainly gypsum and jarosite) are seen forming just a few meters below the surface thus indicating that leachate oversaturation with respect to these minerals is reached at these shallow depths.

Advection plays a large role in heat transfer but it has a great impact as well on the AMD production rate since it is the main source of oxygen supply for pyrite oxidation. Actually, the pyrite oxidation rates, indicated by this study, would require unrealistic oxygen diffusion rates if advection were not controlling oxygen supply. The conceptual model for air circulation in the dump is based on the monitoring data available. However, numerical models developed by Cathles and Schlitt (1980) and by Pantellis and Ritchie (1991) also predicted the formation of convection currents in waste rock piles. The measurements, observations, and data analysis done for this project actually confirm the importance of advection for heat transfer in waste rock dumps. The next step will be to model these processes numerically in order, first to further characterize the properties of the dump and then to better describe the mechanisms responsible for AMD production in waste rock dumps.

5 - Conclusion

Significant heat is generated by pyrite oxidation during the production of acid mine drainage in waste rock dumps. The maximum temperatures recorded in the South Dump at the Doyon mine range from about 40 to 65 °C (one well only reaches 14 °C) in an area where the mean surface temperature is 2 °C.

Fourier analysis was used to characterize the recorded cyclic temperature variations at depth resulting from annual surface changes. The amplitude and phase of the sinusoidal variations may be used to derive the thermal properties of the waste rocks as wells as the magnitude and direction of advectional heat transfer. Advectional heat transfer is found to be significant and influences the shape of the temperature profiles.

The heat production rate can be derived from the mean temperature profiles. A simple conduction model or one considering both conduction and advection may be used for that purpose. The heat production rate may be related to the pyrite oxidation rate and oxygen consumption. Thermal data thus provides a way to determine the rate of AMD production independently of any model. This information can be used to calibrate and validate AMD models and also to follow the evolution of AMD production with time before and after the use of control measures.

The analysis presented here is relatively simple and based solely on analytical models. Numerical modeling in two dimensions will be required in order to better understand the interaction between pyrite oxidation, heat transfer, air convection and water infiltration. The present report should be a helpful guide on temperature monitoring, on methods to analyze the data, and as an illustration of the important physical mechanisms controlling AMD production in waste rock dumps.

6 - References

- Burden, R.L., and Faires, J.D., 1989: Numerical analysis, 4th ed. PWS-Kent Publ. Co., 729 p.
- Cathles, L.M., and Apps, J.A., 1975: A model of the dump leaching process that incorporates oxygen balance, heat balance, and air convection. *Metal. Trans. B*, vol. 6B, p. 617-624.
- Cathles, L.M., and Schlitt, W.J., 1980: A model of the dump leaching process that incorporates oxygen balance, heat balance, and two dimensional air convection. In Schlitt, W.J., ed., Leaching and recovering copper from as-mined materials. Proc. of the Las Vegas Symp., 26 Feb., 1980, Solution Mining Committee, Soc. of Mining Eng. of AIME, p. 9-27.
- Davis, G.B., and Ritchie, A.I.M., 1986: A model of oxidation in pyritic mine wastes: part 1 - equations and approximate solution. *Appl. Math. Modeling*, 1986, vol. 10, October, pp. 314-322.
- Davis, J.C., 1973: Statistics and data analysis in geology. John Wiley & Sons, New York, 550p.
- Gélinas, P., Lefebvre, R., Choquette, M., 1992: Characterization of acid mine drainage production from waste rock dumps at La Mine Doyon, Québec. Second Int. Conf. on Environ. Issues and Manag. of Waste in Energy and Mineral Prod., Calgary, Sept. 1992.
- Harries, J.R., and Ritchie, A.I.M., 1985: Pore gas composition in waste rock dumps undergoing pyritic oxidation. *Soil Science*, August 1985, vol.140, no.2, p. 143-152.
- Hart, W.M., Batarseh, K.I., Swaney, G.P., and Stiller, A.H., 1991: A rigorous model to predict the AMD production rate of mine waste rock. In MEND, ed., Proc. of the Second Int. Conf. on the Abatement of Acidic Drainage, Montreal, sept.16-18, vol.2, p.257-269.
- Hiskey, J.B., and Schlitt, W.J., 1981: Aqueous oxidation of pyrite. In Schlitt, W.J., ed., Interfacing technologies in solution mining. Proc. of the second SME-SPE int. solution mining symp., Denver, Colorado, 18-20 Nov. 1981, p. 55-74.
- Jaynes, D.B., Rogowski, A.S., and Pionke, H.B., 1984a: Acid mine drainage from reclaimed coal strip mines - 1. Model Description. *Water Resources Research*, vol. 20, no. 2, Febr., p. 233-242.
- Jaynes, D.B., Rogowski, A.S., Pionke, H.B., and Jacoby, E.L., Jr., 1983: Atmosphere and temperature changes within a reclaimed coal strip mine. *Soil Science*, Sept. 1983, vol. 136, no. 3, p. 164-177.

- Lefebvre, R., 1992: Halde sud de la mine Doyon - Phase 2: Rapport de terrain - Été 1992. Rapport GREGI 1992-16, Univ. Laval, 29 p. and appendices.
- Lefebvre, R., Gélinas, P., and Isabel, D., 1992: Heat transfer analysis applied to acid mine drainage production in a waste rock dump, La Mine Doyon (Québec). 1992 Int. Ass. of Hydrogeol., Hamilton, May 1992.
- Lowson, R.T., 1982: Aqueous oxidation of pyrite by molecular oxygen. Chemical Reviews, vol. 82, no. 5, October.
- Nordstrom, D.K., 1977: Hydrogeochemistry and microbiological factors affecting the heavy metal chemistry of an acid mine drainage system. Ph. D. Thesis, Stanford Univ., 210 p.
- Pantelis, G., and Ritchie, A.I.M., 1991: Macroscopic transport mechanisms as rate-limiting factor in dump leaching of pyritic ores. Appl. Math. Modeling, vol.15, March, p. 136-143.
- Stallman, R.W., 1965: Steady One-Dimensional Fluid Flow in a Semi-Infinite Porous Medium with Sinusoidal Surface Temperature. Jour. of Geoph. Res., v.70, no.12, p.2821-2827.

Table 1.
Properties of the South Dump
and waste rocks.

Volume (m ³)	11 450 000
Equivalent surface (m ²)	369 334
Mean thickness (m)	31
Porosity	0,33
Water saturation	0,32
Dry bulk density (kg/m ³)	1 840
Grain density (kg/m ³)	2 740
Grain size (d ₁₀ -d ₉₀) (mm)	2-150

Table 2.
Thermal conductivity and fluid flux from Stallman's solution.

Well	a (m ⁻¹)	b (m ⁻¹)	k _t (W/m °C)	q _{air} (m/d)	q _{water} (m/y)
1	0.336	0.255	2.92	-7.2	-3.1
2	0.168	0.385	0.97	12.0	5.3
3	0.163	0.260	2.62	11.4	5.0
4	0.221	0.287	2.31	6.1	2.6
5	0.239	0.295	2.22	4.8	2.1
6	0.364	0.095	10.67	-62.6	-27.3

Table 3.
Parameters and heat production for the
conduction and advection model.

Parameter	Well #1	Well #2	Well #3	Well #4	Well #5	Well #6
D _e (m ² /d)	10.1	5.0	1.0	8.5	7.0	12.5
C _o (mol/m ³)	9.38	9.38	9.38	9.38	9.38	9.38
k _t (J/d m °C)	217 728	217 728	217 728	217 728	217 728	217 728
K _{ox} (d ⁻¹)	0.03	0.03	0.03	0.03	0.03	0.03
v (m/d)	-5	1	7	-4.05	1	-5.41
C _v (J/m ³ °C)	5000	5000	5000	5000	5000	5000
T _b (°C/m)	-1.1	-1.1	-0.1	-1.1	-1.1	-1.1
B (m)	31	31	31	31	31	31
T _m (°C)	5	5	5	5	5	5
Q _t (W/m ²)	19.6	15.4	7.6	18.6	17.4	20.9

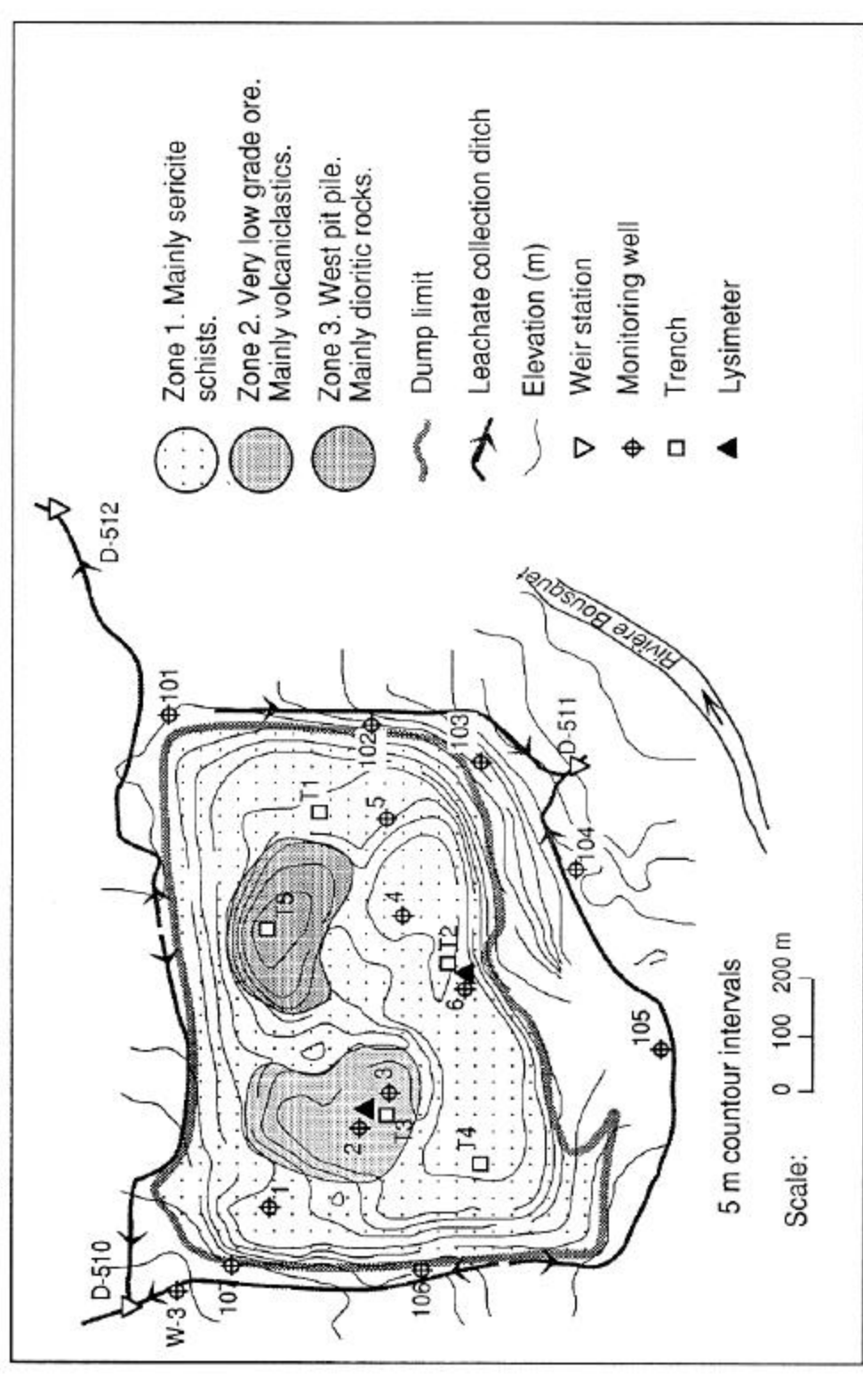


Figure 1. South Dump instrumentation

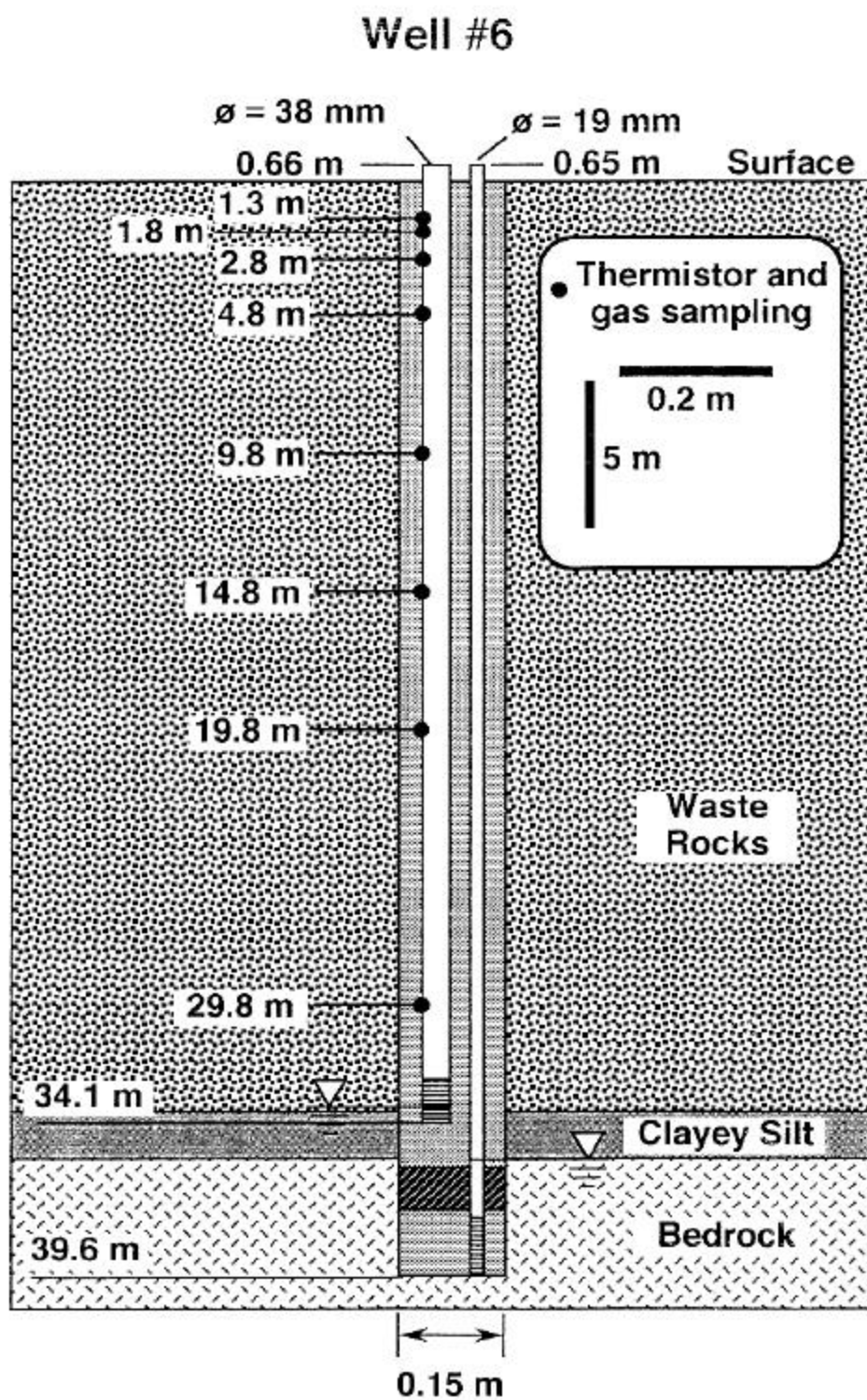


Figure 2. Monitoring well instrumentation complete.

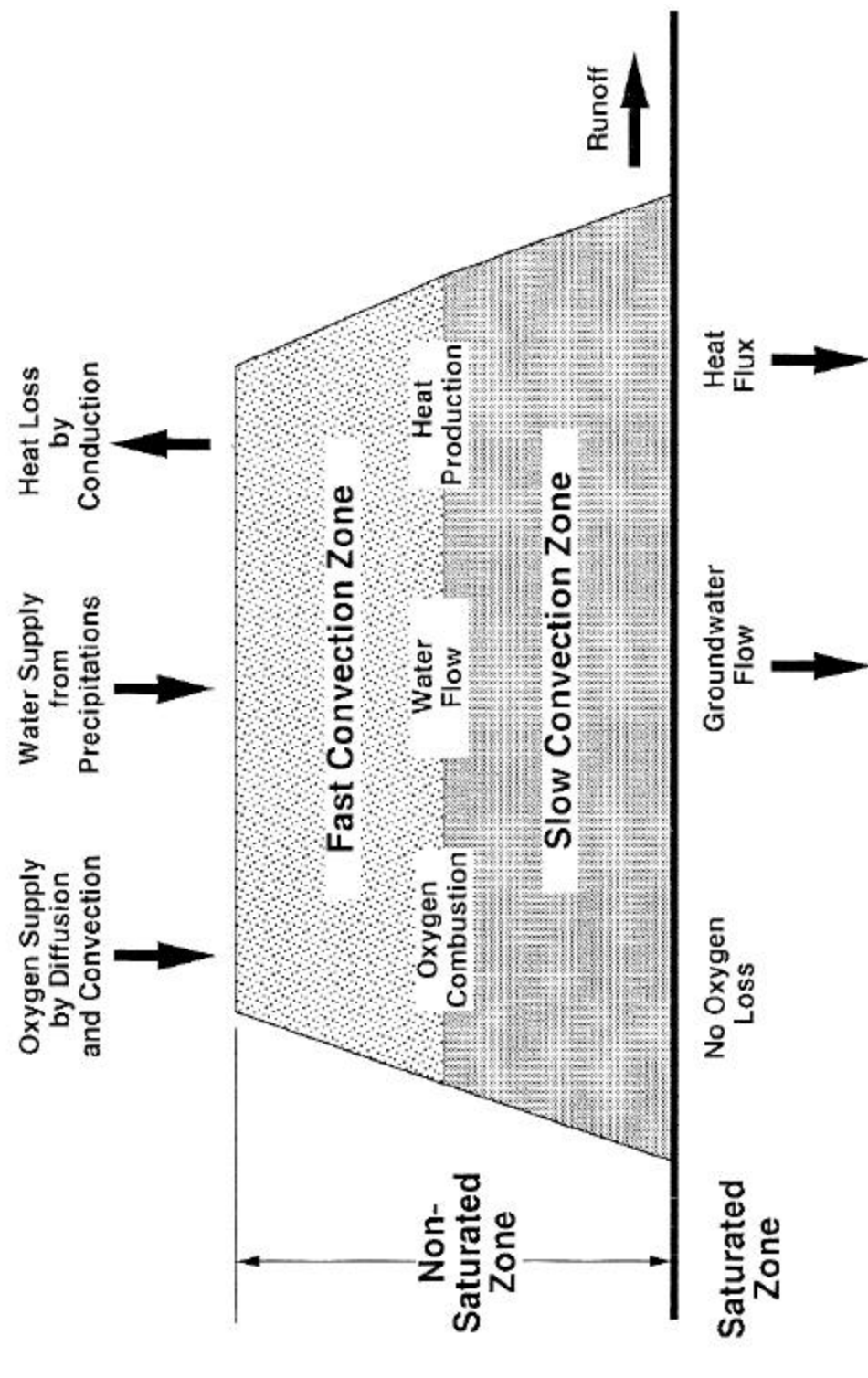


Figure 3. Physical mechanisms operating in AMD-producing waste rock dumps.

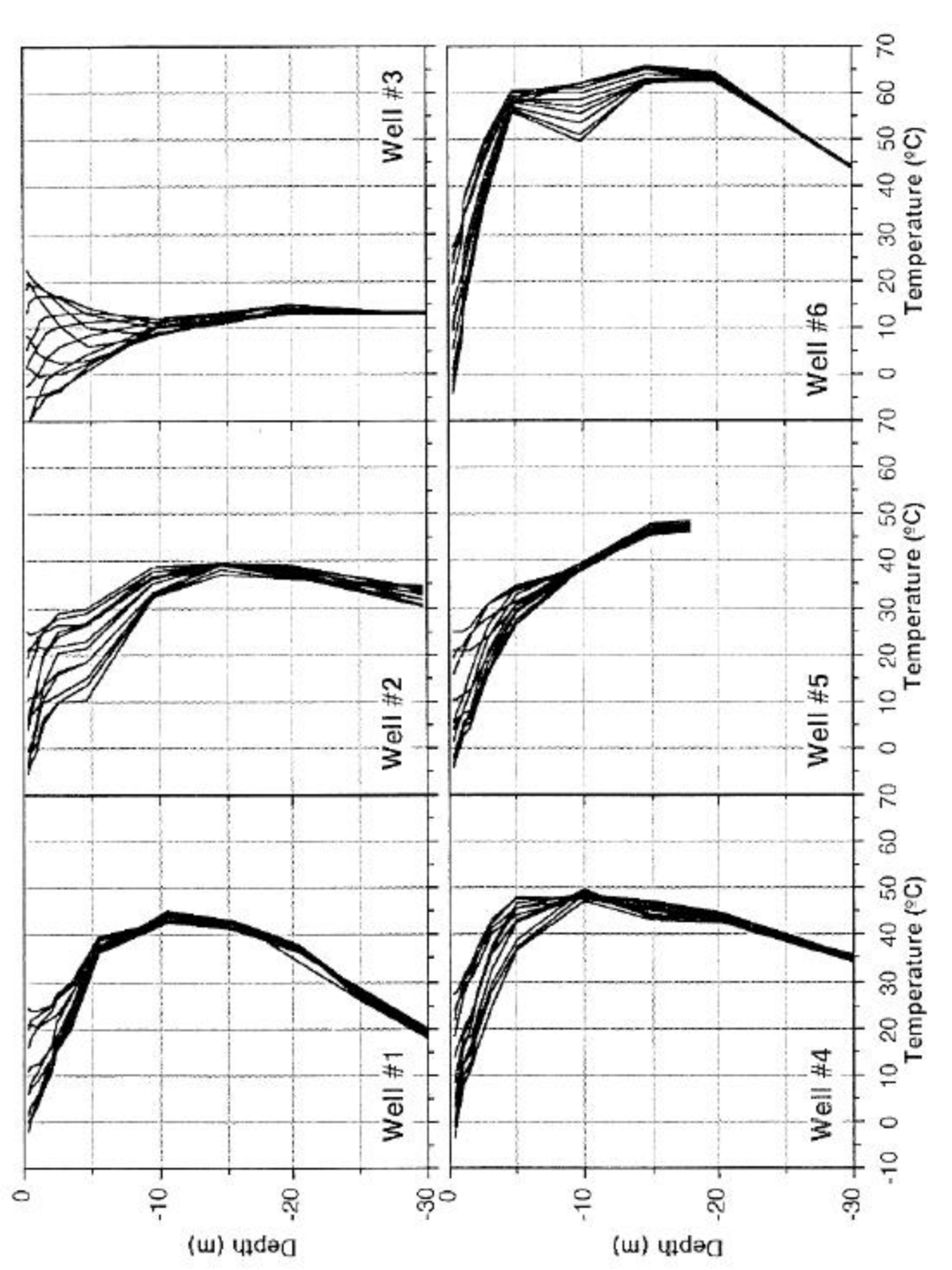


Figure 4. Mid-month temperature profiles for the first monitoring year.

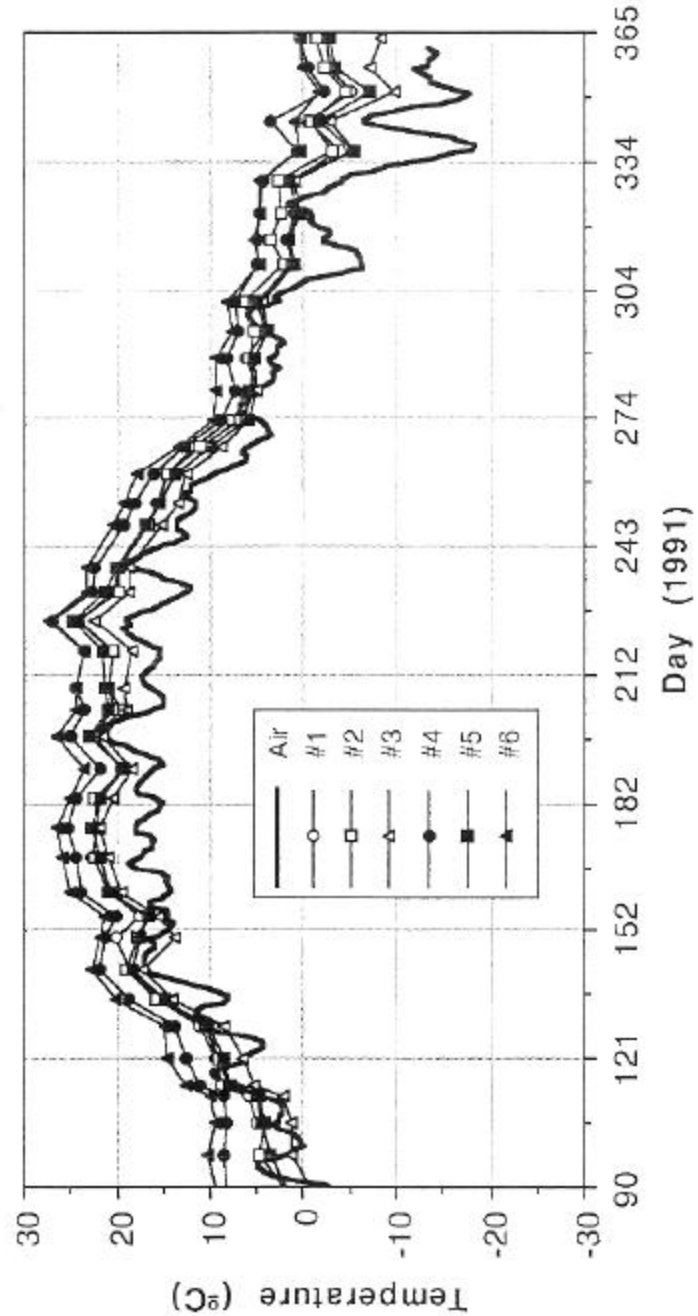


Figure 5. Air temperature compared with near surface temperature.

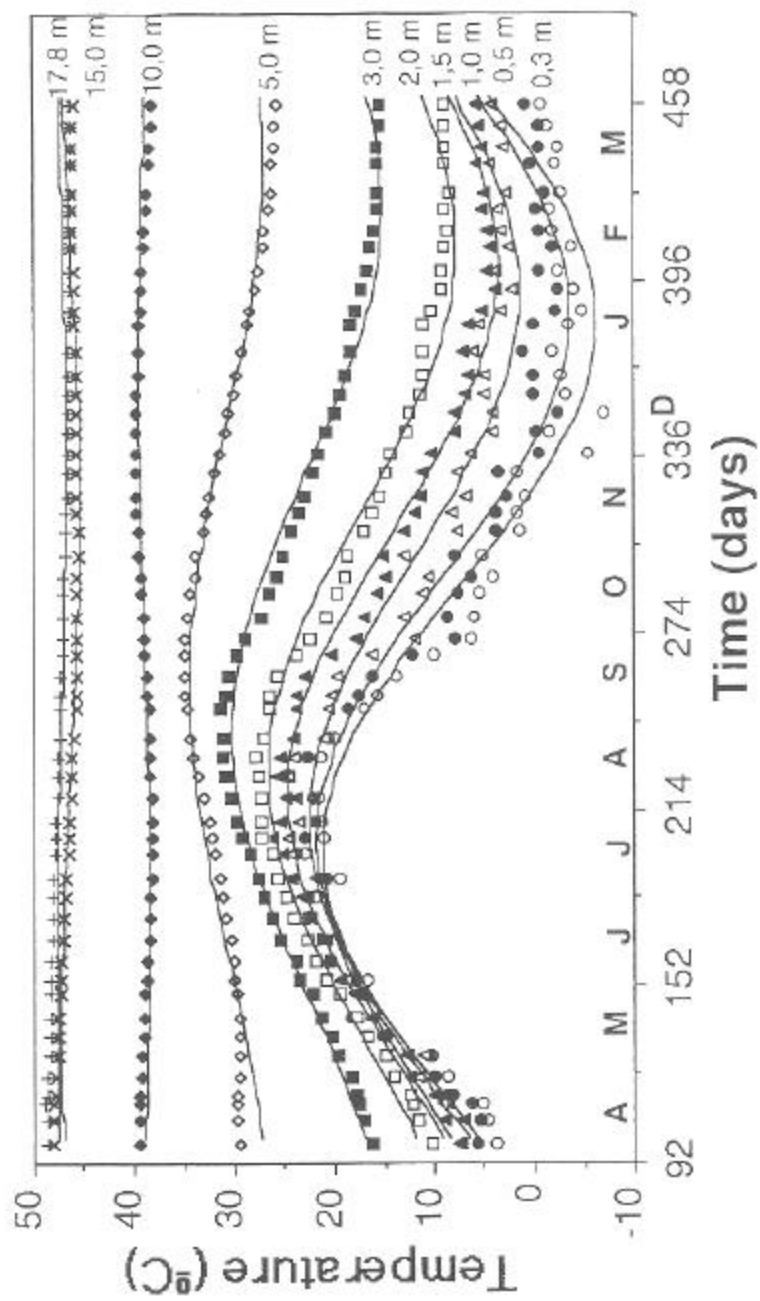


Figure 6. Cyclic temperature variations for monitoring well #5.

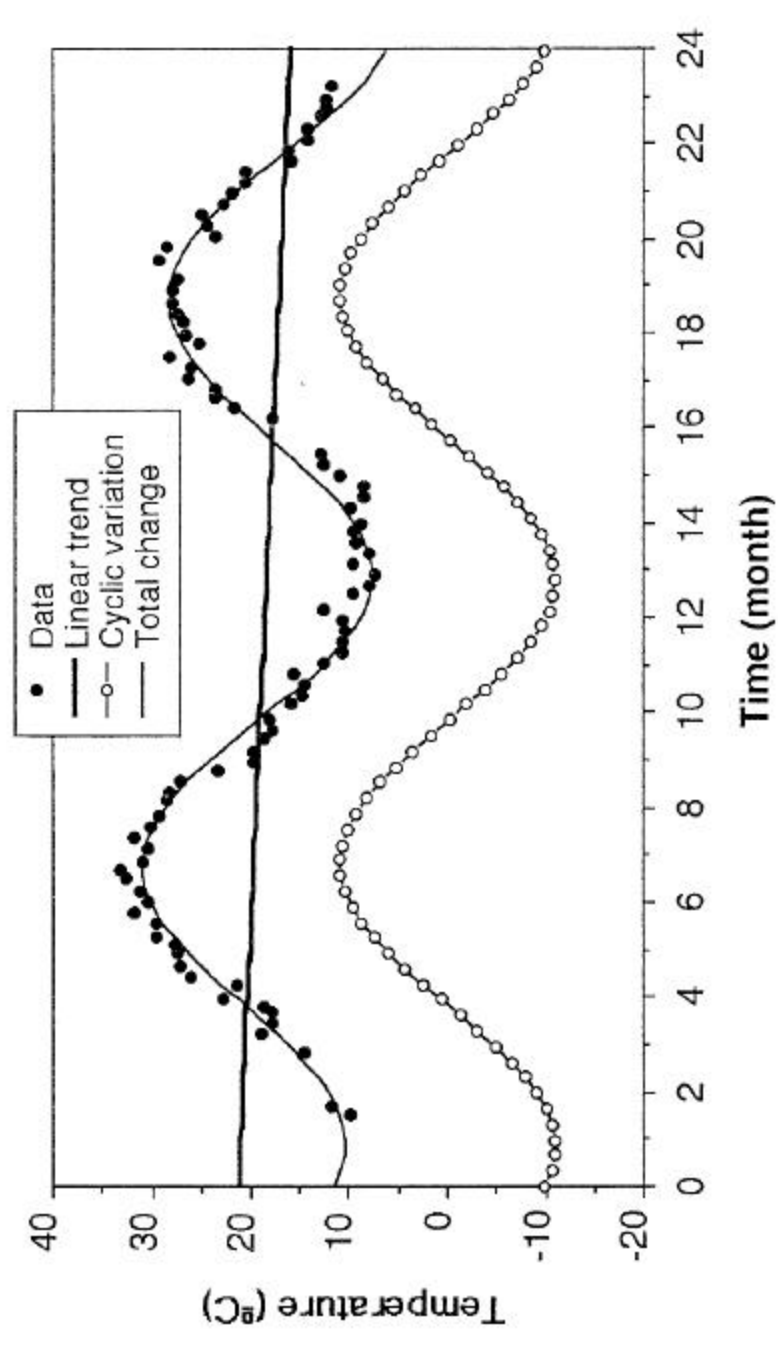


Figure 7. Cyclic temperature variations analysis for Well #6 (1.0).

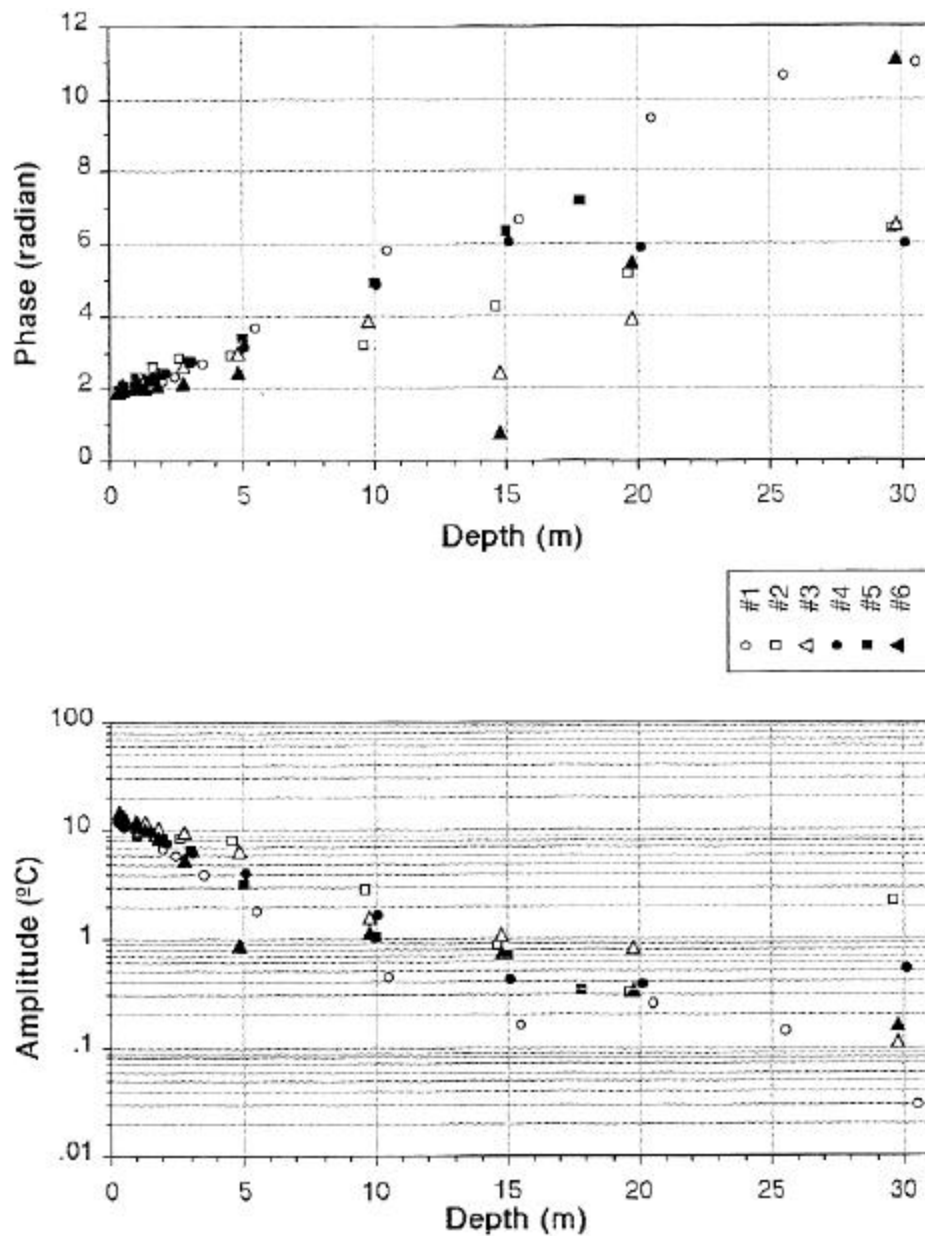


Figure 8. Amplitude and phase as a function of depth for all wells.

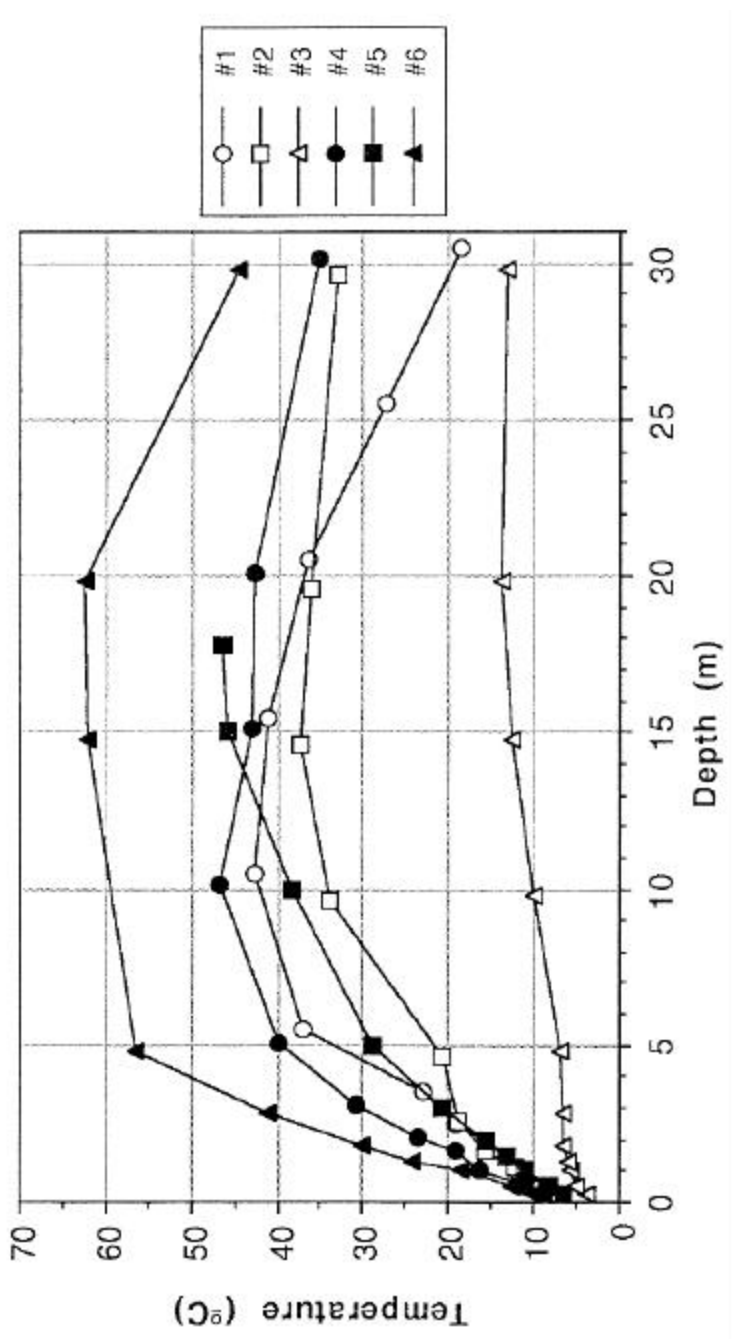


Figure 9. Mean temperature profiles for all wells.

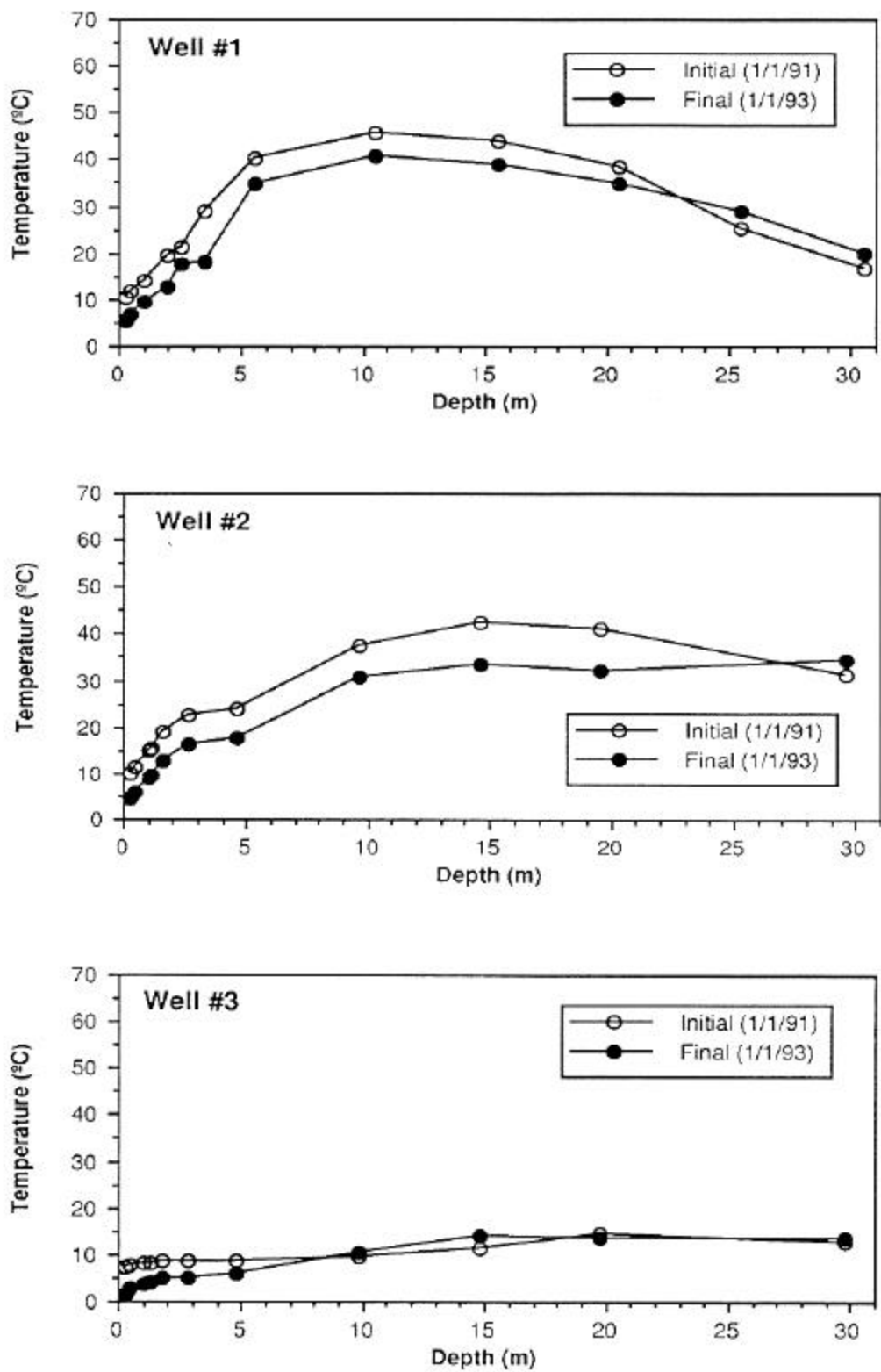


Figure 10. Initial and final temperature profiles.

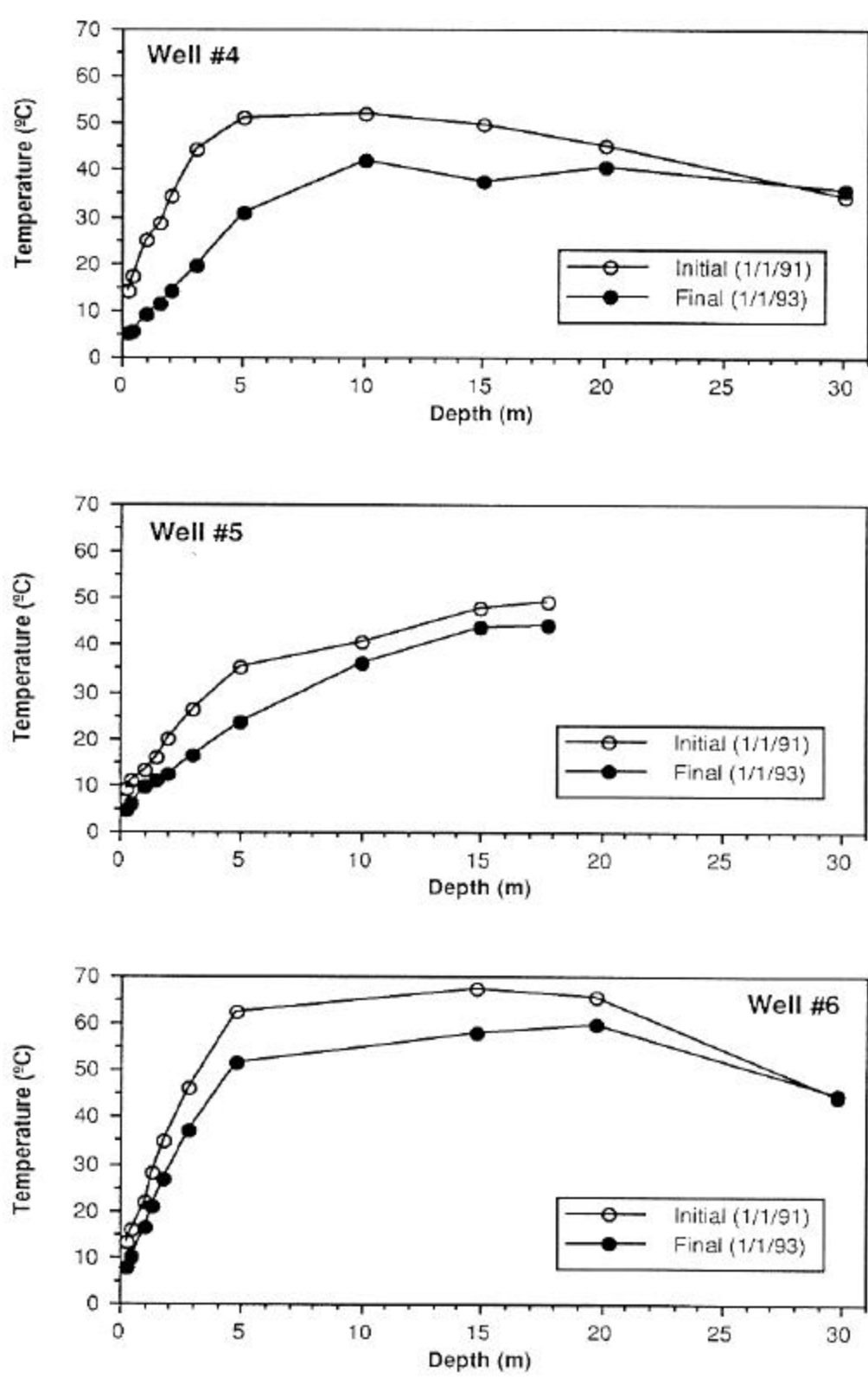


Figure 10 (continued). Initial and final temperature profiles.

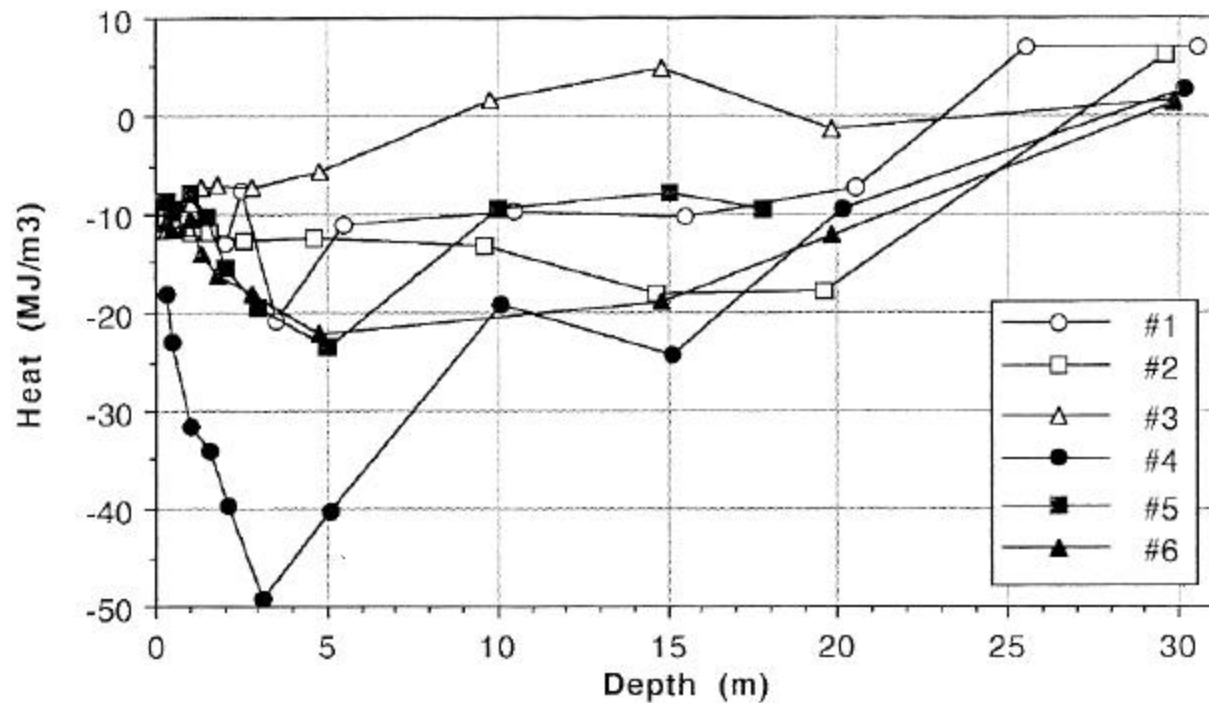


Figure 11. Change in heat stored during the monitoring period.

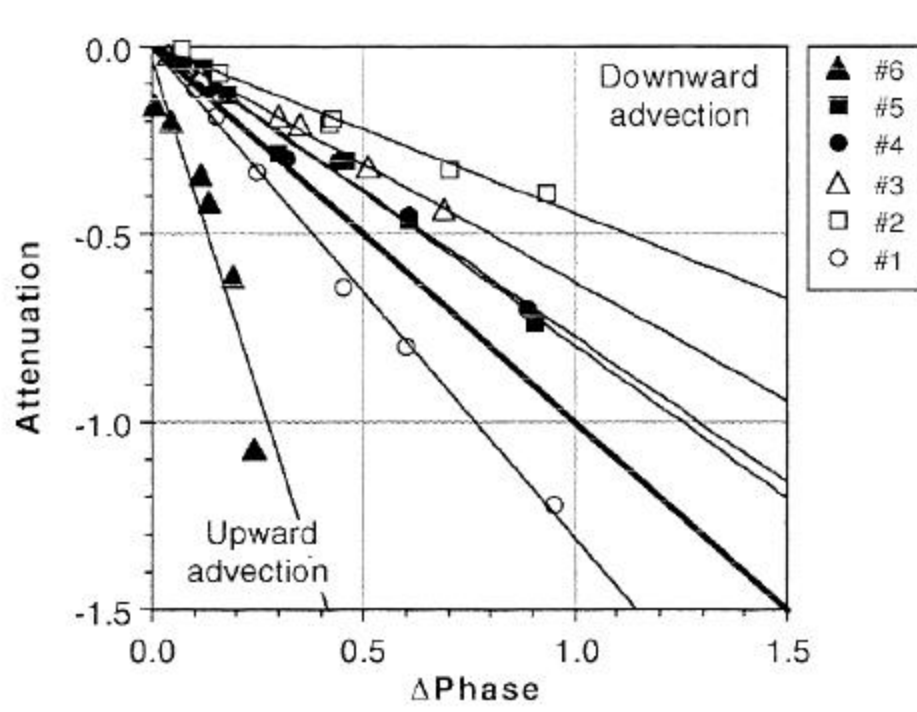


Figure 12. Relationship between attenuation and phase for all wells.

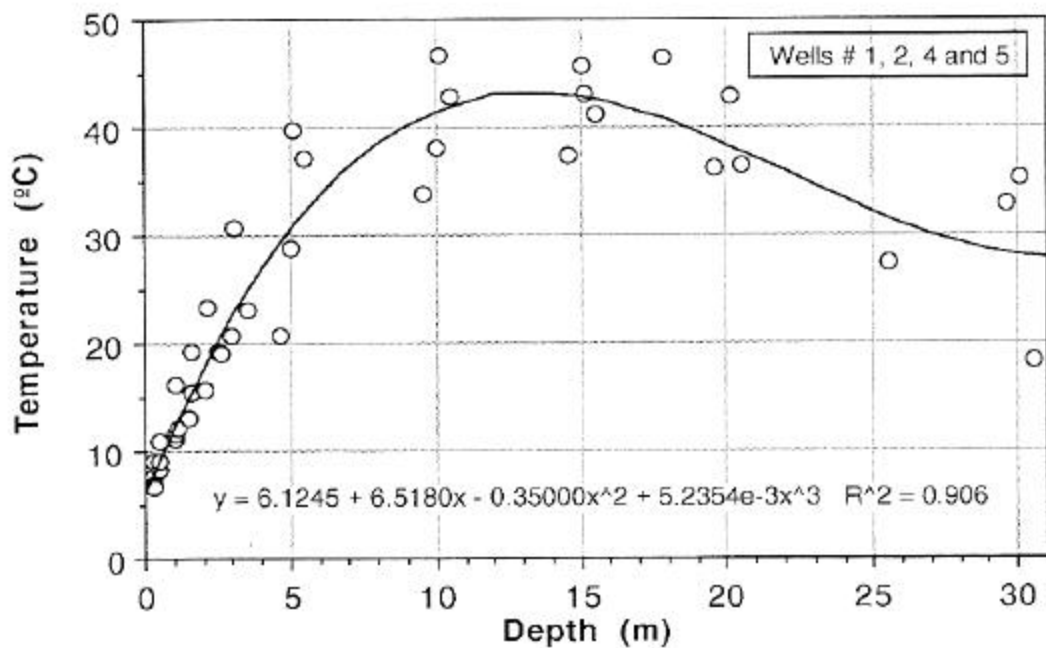


Figure 13. a) Polynomial temperature correlation with depth.

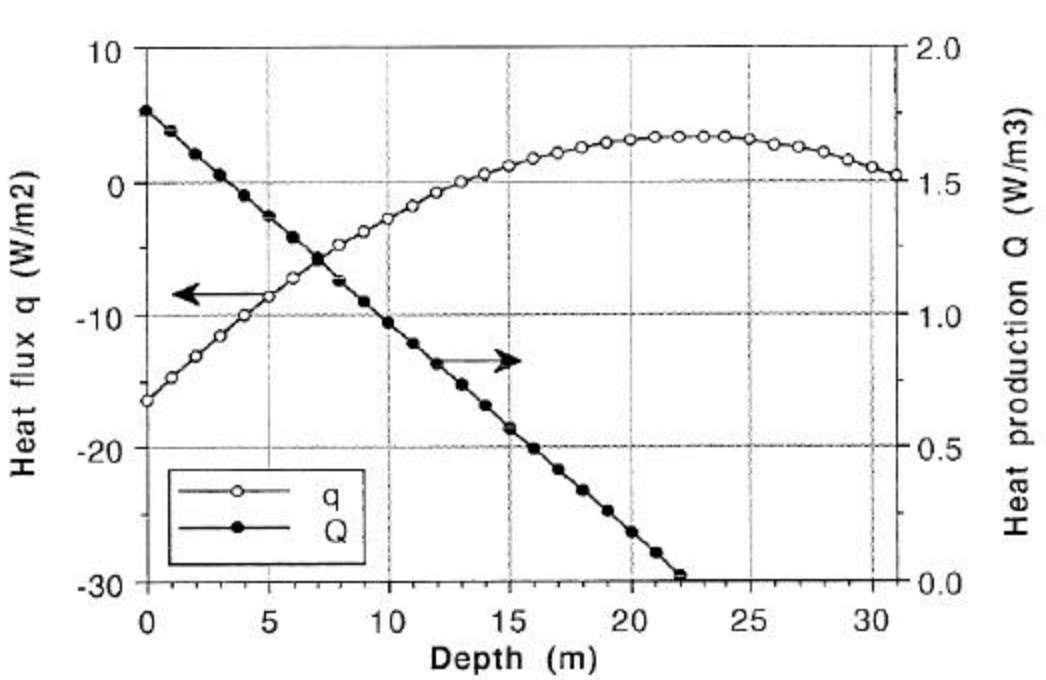


Figure 13. b) Heat flux and production from the conduction model.

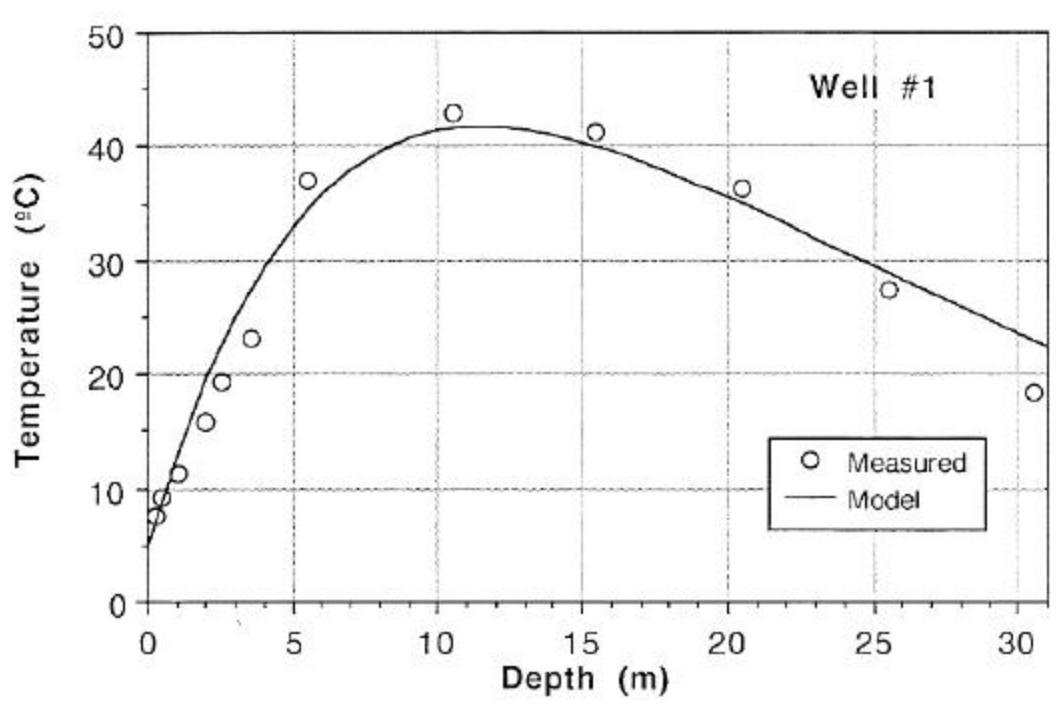


Figure 14. a) Temperature computed from the advection model.

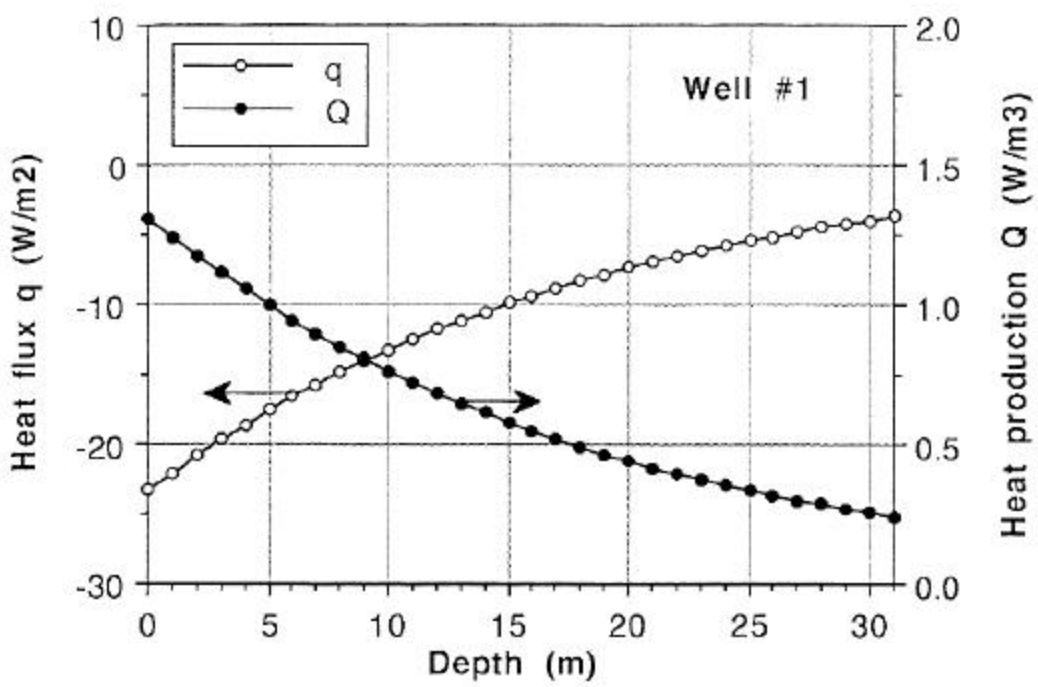


Figure 14. b) Heat flux and production from the advection model.

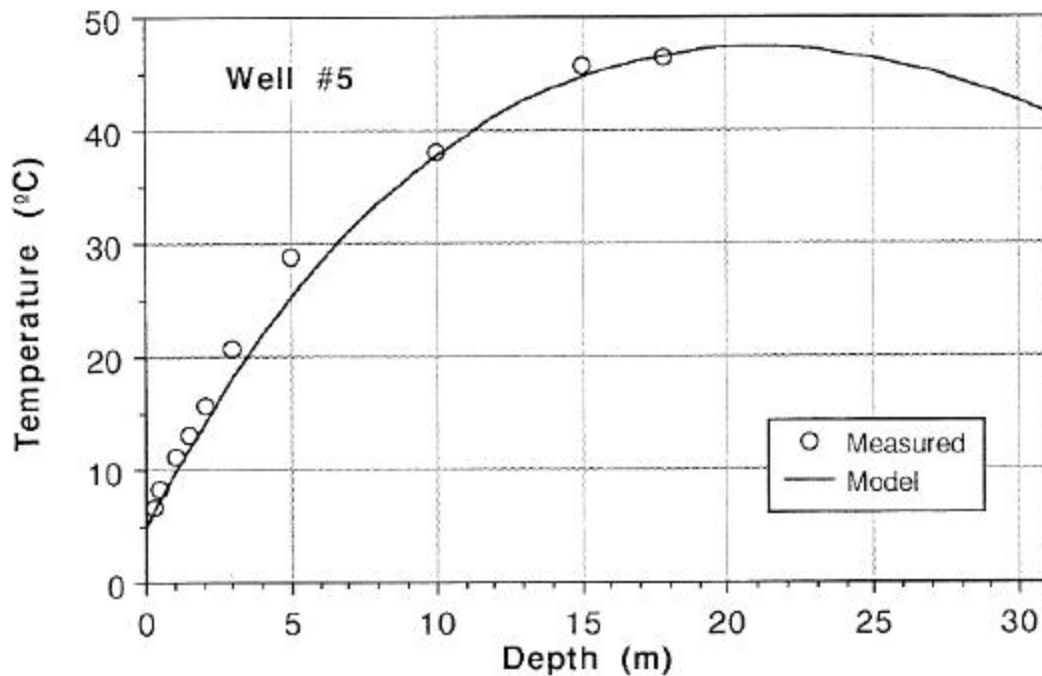


Figure 15. a) Temperature computed from the advection model.

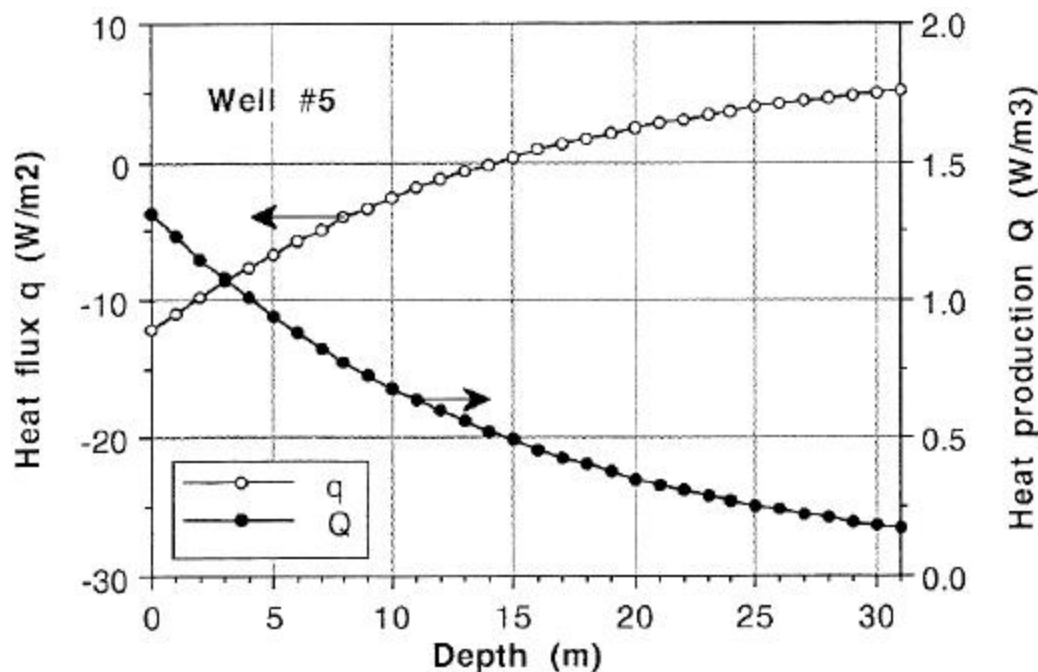


Figure 15. b) Heat flux and production from the advection model.

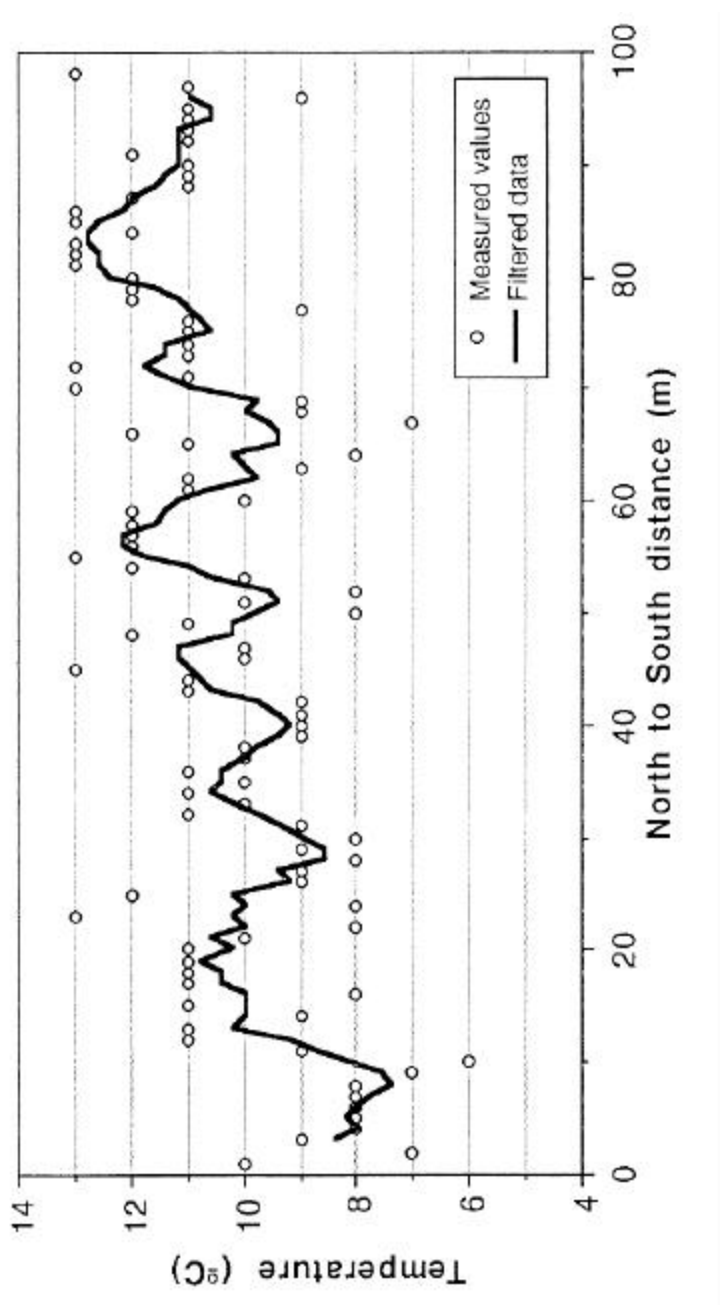


Figure 16. Thermographic survey measured at the dump surface.

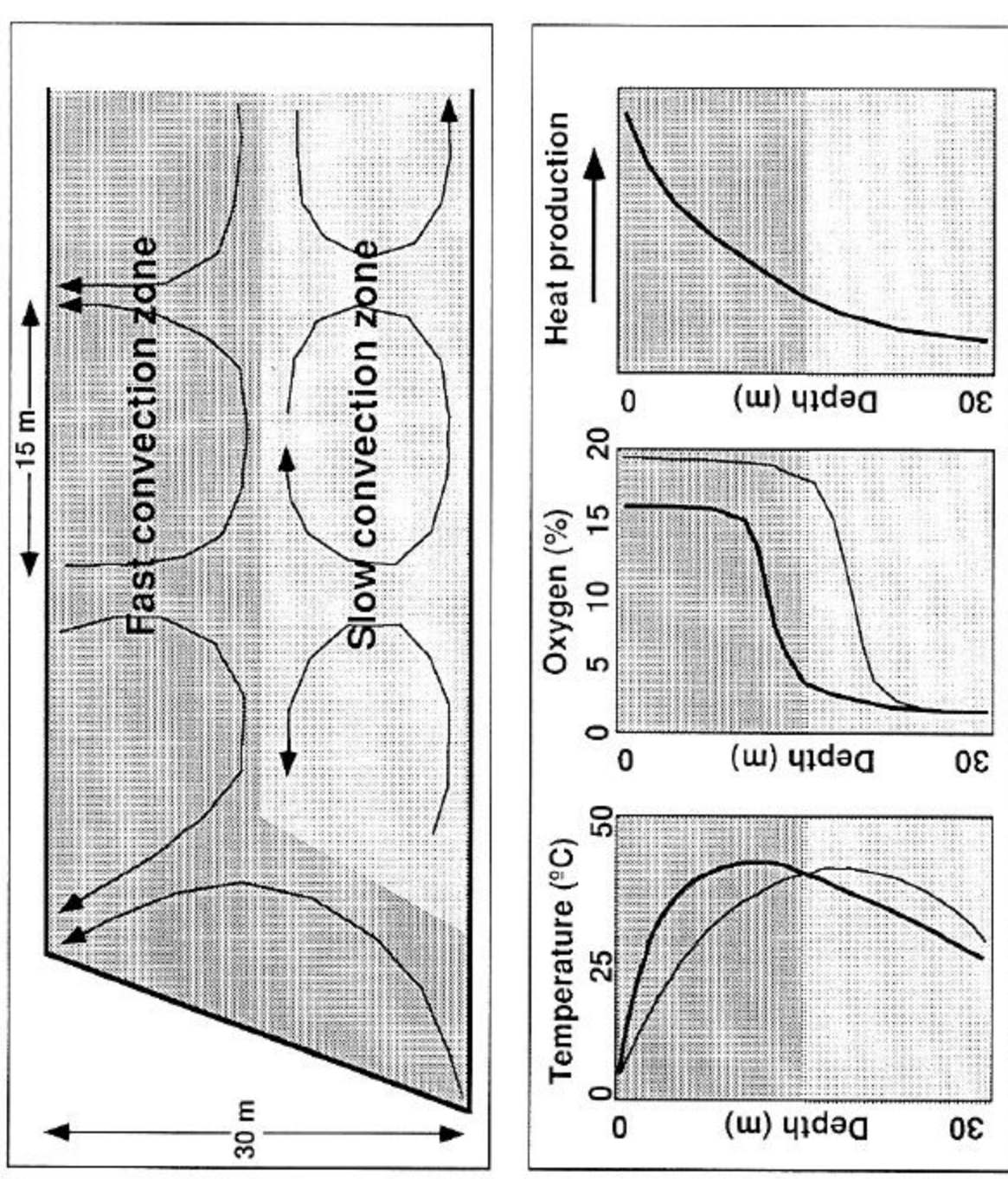


Figure 17. Schematic diagram of air convection patterns.

Appendices

A - Fourier analysis of cyclic temperature changes

We wish to represent the seasonal cyclic temperature changes with time, recorded at different depths within the waste rock dump, as a sinusoidal variation with a one year period superposed on a linearly trending average temperature. This type of representation is chosen because the temperature data shows a generally declining trend. However, the observation period (nearly 2 years) is not long enough to be able to extract from the data more than a linear representation of the declining tendency of the average temperature.

The average temperature $T_a(t)$ ($^{\circ}\text{C}$) is then represented as a linear change in time from an original temperature T_0 ($^{\circ}\text{C}$) at time t (day) zero with a slope m ($^{\circ}\text{C}/\text{d}$):

$$T_a = T_0 + m t . \quad (\text{A.1})$$

The cyclic temperature variation with time $\Delta T(t)$ may be expressed as the first harmonic of the Fourier series representing this variation (Davis, 1973; Burden and Faires, 1989):

$$\Delta T(t) = a \cos \frac{2\pi t}{T} + b \sin \frac{2\pi t}{T} = a C + b S , \quad (\text{A.2})$$

where,	t :	time (days),	a :	cosine coefficient,
	b :	sine coefficient,	t :	variation period (365 days),
	C :	$\cos(2\pi t/T)$,	S :	$\sin(2\pi t/T)$.

The change in temperature with time $T(t)$ will then be the sum of the contributions of the linear trend $T_a(t)$ added to the cyclic trend $\Delta T(t)$:

$$T(t) = T_a(t) + \Delta T(t) = T_0 + m t + a C + b S . \quad (\text{A.3})$$

The four parameters T_0 , m , a and b defining the change in temperature with time may be computed from the temperature measurements as a function of time at different depths. The method of least squares is used to determine the parameters which allow the best description of the observed temperature (n values) as equation A.3.

The least squares method minimizes the square of the error between the estimated temperature $\mathbf{T}(t)$ using A.3 and the measured values \mathbf{T}_i . The square of the error is a function of the parameters T_0 , m , a and b :

$$f(T_0, m, a, b) = \sum_{i=1}^n [T_i - (T_0 + mt_i + aC_i + bS_i)]^2 . \quad (\text{A.4})$$

We have to find the values of these parameters which will minimize function A.4. These correspond to the values for which the derivatives of function A.4 with respect to T_0 , m , a and b are zero:

$$\frac{\partial f}{\partial T_0} = 2 \sum_{i=1}^n [b_i - T_0 - mt_i - aC_i - bS_i] = 0 \quad (\text{A.5a})$$

$$\frac{\partial f}{\partial m} = 2 \sum_{i=1}^n [b_i - T_0 - mt_i - aC_i - bS_i] = 0 \quad (\text{A.5b})$$

$$\frac{\partial f}{\partial a} = 2 \sum_{i=1}^n [b_i - T_0 - mt_i - aC_i - bS_i] = 0 \quad (\text{A.5c})$$

$$\frac{\partial f}{\partial b} = 2 \sum_{i=1}^n [b_i - T_0 - mt_i - aC_i - bS_i] = 0 \quad (\text{A.5d})$$

The equation system A.5 becomes (the notation is simplified by replacing $\sum_{i=1}^n$ simply by ?):

$$-T_i = nT_0 + m?t_i + a?C_i + b?S_i . \quad (\text{A.6a})$$

$$?T_i t_i = nT_0 + m?t_i^2 + a?C_i t_i + b?S_i t_i . \quad (\text{A.6b})$$

$$?T_i C_i = T_0?C_i + m?C_i t_i + a?C_i^2 + b?S_i C_i . \quad (\text{A.6c})$$

$$?T_i S_i = T_0?S_i + m?S_i t_i + a?C_i S_i + b?S_i^2 . \quad (\text{A.6d})$$

The equation system A.6 may be expressed in a matrix form:

$$\begin{bmatrix} n & -t_i & -C_i & -S_i \\ -t_i & -t_i^2 & -C_i t_i & -S_i t_i \\ -C_i & -C_i t_i & -C_i^2 & -C_i S_i \\ -S_i & -S_i t_i & -S_i C_i & -S_i^2 \end{bmatrix} \begin{bmatrix} T_0 \\ m \\ a \\ b \end{bmatrix} = \begin{bmatrix} -T_i \\ -T_i t_i \\ -T_i C_i \\ -T_i S_i \end{bmatrix} \quad (\text{A.7})$$

If matrix $[A]$ is defined as follows:

$$[\mathbf{A}] = \begin{bmatrix} n & -t_i & -C_i & -S_i \\ -t_i & -t_{i^2} & -C_i t_i & -S_i t_i \\ -C_i & -C_i t_i & -C_{i^2} & -C_i S_i \\ -S_i & -S_i t_i & -S_i C_i & -S_{i^2} \end{bmatrix}, \quad (\text{A.8})$$

the solution required (coefficients \mathbf{T}_o , \mathbf{m} , \mathbf{a} and \mathbf{b}) is found by inverting matrix $[\mathbf{A}]$:

$$\begin{bmatrix} T_o \\ m \\ a \\ b \end{bmatrix} = [\mathbf{A}]^{-1} \begin{bmatrix} ?T_i \\ \hat{e} ?T_i t_i \\ \hat{e} ?T_i C_i \\ \hat{e} ?T_i S_i \end{bmatrix} \quad (\text{A.9})$$

Once coefficients \mathbf{T}_o , \mathbf{m} , \mathbf{a} and \mathbf{b} are determined, cyclic variations may be expressed in terms of the amplitude \mathbf{A} and phase \mathbf{P} of a sinusoidal wave using the transformation:

$$DT(t) = a \cos x + b \sin x = T_o \sin(x - P), \quad (\text{A.10})$$

where,

$$A = \sqrt{a^2 + b^2} \quad \text{and} \quad \tan P = -\frac{a}{b}. \quad (\text{A.11})$$

Relationship A.11 always holds. If we limit angle P in the close-ended interval of $[-\pi/2, \pi/2]$, there is only one angle P $[-\pi/2, \pi/2]$ corresponding to each value of $-\pi/2$. The angle $P+2\pi$ desired for plotting against time can be obtained by $P+n$, where $n=0, 1$ or 2 and is easily determined as the value that makes each successive depth show the smallest, positive increase in the phase shift $P+2\pi$ from the previous depth. Also, for plotting purposes, a multiple of 2π may be added to the positive phase angle if that angle is lower than the one calculated for the preceding depth. This rule is relatively straight forward to apply to the shallow depths where measurements are made close to one another but it becomes more arbitrary when applied to deeper measurements. In any case, the original phase value may be determined by removing a multiple of 2π from the compiled phase estimate.

a	b	P
+	+	P = - atan(a/b)

+	0	$P = p/2$
-	0	$P = -p/2 \text{ or } 3p/2$
-	-	$P = -(\tan(a/b) + p)$
+	-	$P = -(\tan(a/b) - p)$
-	+	$P = -\tan(a/b)$

In order to be able to judge how well the model applies to the data, statistical parameters have to be derived. The statistical parameter which conveys best this information is the determination coefficient R^2 (also termed goodness of fit) (Davis, 1973): it is the ratio between the variation explained by the regression model over the total variation in the data. For N measured T_i and estimated $T_i(T_0, m, a, b, t_i)$ (simply noted T_i^*) temperature values, the total variation is obtained from the total sum of squares **SST** whereas the variation explained by the regression model is derived from the regression sum of squares **SSR**:

$$SST = \sum_{i=1}^n \left[T_i - \frac{\sum_{i=1}^n T_i}{N} \right]^2, \quad (\text{A.12})$$

$$SSR = \sum_{i=1}^n \left[T_i^* - \frac{\sum_{i=1}^n T_i^*}{N} \right]^2. \quad (\text{A.13})$$

So, the determination coefficient is:

$$R^2 = \frac{SSR}{SST} . \quad (\text{A.14})$$

The entire procedure to characterize cyclic temperature variations is implemented in a simple MSQuickBasic program for Macintosh computers. The program could easily be adapted to IBM PC and compatibles since machine-dependent commands are kept to a minimum. A listing of the program is appended next, following tables summarizing the computation results. The program is commented in French but the procedure follows exactly the explanations provided in the text so its use should not be too difficult.

Results of Fourier analysis of cyclic temperature variations

Well #1

Depth (m)	Tinit. °C 1/1/91	Slope (°C/j)	Amplit. (°C)	Phase (rad)	Tavg °C 2/1/92	Tfinal °C 1/1/93	A_o		R^2
							P _o	13.093	
0.3	10.29	-0.0067	11.67	1.84	7.65	5.42	-0.12	0.10	0.92
0.5	11.83	-0.0069	10.90	1.89	9.10	6.80	-0.18	0.15	0.94
1.0	13.82	-0.0062	9.38	1.99	11.35	9.27	-0.33	0.25	0.94
2.0	19.25	-0.0089	6.90	2.20	15.72	12.75	-0.64	0.45	0.94
2.5	21.34	-0.0052	5.89	2.34	19.27	17.53	-0.80	0.60	0.94
3.5	28.69	-0.0144	3.87	2.69	23.00	18.20	-1.22	0.95	0.96
5.5	40.12	-0.0076	1.77	3.69	37.10	34.55	-2.00	1.94	0.98
10.5	45.50	-0.0068	0.44	5.84	42.81	40.54	-3.39	4.10	0.98
15.5	43.95	-0.0070	0.16	6.66	41.16	38.80	-4.40	4.92	0.98
20.5	38.40	-0.0050	0.25	9.46	36.43	34.77	-3.96	7.72	0.94
25.5	25.37	0.0049	0.14	10.63	27.29	28.92	-4.54	8.89	0.98
30.5	16.53	0.0048	0.03	11.00	18.42	20.02	-6.08	9.25	1.00

Well #2

Depth (m)	Tinit. °C 1/1/91	Slope (°C/j)	Amplit. (°C)	Phase (rad)	Tavg °C 2/1/92	Tfinal °C 1/1/93	A_o		R^2
							P _o	12.507	
0.3	9.77	-0.0074	12.39	1.96	6.84	4.37	-0.01	0.07	0.92
0.5	11.49	-0.0079	11.69	2.05	8.36	5.71	-0.07	0.16	0.92
1.0	14.98	-0.0083	10.32	2.32	11.69	8.92	-0.19	0.43	0.92
1.1	15.34	-0.0079	10.15	2.31	12.22	9.59	-0.21	0.42	0.94
1.6	18.82	-0.0082	9.03	2.59	15.58	12.85	-0.33	0.70	0.94
2.6	22.44	-0.0087	8.45	2.83	18.99	16.07	-0.39	0.94	0.96
4.6	24.11	-0.0087	8.14	2.89	20.67	17.76	-0.43	1.00	0.98
9.6	37.54	-0.0091	2.84	3.18	33.92	30.87	-1.48	1.29	0.96
14.6	42.35	-0.0125	0.88	4.30	37.41	33.24	-2.65	2.41	0.94
19.6	40.97	-0.0123	0.32	5.16	36.11	32.01	-3.67	3.27	1.00
29.6	31.18	0.0043	2.23	6.42	32.87	34.30	-1.72	4.54	0.96

Well #3

Depth (m)	Tinit. °C 1/1/91	Slope (°C/j)	Amplit. (°C)	Phase (rad)	Tavg °C 2/1/92	Tfinal °C 1/1/93	A_o		R^2
							P _o	14.913	
0.3	7.01	-0.0080	14.59	1.97	3.86	1.19	-0.02	0.04	0.94
0.5	7.54	-0.0067	13.75	2.05	4.88	2.63	-0.08	0.12	0.94
1.0	8.08	-0.0061	12.34	2.24	5.67	3.63	-0.19	0.30	0.96
1.3	8.03	-0.0051	12.12	2.28	6.00	4.28	-0.21	0.35	0.94
1.8	8.45	-0.0050	10.83	2.44	6.49	4.84	-0.32	0.51	0.96
2.8	8.54	-0.0050	9.66	2.62	6.56	4.90	-0.43	0.69	0.98
4.8	8.53	-0.0039	6.43	2.99	6.99	5.70	-0.84	1.06	1.00
9.8	9.69	0.0012	1.56	3.88	10.17	10.57	-2.26	1.95	0.96
14.8	11.37	0.0034	1.10	2.44	12.70	13.83	-2.61	0.51	0.90
19.8	14.27	-0.0009	0.84	3.91	13.92	13.63	-2.88	1.98	0.94
29.8	12.69	0.0012	0.11	6.55	13.15	13.54	-4.91	4.62	0.94

Results of Fourier analysis (continued)

Well #4

Depth (m)	Tinit. °C 1/1/91	Slope (°C/l)	Amplit. (°C)	Phase (rad)	Tavg °C 2/1/92	Tfinal °C 1/1/93	A_o	P_o
							In (A/A _o)	ΔP
0.3	13.91	-0.0125	11.67	1.93	8.95	4.77	-0.04	0.08
0.5	17.20	-0.0160	10.93	2.00	10.88	5.56	-0.11	0.14
1.0	24.85	-0.0219	9.05	2.17	16.19	8.88	-0.30	0.31
1.6	28.56	-0.0237	8.97	2.29	19.19	11.28	-0.31	0.44
2.1	34.30	-0.0276	7.79	2.46	23.39	14.19	-0.45	0.60
3.1	44.29	-0.0341	6.06	2.75	30.78	19.38	-0.70	0.89
5.1	50.86	-0.0279	4.14	3.12	39.82	30.50	-1.08	1.26
10.1	51.91	-0.0133	1.68	4.85	46.63	42.18	-1.98	3.00
15.1	49.75	-0.0169	0.43	6.03	43.07	37.44	-3.34	4.17
20.1	45.36	-0.0066	0.39	5.89	42.77	40.58	-3.44	4.04
30.1	34.43	-0.0018	0.52	5.99	35.16	35.77	-3.15	4.14

Well #5

Depth (m)	Tinit. °C 1/1/91	Slope (°C/l)	Amplit. (°C)	Phase (rad)	Tavg °C 2/1/92	Tfinal °C 1/1/93	A_o	P_o
							In (A/A _o)	ΔP
0.3	9.06	-0.0060	12.64	1.92	6.68	4.67	-0.06	0.10
0.5	10.79	-0.0065	11.81	1.98	8.23	6.07	-0.13	0.16
1.0	13.28	-0.0055	10.06	2.10	11.11	9.29	-0.29	0.28
1.5	15.88	-0.0072	9.87	2.26	13.03	10.62	-0.31	0.44
2.0	19.89	-0.0107	8.43	2.41	15.67	12.11	-0.47	0.59
3.0	26.17	-0.0135	6.44	2.71	20.83	16.32	-0.73	0.89
5.0	35.14	-0.0162	3.32	3.40	28.73	23.32	-1.40	1.58
10.0	40.70	-0.0065	1.06	4.96	38.14	35.98	-2.54	3.14
15.0	47.81	-0.0053	0.69	6.36	45.69	43.91	-2.97	4.53
17.8	49.03	-0.0065	0.33	7.20	46.45	44.28	-3.71	5.38

Well #6

Depth (m)	Tinit. °C 1/1/91	Slope (°C/l)	Amplit. (°C)	Phase (rad)	Tavg °C 2/1/92	Tfinal °C 1/1/93	A_o	P_o
							In (A/A _o)	ΔP
0.3	13.00	-0.0075	13.23	1.90	10.02	7.51	-0.16	0.01
0.5	15.86	-0.0081	12.63	1.94	12.65	9.95	-0.20	0.04
1.0	21.48	-0.0072	10.97	2.01	18.61	16.20	-0.34	0.11
1.3	28.04	-0.0097	10.21	2.03	24.19	20.95	-0.41	0.14
1.8	34.69	-0.0113	8.38	2.10	30.23	26.47	-0.61	0.20
2.8	46.08	-0.0126	5.31	2.14	41.08	36.87	-1.07	0.25
4.8	62.43	-0.0153	0.87	2.41	56.37	51.26	-2.88	0.52
14.8	67.33	-0.0130	0.72	0.77	62.17	57.82	-3.07	5.15
19.8	65.68	-0.0084	0.33	5.45	62.35	59.55	-3.85	3.56
29.8	44.12	0.0010	0.16	11.12	44.52	44.86	-4.57	9.22

Microsoft QuickBASIC Listing 01/06/93

Page 1

Source File: fourier2.bas

Program Unit: MAIN

Entry: 00000022

```
00001 REM Programme pour l'analyse de Fourier des données de température.
00002 REM Détermine l'amplitude et la phase de variations sinusoïdales,
00003 REM en plus de décrire la tendance linéaire superposée à ces variations.
00004 REM
00005 REM ****
00006 REM
00007 REM Programme par: René Lefebvre.
00008 REM Crédit: Janvier 1993.
00009 REM Modifications: Description de la tendance linéaire des données
00010 REM par rapport au programme initial FOURIER.BAS.
00011 REM
00012 REM Les données sont lues à partir d'un fichier texte (ASCII) et les
00013 REM résultats sont inscrits dans un autre fichier texte.
00014 REM
00015 REM Le programme fait les calculs pour une seule série de données de
00016 REM temps et de température à la fois. À la fin des calculs pour une
00017 REM série de données, le programme permet d'ouvrir un autre fichier de
00018 REM données si besoin est.
00019 REM
00020 REM Le format du fichier de données est le suivant. Chaque donnée est
00021 REM séparée des autres par une virgule ou un changement de ligne:
00022 REM
00023 REM 1) Nom du puits: PUIT$%
00024 REM
00025 REM 2) Profondeur, Nombre de points de mesure: PROF$,NPT
00026 REM
00027 REM 3) Jour, Température (NPT lignes): JOUR(NPT),T(NPT)
00028 REM
00029 REM ****
00030 REM
00031 REM *** Déclarations:
00032 REM
00033 DEFDBL A-H, O-Z
00034 DEFINT I-N
00035 REM
00036 DIM STATIC JOUR(200),T(200),A(4,4),B(4),STAT(200,2)
00037 REM
00038 REM *** Valeur considérée comme zéro pour l'inversion de matrice:
00039 ZERO = .000001
00040 REM *** Fréquence angulaire (2*pi/Période):
00041 PI = 3.141592654#
00042 F = 2!*PI/365.25
00043 REM
00044 REM *** Sélection des fichiers d'entrée et de sortie:
00045 REM
00046 DEBUT:
00047 CLS
00048 PRINT "Sélectionner le fichier de données à ouvrir."
00049 FINP$ = FILES$(1)
00050 CLS
00051 PRINT "Donner le nom du nouveau fichier de sortie à créer."
00052 FOUT$ = FILES$(0)
00053 CLS
00054 PRINT
00055 PRINT "Le fichier d'entrée est: ",FINP$
```

Source File: fourier2.bas

```
00056 PRINT
00057 PRINT "Le fichier de sortie est: ",FOUT$
00058 PRINT
00059 PRINT
00060 REM *** Ouverture des fichiers d'entrée et de sortie:
00061 REM
00062 OPEN FINP$ FOR INPUT AS #1
00063 OPEN FOUT$ FOR OUTPUT AS #6
00064 REM
00065 REM *** Lecture des données:
00066 REM
00067 PRINT "Lecture des données ... "
00068 REM
00069 INPUT #1,PUITS$
00070 INPUT #1,PROF$,NPT
00071 FOR NL=1 TO NPT
00072     INPUT #1,JOUR(NL),T(NL)
00073 NEXT NL
00074 REM
00075 REM *** Fermeture du fichier de données
00076 REM
00077 CLOSE #1
00078 REM
00079 REM *** Calcul des paramètres:
00080 REM
00081 PRINT "Calcul des paramètres ... "
00082 REM
00083 REM *** Calcul des valeurs des éléments des matrices A et B ***
00084 REM
00085 REM *** Somme des cosinus, sinus, temps (jours) et températures:
00086 SJOUR=0!
00087 SCOS=0!
00088 SSIN=0!
00089 SJOUR2=0!
00090 SCOS2=0!
00091 SSIN2=0!
00092 SCJ=0!
00093 SSJ=0!
00094 SCS=0!
00095 ST=0!
00096 STJ=0!
00097 STC=0!
00098 STS=0!
00099 FOR NL=1 TO NPT
00100     SJOUR=SJOUR+JOUR(NL)
00101     SCOS=SCOS+COS(F*JOUR(NL))
00102     SSIN=SSIN+SIN(F*JOUR(NL))
00103     SJOUR2=SJOUR2+JOUR(NL)^2
00104     SCOS2=SCOS2+(COS(F*JOUR(NL)))^2
00105     SSIN2=SSIN2+(SIN(F*JOUR(NL)))^2
00106     SCJ=SCJ+COS(F*JOUR(NL))*JOUR(NL)
00107     SSJ=SSJ+SIN(F*JOUR(NL))*JOUR(NL)
00108     SCS=SCS+COS(F*JOUR(NL))*SIN(F*JOUR(NL))
00109     ST=ST+T(NL)
00110     STJ=STJ+T(NL)*JOUR(NL)
00111     STC=STC+T(NL)*COS(F*JOUR(NL))
00112     STS=STS+T(NL)*SIN(F*JOUR(NL))
00113 NEXT NL
```

Source File: fourier2.bas

```
00114 REM
00115 REM *** Assignment des valeurs des éléments des matrices A et B:
00116 A(1,1)=NPT
00117 A(1,2)=SJOUR
00118 A(1,3)=SCOS
00119 A(1,4)=SSIN
00120 A(2,1)=SJOUR
00121 A(2,2)=SJOUR2
00122 A(2,3)=SCJ
00123 A(2,4)=SSJ
00124 A(3,1)=SCOS
00125 A(3,2)=SCJ
00126 A(3,3)=SCOS2
00127 A(3,4)=SCS
00128 A(4,1)=SSIN
00129 A(4,2)=SSJ
00130 A(4,3)=SCS
00131 A(4,4)=SSIN2
00132 B(1)=ST
00133 B(2)=STJ
00134 B(3)=STC
00135 B(4)=STS
00136 REM
00137 REM *** Solution du système d'équations linéaires (Davis, 1973, p.144):
00138 REM
00139 PRINT "Solution du système d'équations linéaires ... "
00140 REM
00141 FOR I=1 TO 4
00142     DIV=A(I,I)
00143     IF ABS(DIV) < ZERO GOTO FIN
00144     FOR J=1 TO 4
00145         A(I,J)=A(I,J)/DIV
00146     NEXT J
00147     B(I)=B(I)/DIV
00148     FOR J=1 TO 4
00149         IF I=J GOTO SUITE
00150         RATIO=A(J,I)
00151         FOR K=1 TO 4
00152             A(J,K)=A(J,K)-RATIO*A(I,K)
00153         NEXT K
00154         B(J)=B(J)-RATIO*B(I)
00155 SUITE:
00156     NEXT J
00157 NEXT I
00158 REM
00159 REM *** Calcul de la tendance linéaire et de la sinusoide:
00160 REM
00161 TZERO=B(1)
00162 PENTE=B(2)
00163 ALPHA=B(3)
00164 BETA=B(4)
00165 AMPL=SQR(ALPHA^2+BETA^2)
00166 PHASE=ATN(-ALPHA/BETA)
00167 REM
00168 REM *** Analyse statistique de la régression ***
00169 REM
00170 PRINT
00171 PRINT "Analyse statistique ..."
```

Source File: fourier2.bas

```

00172 REM
00173 REM *** Calcul des valeurs de température prédictes et des écarts:
00174 REM
00175 FOR I=1 TO NPT
00176     STAT(I,1)=TZERO+PENTE*JOUR(I)+ALPHA*COS(F*JOUR(I))+BETA*SIN(F*JOUR(I))
00177     STAT(I,2)=T(I)-STAT(I,1)
00178 NEXT I
00179 REM
00180 REM *** Calcul des mesures d'erreur (Davis, 1973, chap.5, progr.5.5):
00181 REM
00182 SY=0!
00183 SY2=0!
00184 SYC=0!
00185 SYC2=0!
00186 FOR I=1 TO NPT
00187 REM Somme des températures mesurées et de leur carrés
00188     SY=SY+T(I)
00189     SY2=SY2+T(I)*T(I)
00190 REM Somme des températures calculées et de leur carrés
00191     SYC=SYC+STAT(I,1)
00192     SYC2=SYC2+STAT(I,1)*STAT(I,1)
00193 NEXT I
00194 REM
00195 REM *** Paramètres statistiques:
00196 REM
00197 REM Somme totale des carrés:
00198 SST = SY2-SY*SY/CDBL(NPT)
00199 REM Somme des carrés due à la régression:
00200 SSR=SYC2-SYC*SYC/CDBL(NPT)
00201 REM Somme des carrés due à la déviation:
00202 SSD=SST-SSR
00203 REM Variance ("Goodness of fit")
00204 R2=SSR/SST
00205 REM Coefficient de corrélation
00206 R=SQR(R2)
00207 REM ***Impression des résultats:
00208 REM
00209 PRINT
00210 PRINT "Impression des résultats ..."
00211 REM
00212 PRINT #6,"PROGRAMME FOURIER: Variations cycliques de température.
00213 PRINT #6,
00214 PRINT #6,"Par René Lefebvre - Version Janvier 93.
00215 PRINT #6,
00216 PRINT #6,"Données de température du puits ";PUITS$;"."
00217 PRINT #6,
00218 PRINT #6,"Mesures à la profondeur de ";PROF$;" m."
00219 PRINT #6,
00220 PRINT #6,"Nombre de mesures ";NPT;"."
00221 PRINT #6,"Température au temps zéro ";
00222 PRINT #6,USING "#.#";TZERO;
00223 PRINT #6," °C."
00224 PRINT #6,"Pente de la tendance linéaire ";
00225 PRINT #6,USING "#.#####";PENTE;
00226 PRINT #6," °C/jour."
00227 PRINT #6,"L'amplitude des variations est de ";
00228 PRINT #6,USING "#.##";AMPL;
00229 PRINT #6," °C."

```

Source File: fourier2.bas

```

00230 PRINT #6,"La phase est de ";
00231 PRINT #6,USING "##.##";PHASE;
00232 PRINT #6," radian."
00233 PRINT #6,"Alpha = ";
00234 PRINT #6,USING "###.##";ALPHA;
00235 PRINT #6," et Beta = ";
00236 PRINT #6,USING "###.##";BETA;
00237 PRINT #6," ."
00238 PRINT #6,
00239 QUOI:
00240 INPUT "Impression des résultats complémentaires ? (oui:O, non:N)";OKC$
00241 IF OKC$ = "N" GOTO STAT
00242 IF OKC$ <> "O" THEN
00243     PRINT
00244     PRINT "Pardon? ... Entrez O pour oui et N pour non !"
00245     PRINT
00246     GOTO QUIT
00247 END IF
00248 PRINT #6,"Résultats complémentaires: "
00249 PRINT #6,"Somme des jours: ";
00250 PRINT #6,USING "##.##^##";SJOUR
00251 PRINT #6,"Somme des cosinus: ";
00252 PRINT #6,USING "##.##";SCOS
00253 PRINT #6,"Somme des sinus: ";
00254 PRINT #6,USING "##.##";SSIN
00255 PRINT #6,"Somme des jours au carré: ";
00256 PRINT #6,USING "##.##^##";SJOUR2
00257 PRINT #6,"Somme des cosinus au carré: ";
00258 PRINT #6,USING "##.##";SCOS2
00259 PRINT #6,"Somme des sinus au carré: ";
00260 PRINT #6,USING "##.##";SSIN2
00261 PRINT #6,"Somme des produits des jours et des cosinus: ";
00262 PRINT #6,USING "##.##^##";SCJ
00263 PRINT #6,"Somme des produits des jours et des sinus: ";
00264 PRINT #6,USING "##.##^##";SSJ
00265 PRINT #6,"Somme des produits des sinus et des cosinus: ";
00266 PRINT #6,USING "##.##";SCS
00267 PRINT #6,"Somme des températures: ";
00268 PRINT #6,USING "####.##";ST
00269 PRINT #6,"Somme des produits des températures et des jours: ";
00270 PRINT #6,USING "##.##^##";STJ
00271 PRINT #6,"Somme des produits des températures et des cosinus: ";
00272 PRINT #6,USING "####.##";STC
00273 PRINT #6,"Somme des produits des températures et des sinus: ";
00274 PRINT #6,USING "####.##";STS
00275 PRINT #6,
00276 STAT:
00277 SCUSEZ:
00278 INPUT "Impression des paramètres statistiques ? (oui:O, non:N)";OKS$
00279 IF OKS$ = "N" GOTO COEF
00280 IF OKS$ <> "O" THEN
00281     PRINT
00282     PRINT "Pardon? ... Entrez O pour oui et N pour non !"
00283     PRINT
00284     GOTO SCUSEZ
00285 END IF
00286 PRINT #6,"Paramètres statistiques: "
00287 PRINT #6,"Somme totale des carrés: ";

```

Source File: fourier2.bas

```
00288 PRINT #6,USING "##.####^^^^";SST
00289 PRINT #6,"Somme des carrés due à la régression: ";
00290 PRINT #6,USING "##.####^^^^";SSR
00291 PRINT #6,"Somme des carrés due à la déviation: ";
00292 PRINT #6,USING "##.####^^^^";SSD
00293 PRINT #6,"Variance (Goodness of fit): ";
00294 PRINT #6,USING "#.##";R2
00295 COEF:
00296 PRINT #6,"Coefficient de corrélation: ";
00297 PRINT #6,USING "#.##";R
00298 FIN:
00299 REM
00300 REM *** Fermeture du fichier de sortie
00301 REM
00302 CLOSE #6
00303 PRINT
00304 PARDON:
00305 INPUT "Voulez-vous ouvrir un autre fichier d'entrée ? (oui:O, non:N)";OK$
00306 IF OK$="O" GOTO DEBUT
00307 IF OK$ <> "N" THEN
00308     PRINT
00309     PRINT "Pardon? ... Entrez O pour oui et N pour non !"
00310     PRINT
00311     GOTO PARDON
00312 END IF
00313 PRINT
00314 PRINT "Fin du programme ..."
00315 REM
00316 END
00317
```

B - Heat transfer with a periodic surface temperature variation

Stallman (1965) presents a solution for heat transfer by conduction and advection in one dimension in a semi-infinite medium subjected to a sinusoidal surface temperature variation. However, Stallman (1965) does not demonstrate his solution and simpler relationships may be derived from his solution to relate thermal conductivity and fluid advection to measured changes in amplitude and phase with depth. Thus, the analytical solution and new relationships are derived here. Heat transfer by conduction and advection are described by the following differential equation:

$$k_t \frac{\partial^2 T}{\partial z^2} - q c_o r_o \frac{\partial T}{\partial z} = c r \frac{\partial T}{\partial t}, \quad (\text{B.1})$$

where: k_t : medium thermal conductivity (solids and water) (W/m °C),

T : temperature (°C), z : depth positive downward (m),

q : fluid flux (m/s), c_o : fluid heat capacity (J/kg°C)

r_o : fluid density (kg/m³), c : medium heat capacity (J/kg°C)

r : medium density (kg/m³), t : time (s).

New variables \mathbf{K} and \mathbf{V} are defined as:

$$K = \frac{pcr}{k_t t} \quad \text{and} \quad V = \frac{qc_o r_o}{2k_t}, \quad (\text{B.2})$$

where \mathbf{t} (s) is the period of the cyclic temperature variation. Differential equation B.1 becomes:

$$\frac{\partial^2 T}{\partial z^2} - 2V \frac{\partial T}{\partial z} = \frac{tK}{p} \frac{\partial T}{\partial t}. \quad (\text{B.3})$$

The following boundary conditions are used. First, the surface ($z=0$) is subjected to a cyclic temperature variation of period \mathbf{t} (s):

$$T_0 = T_{mo} + \Delta T_0 \sin 2\pi t/\mathbf{t}, \quad (\text{B.4})$$

where, T_0 : surface temperature (°C), T_{mo} : mean surface temperature (°C),

ΔT_0 : amplitude of the surface temperature variation.

Second, as depth becomes infinite ($z \rightarrow \infty$), temperature becomes equal to the mean temperature at that level T_{mz} . The solution for the temperature $T(t,z)$ (°C) as a function of time t (s) at a given depth z (cm) is supposed to be of the form:

$$T(t,z) = T_{mz} + \Delta T e^{-az} \sin(2\pi t/T - bz), \quad (\text{B.5})$$

where, T_{mz} : mean temperature ($^{\circ}\text{C}$), t : variation period (s),
 ΔT : temperature variation amplitude ($^{\circ}\text{C}$).

We have to find expressions relating parameters a and b to K and V such that the differential equation B.3 is satisfied when the boundary conditions are applied. We then have to find the first and second derivatives of temperature as a function of depth as well as its time derivative using B.5:

$$\frac{\partial T}{\partial z} = -a\Delta T e^{-az} \sin(2\pi t/T - bz) - b\Delta T e^{-az} \cos(2\pi t/T - bz), \quad (\text{B.6a})$$

$$\begin{aligned} \frac{\partial^2 T}{\partial z^2} &= a^2 \Delta T e^{-az} \sin(2\pi t/T - bz) + 2ab\Delta T e^{-az} \cos(2\pi t/T - bz) \\ &\quad - b^2 \Delta T e^{-az} \sin(2\pi t/T - bz), \end{aligned} \quad (\text{B.6b})$$

$$\frac{\partial T}{\partial t} = 2\pi \Delta T e^{-az} \cos(2\pi t/T - bz), \quad (\text{B.6c})$$

B.6 is substituted in B.3 to get:

$$\begin{aligned} DT e^{-az} [\{ (a^2 - b^2) + 2aV \} \sin(2\pi t/T - bz) + \{ 2ab + 2bV \} \cos(2\pi t/T - bz)] \\ = 2K DT e^{-az} \cos(2\pi t/T - bz), \end{aligned} \quad (\text{B.7})$$

If we apply the first boundary condition B.4, we get the following relationships in order for B.7 to be verified:

$$V = \frac{b^2 - a^2}{2a}, \quad (\text{B.8})$$

and

$$K = ab + bV = ab + b \frac{b^2 - a^2}{2a}. \quad (\text{B.9})$$

Inversely, we can also express parameters a and b in terms of K and V . We first define b from B.8:

$$b^2 = 2aV + a^2 = (a + V)^2 - V^2, \quad (\text{B.10})$$

and

$$a = (b^2 + V^2)^{1/2} - V. \quad (\text{B.11})$$

From B.9 we have another relationship for parameter **a**:

$$\mathbf{a} = \frac{\mathbf{K}}{\mathbf{b}} \cdot \mathbf{V} . \quad (\text{B.12})$$

Equating B.11 and B.12, we get an expression containing only **b**, **K** and **V**:

$$(\mathbf{b}^2 + \mathbf{V}^2)^{1/2} \cdot \mathbf{V} = \frac{\mathbf{K}}{\mathbf{b}} \cdot \mathbf{V} , \quad (\text{B.13})$$

which becomes

$$\mathbf{K}^2 = \mathbf{b}^2(\mathbf{b}^2 + \mathbf{V}^2) = \mathbf{b}^4 + \mathbf{b}^2\mathbf{V}^2 = (\mathbf{b}^2 + \mathbf{V}^2/2)^2 - \mathbf{V}^4/4 , \quad (\text{B.14})$$

and,

$$\boxed{\mathbf{b} = [(\mathbf{K}^2 + \mathbf{V}^4/4)^{1/2} - \mathbf{V}^2/2]^{1/2}} . \quad (\text{B.15})$$

Similarly, to define parameter **a**, we equate the two relationships B.10 and B.9 defining parameter **b** to derive an expression containing only **a**, **K** and **V**:

$$\mathbf{b} = [(\mathbf{a} + \mathbf{V})^2 - \mathbf{V}^2]^{1/2} = \frac{\mathbf{K}}{\mathbf{a} + \mathbf{V}} , \quad (\text{B.16})$$

which becomes

$$\mathbf{K}^2 = (\mathbf{a} + \mathbf{V})^2 [(\mathbf{a} + \mathbf{V})^2 - \mathbf{V}^2] = [(\mathbf{a} + \mathbf{V})^2 - \mathbf{V}^2/2]^2 - \mathbf{V}^4/4 \quad (\text{B.17})$$

and,

$$\boxed{\mathbf{a} = [(\mathbf{K}^2 + \mathbf{V}^4/4)^{1/2} + \mathbf{V}^2/2]^{1/2} - \mathbf{V}} . \quad (\text{B.18})$$

C - Heat transfer by conduction and advection with a heat source

Steady state heat transfer by conduction and advection in a porous medium with heat sources or sinks is described by the following differential equation (in one dimension x):

$$k_t \frac{\partial^2 T}{\partial x^2} - qc_o r_o \frac{\partial T}{\partial x} = -Q(x), \quad (\text{C.1})$$

where: k_t : thermal conductivity (W/m°), Q : heat source (W/m^3),
 T : temperature ($^\circ$), x : distance (m),
 q : fluid flux (m/s), c_o : fluid heat capacity (J/kg°)
 r_o : fluid density (kg/m^3).

The source of heat is provided by pyrite oxidation which implies oxygen consumption. If pyrite oxidation is supposed having first order kinetics with respect to oxygen concentration C_{Ox} (mol/m^3), the rate of oxygen consumption R_{Ox} ($\text{mol/m}^3\text{s}$) will depend on the kinetic constant K_{Ox} (s^{-1}):

$$R_{\text{Ox}}(x) = K_{\text{Ox}} C_{\text{Ox}}(x) . \quad (\text{C.2})$$

In order for the system to remain in a steady state, oxygen has to be supplied by some means. Even though we know that advection is a major mechanism providing oxygen, we will suppose in this model that all oxygen is supplied by diffusion from the surface. This is equivalent to saying that heat production exponentially declines from the surface, which is a reasonable supposition even if advection is important. Oxygen concentration in a system subjected to a first order reaction is given by:

$$C_{\text{Ox}}(x) = C_o e^{-x\sqrt{K_{\text{Ox}}/D_e}} , \quad (\text{C.3})$$

where D_e (m^2/s) is the effective diffusion coefficient and C_o (mol/m^3) is the oxygen concentration at the surface. Since 3,5 moles of oxygen are consumed per mole of pyrite oxidized which releases 1,41 MJ of heat, there is a factor F of 0,4 MJ/mol of heat released per mole of oxygen consumed. The heat source term may be written as:

$$Q(x) = F K_{\text{Ox}} C_o e^{-x\sqrt{K_{\text{Ox}}/D_e}} . \quad (\text{C.4})$$

We then have the following differential equation to solve:

$$\frac{\frac{d^2T}{dx^2}}{k_x} - A \frac{dT}{dx} = -Be^{-Ex}, \quad (C.5)$$

where,

$$A = \frac{qc_o R_o}{k_t} \quad B = \frac{FC_o K_{ox}}{k_t} \quad E = \sqrt{\frac{K_{ox}}{D_e}}.$$

The characteristic equation of the homogeneous part of C.5 has two real roots and its general solution is of the form:

$$T_h = C_1 e^{Ax} + C_2, \quad (C.6)$$

where C_1 and C_2 are constants. If we suppose an exponential form ($T_p = Ke^{-Ex}$) for the solution of the non homogeneous term, we obtain the value of K after substitution of the derivatives in the homogeneous term:

$$T_p = \frac{-B}{E^2 + AE} e^{-Ex}. \quad (C.7)$$

The general solution is obtained from the sum of solutions C.6 and C.7:

$$T = \frac{-B}{E^2 + AE} e^{-Ex} + C_1 e^{Ax} + C_2. \quad (C.8)$$

Constants C_1 and C_2 are found by applying the following boundary conditions:

- 1) $T(0) = T_m$: the temperature at the surface is equal to the mean surface temperature.
- 2) $\frac{dT}{dx}(b) = T_b$: the temperature gradient at the base (at depth b) is constant.

The solution for temperature is then:

$$T(x) - T_m = \frac{\frac{T'b}{e^{Ab}} - \frac{B}{EA+A^2} e^{-(E+A)b}}{(e^{Ax}-1) + \frac{B}{E^2+AE} (1-e^{-Ex})} \quad (C.9)$$

Once an analytical expression is available to describe the temperature distribution, the heat flux can be derived. The total heat flux is the sum of the conductive (equation 4) and convective (equation 9) components. The model was applied to all temperature monitoring wells and the results are compiled next as tables and figures.

Conduction and advection model - Well #1

Effective diffusion coefficient	De	10.1	m ² /j
Oxygen concentration at the surface	Co	9.38	mol/m ³
Thermal conductivity	Kt	217728	J/j m °C
Kinetic constant (Oxygen combustion)	Kox	0.03	1/j
Gas flux	v	-5	m/j
Air volumetric heat capacity	Cv	5000	J/m ³ °C
Temperature gradient at the dump's base	T	-1.1	°C/m
Dump thickness	B	31	m
Average dump surface temperature	Tm	5	°C
Conversion factor	F	402629	J/mol
Constant A	CA	-0.11	v•Cv/Kt
Constant E	CE	0.055	√(Kox/De)
Constant M	CM	-150.76	
Constant N	CN	-158.29	
Constant B	CB	0.52	F Co Kox/Kt

x	Tx	q (W/m)	Q (W/m ³)
0	5.0	-23.33	1.31
1	13.0	-22.06	1.24
2	19.6	-20.85	1.18
3	25.1	-19.70	1.11
4	29.5	-18.62	1.05
5	33.1	-17.59	1.00
6	35.9	-16.62	0.95
7	38.1	-15.70	0.90
8	39.7	-14.83	0.85
9	40.8	-14.00	0.80
10	41.4	-13.22	0.76
11	41.8	-12.48	0.72
12	41.8	-11.78	0.68
13	41.5	-11.12	0.65
14	41.1	-10.49	0.61
15	40.4	-9.89	0.58
16	39.6	-9.33	0.55
17	38.7	-8.80	0.52
18	37.7	-8.29	0.49
19	36.7	-7.81	0.47
20	35.5	-7.36	0.44
21	34.3	-6.93	0.42
22	33.1	-6.52	0.40
23	31.9	-6.14	0.37
24	30.7	-5.78	0.35
25	29.5	-5.43	0.34
26	28.2	-5.10	0.32
27	27.0	-4.79	0.30
28	25.8	-4.50	0.29
29	24.7	-4.22	0.27
30	23.5	-3.96	0.26
31	22.4	-3.71	0.24
Q _t (W/m ²)			19.6

Conduction and advection model - Well #2

Effective diffusion coefficient	De	5	m ² /j
Oxygen concentration at the surface	Co	9.38	mol/m ³
Thermal conductivity	Kt	217728	J/j m °C
Kinetic constant (Oxygen combustion)	Kox	0.03	1/j
Gas flux	v	1	m/j
Air volumetric heat capacity	Cv	5000	J/m ³ °C
Temperature gradient at the dump's base	T	-1.1	°C/m
Dump thickness	B	31	m
Average dump surface temperature	Tm	5	°C
Conversion factor	F	402629	J/mol
Constant A	CA	0.02	v•Cv/Kt
Constant E	CE	0.077	√(Kox/De)
Constant M	CM	-33.54	
Constant N	CN	66.90	
Constant B	CB	0.52	F Co Kox/Kt

x	Tx	q (W/m)	Q (W/m ³)
0	5.0	-10.83	1.31
1	9.2	-9.57	1.21
2	13.0	-8.40	1.12
3	16.5	-7.32	1.04
4	19.6	-6.32	0.96
5	22.4	-5.39	0.89
6	24.9	-4.53	0.82
7	27.2	-3.74	0.76
8	29.1	-3.01	0.71
9	30.9	-2.33	0.65
10	32.4	-1.70	0.60
11	33.7	-1.12	0.56
12	34.8	-0.58	0.52
13	35.8	-0.08	0.48
14	36.6	0.38	0.44
15	37.2	0.80	0.41
16	37.6	1.20	0.38
17	38.0	1.56	0.35
18	38.1	1.90	0.33
19	38.2	2.22	0.30
20	38.1	2.51	0.28
21	38.0	2.77	0.26
22	37.7	3.02	0.24
23	37.3	3.25	0.22
24	36.8	3.46	0.20
25	36.2	3.66	0.19
26	35.6	3.84	0.18
27	34.8	4.01	0.16
28	34.0	4.17	0.15
29	33.1	4.31	0.14
30	32.1	4.44	0.13
31	31.0	4.57	0.12
Qt (W/m ²)			15.4

Conduction and advection model - Well #3

Effective diffusion coefficient	De	1	m ² /j
Oxygen concentration at the surface	Co	9.38	mol/m ³
Thermal conductivity	Kt	217728	J/j m °C
Kinetic constant (Oxygen combustion)	Kox	0.03	1/j
Gas flux	v	7	m/j
Air volumetric heat capacity	Cv	5000	J/m ³ °C
Temperature gradient at the dump's base	T	-0.1	°C/m
Dump thickness	B	31	m
Average dump surface temperature	Tm	5	°C
Conversion factor	F	402629	J/mol
Constant A	CA	0.16	v·Cv/Kt
Constant E	CE	0.173	✓(Kox/De)
Constant M	CM	0.00	
Constant N	CN	9.00	
Constant B	CB	0.52	F Co Kox/Kt

x	Tx	q (W/m)	Q (W/m ³)
0	5.0	-1.90	1.31
1	6.4	-0.70	1.10
2	7.6	0.32	0.93
3	8.6	1.17	0.78
4	9.5	1.88	0.66
5	10.2	2.49	0.55
6	10.8	2.99	0.46
7	11.3	3.42	0.39
8	11.7	3.78	0.33
9	12.1	4.08	0.28
10	12.4	4.33	0.23
11	12.6	4.55	0.20
12	12.8	4.72	0.16
13	13.0	4.88	0.14
14	13.2	5.00	0.12
15	13.3	5.11	0.10
16	13.4	5.20	0.08
17	13.5	5.27	0.07
18	13.5	5.34	0.06
19	13.6	5.39	0.05
20	13.6	5.43	0.04
21	13.6	5.47	0.03
22	13.6	5.50	0.03
23	13.6	5.53	0.02
24	13.6	5.55	0.02
25	13.6	5.57	0.02
26	13.6	5.59	0.01
27	13.6	5.60	0.01
28	13.5	5.61	0.01
29	13.5	5.62	0.01
30	13.4	5.63	0.01
31	13.3	5.64	0.01

G1 (W/m²)

75

Conduction and advection model - Well #4

Effective diffusion coefficient	De	8.5	m ² /j
Oxygen concentration at the surface	Co	9.38	mol/m ³
Thermal conductivity	Kt	217728	J/j m °C
Kinetic constant (Oxygen combustion)	Kox	0.03	1/j
Gas flux	v	-4.05	m/j
Air volumetric heat capacity	Cv	5000	J/m ³ °C
Temperature gradient at the dump's base	T	-1.1	°C/m
Dump thickness	B	31	m
Average dump surface temperature	Tm	5	°C
Conversion factor	F	402629	J/mol
Constant A	CA	-0.09	v*Cv/Kt
Constant E	CE	0.059	✓(Kox/De)
Constant M	CM	-260.51	
Constant N	CN	-260.71	
Constant B	CB	0.52	F Co Kox/Kt

x	Tx	q (W/m)	Q (W/m ³)
0	5.0	-23.20	1.31
1	13.1	-21.92	1.24
2	20.0	-20.72	1.16
3	25.9	-19.59	1.10
4	30.8	-18.53	1.03
5	34.9	-17.52	0.97
6	38.2	-16.58	0.92
7	41.0	-15.69	0.87
8	43.1	-14.85	0.82
9	44.7	-14.06	0.77
10	45.9	-13.31	0.72
11	46.8	-12.61	0.68
12	47.3	-11.94	0.64
13	47.5	-11.32	0.61
14	47.4	-10.73	0.57
15	47.2	-10.18	0.54
16	46.7	-9.66	0.51
17	46.2	-9.16	0.48
18	45.4	-8.70	0.45
19	44.6	-8.26	0.42
20	43.7	-7.85	0.40
21	42.7	-7.46	0.38
22	41.7	-7.10	0.35
23	40.6	-6.75	0.33
24	39.5	-6.43	0.32
25	38.4	-6.12	0.30
26	37.2	-5.83	0.28
27	36.1	-5.56	0.26
28	34.9	-5.31	0.25
29	33.8	-5.07	0.23
30	32.7	-4.84	0.22
31	31.6	-4.62	0.21
Q1 (W/m ²)			18.6

Conduction and advection model - Well #5

Effective diffusion coefficient	De	7	m ² /j
Oxygen concentration at the surface	Co	9.38	mol/m ³
Thermal conductivity	Kt	217728	J/j m °C
Kinetic constant (Oxygen combustion)	Kox	0.03	1/j
Gas flux	v	1	m/j
Air volumetric heat capacity	Cv	5000	J/m ³ °C
Temperature gradient at the dump's base	T	-1.1	°C/m
Dump thickness	B	31	m
Average dump surface temperature	Tm	5	°C
Conversion factor	F	402629	J/mol
Constant A	CA	0.02	v•Cv/Kt
Constant E	CE	0.065	√(Kox/De)
Constant M	CM	-40.03	
Constant N	CN	89.89	
Constant B	CB	0.52	F Co Kox/Kt

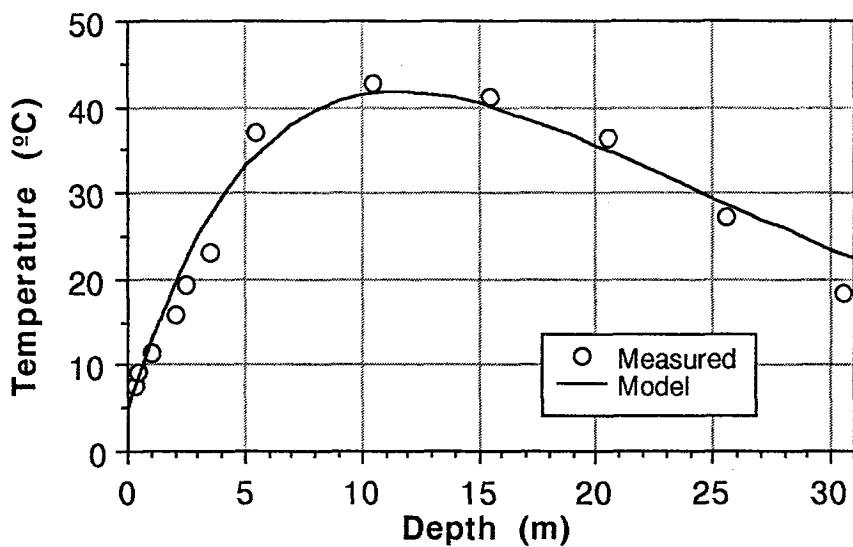
x	Tx	q (W/m)	G (W/m ³)
0	5.0	-12.22	1.31
1	9.8	-10.95	1.23
2	14.1	-9.77	1.15
3	18.2	-8.65	1.08
4	21.9	-7.61	1.01
5	25.2	-6.63	0.95
6	28.3	-5.72	0.89
7	31.1	-4.86	0.83
8	33.6	-4.06	0.78
9	35.8	-3.31	0.73
10	37.8	-2.60	0.68
11	39.6	-1.94	0.64
12	41.2	-1.32	0.60
13	42.6	-0.74	0.56
14	43.8	-0.20	0.52
15	44.8	0.30	0.49
16	45.6	0.78	0.46
17	46.2	1.23	0.43
18	46.7	1.64	0.40
19	47.1	2.03	0.38
20	47.3	2.40	0.35
21	47.3	2.74	0.33
22	47.3	3.06	0.31
23	47.1	3.36	0.29
24	46.8	3.65	0.27
25	46.3	3.91	0.26
26	45.8	4.16	0.24
27	45.2	4.39	0.22
28	44.4	4.60	0.21
29	43.5	4.81	0.20
30	42.6	5.00	0.18
31	41.5	5.18	0.17
Qf (W/m ²)			17.4

Conduction and advection model - Well #6

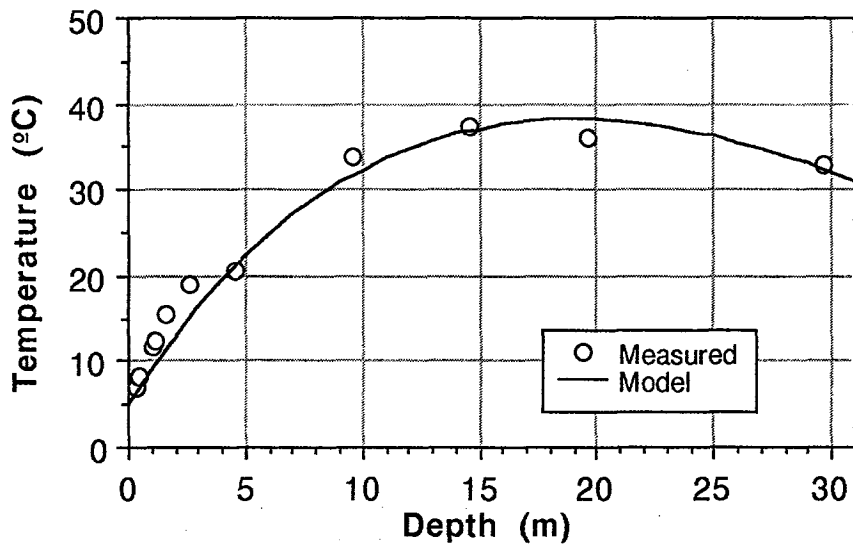
Effective diffusion coefficient	De	12.5	m ² /j
Oxygen concentration at the surface	Co	9.38	mol/m ³
Thermal conductivity	Kt	217728	J/j m °C
Kinetic constant (Oxygen combustion)	Kox	0.03	1/j
Gas flux	v	-5.41	m/j
Air volumetric heat capacity	Cv	5000	J/m ³ °C
Temperature gradient at the dump's base	T	-1.1	°C/m
Dump thickness	B	31	m
Average dump surface temperature	Tm	5	°C
Conversion factor	F	402629	J/mol
Constant A	CA	-0.12	v•Cv/Kt
Constant E	CE	0.049	√(Kox/De)
Constant M	CM	-156.99	
Constant N	CN	-141.16	
Constant B	CB	0.52	F Co Kox/Kt

x	Tx	q (W/m)	Q (W/m ³)
0	5.0	-33.29	1.31
1	16.6	-32.01	1.25
2	26.4	-30.79	1.19
3	34.6	-29.63	1.13
4	41.4	-28.53	1.08
5	47.0	-27.47	1.03
6	51.5	-26.47	0.98
7	55.2	-25.52	0.93
8	58.1	-24.61	0.89
9	60.3	-23.75	0.84
10	62.0	-22.92	0.80
11	63.2	-22.14	0.77
12	63.9	-21.39	0.73
13	64.3	-20.68	0.69
14	64.4	-20.00	0.66
15	64.2	-19.36	0.63
16	63.8	-18.75	0.60
17	63.2	-18.16	0.57
18	62.5	-17.60	0.54
19	61.7	-17.08	0.52
20	60.7	-16.57	0.49
21	59.7	-16.09	0.47
22	58.7	-15.63	0.45
23	57.6	-15.20	0.42
24	56.4	-14.78	0.40
25	55.3	-14.39	0.39
26	54.1	-14.01	0.37
27	53.0	-13.65	0.35
28	51.8	-13.31	0.33
29	50.7	-12.99	0.32
30	49.5	-12.68	0.30
31	48.4	-12.38	0.29
Gt (W/m ²)			20.9

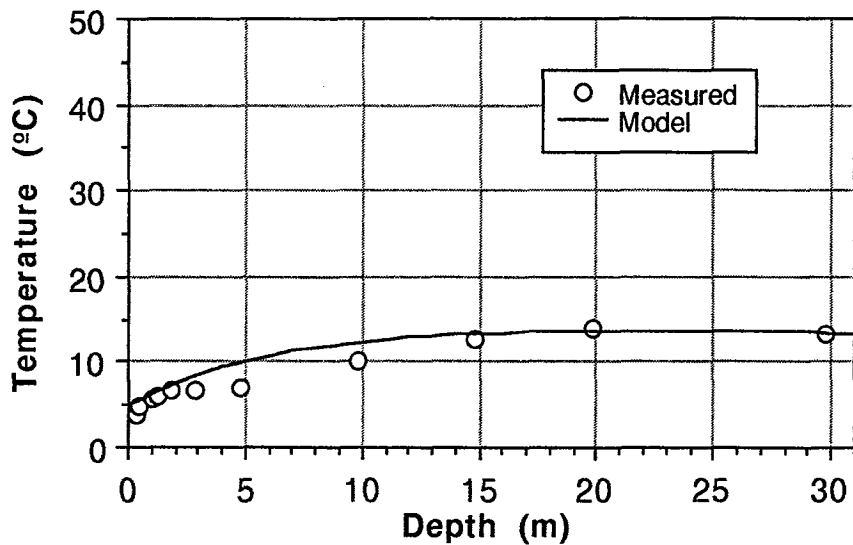
Temperature computed from the advection model - Well #1



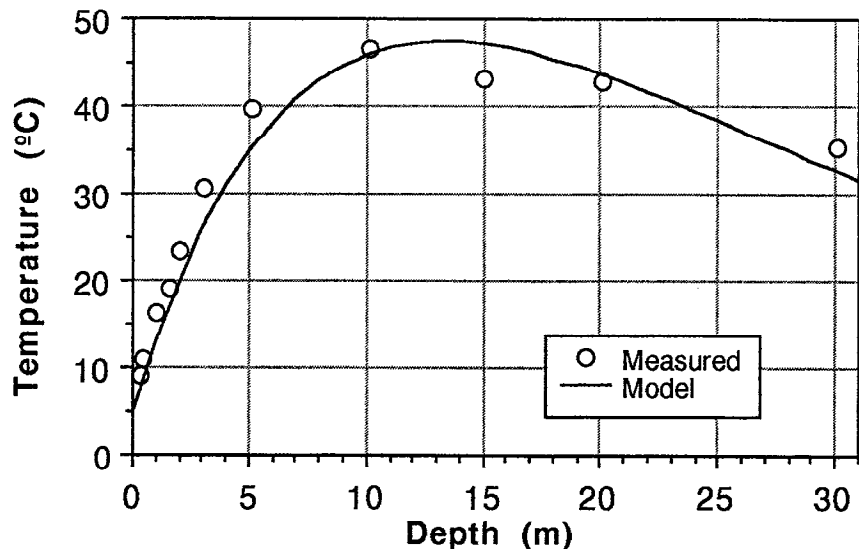
Temperature computed from the advection model - Well #2



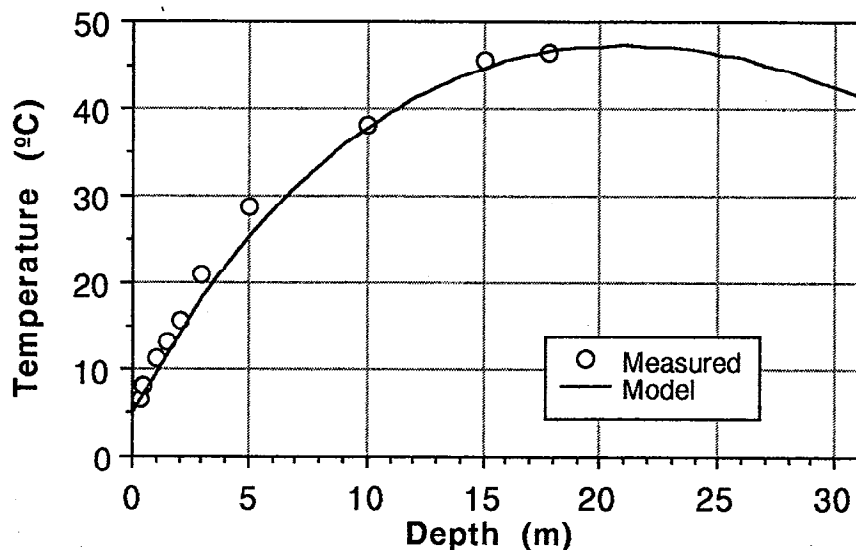
Temperature computed from the advection model - Well #3



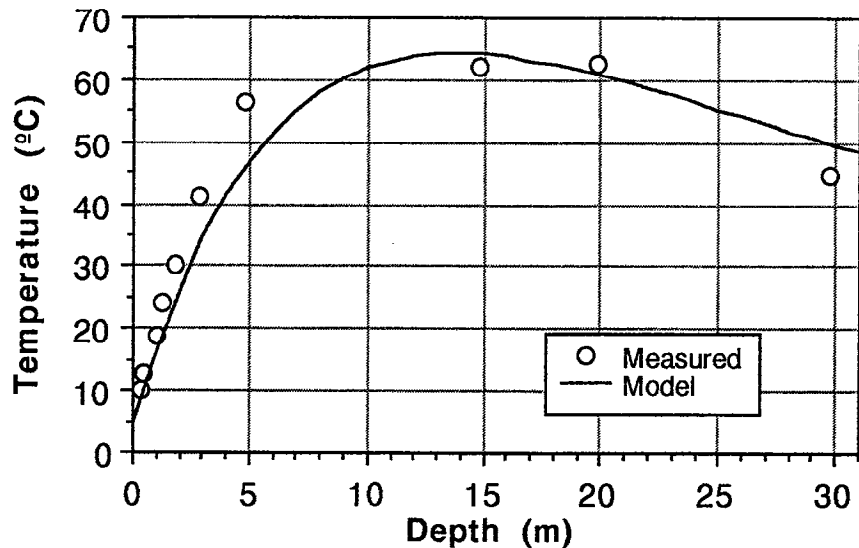
Temperature computed from the advection model - Well #4



Temperature computed from the advection model - Well #5



Temperature computed from the advection model - Well #6



D - Calculation of the heat stored within the dump

Results of the calculations of the heat stored in the dump for all wells are presented next in tables. For each well, we first present the calculation of the average heat stored within the dump at the beginning (initial temperature) and end (final temperature) of the monitoring period. We then present the calculation of the cyclic annual variations in heat storage.

Average heat stored within the dump

Calculations done using the initial (1/1/91) and final (1/1/93) average temperature profiles.

Average heat stored within the dump (per unit volume):

$$H = (T_{\text{measured}} - T_{\text{base}}) \cdot C_v$$

Average heat stored within the dump (per unit area):

Integration of the area under the volumetric heat stored between two different depths:

$$\text{Trapezoidal rule: } H = 0.5 \cdot \Delta Z \cdot (H_1 + H_2)$$

Cyclic annual variation in heat storage (per unit area):

Integration of the cyclic temperature variations half envelope: $\Delta H_c = C_v \cdot \Delta T / a$

Parameters:

C_v	1.98	MJ/ $^{\circ}\text{C}$ m 3	Global volumetric heat capacity
T_{base}	5	$^{\circ}\text{C}$	Base temperature (reference)

Note: ΔH in % computed with respect to the average heat stored during the monitoring period (at 1/1/92).

Well #1

Average heat stored within the dump:

Depth (m)	$T_{\text{init.}}$ $^{\circ}\text{C}$ 1/1/91	T_{final} $^{\circ}\text{C}$ 1/1/93	H_{init} (MJ/m 3)	H_{final} (MJ/m 2)	H_{final} (MJ/m 3)	H_{final} (MJ/m 2)	ΔH (MJ/m 3)	ΔH (MJ/m 2)
0.3	10.29	5.42	10.47		0.83		-9.64	
0.5	11.83	6.80	13.51	2.40	3.57	0.44	-9.95	-1.96
1.0	13.82	9.27	17.45	7.74	8.45	3.00	-9.00	-4.74
2.0	19.25	12.75	28.19	22.82	15.32	11.89	-12.87	-10.93
2.5	21.34	17.53	32.33	15.13	24.78	10.03	-7.54	-5.10
3.5	28.69	18.20	46.87	39.60	26.12	25.45	-20.75	-14.15
5.5	40.12	34.55	69.48	116.35	58.45	84.57	-11.03	-31.78
10.5	45.50	40.54	80.12	374.02	70.31	321.91	-9.81	-52.10
15.5	43.95	38.80	77.06	392.96	66.88	342.97	-10.18	-49.99
20.5	38.40	34.77	66.08	357.84	58.90	314.44	-7.18	-43.40
25.5	25.37	28.92	40.30	265.95	47.32	265.54	7.02	-0.40
30.5	16.53	20.02	22.81	157.78	29.71	192.58	6.90	34.81
Total:				1752.6	Total:	1572.8	Total:	-179.7
							%:	-10.8%

Cyclic annual variation in heat stored within the dump (MJ/m 2):

ΔT	a	ΔH_c	$\Delta H_c \%$
13.1	0.336	123.0	7.3

Well #2**Average heat stored within the dump:**

Depth (m)	Tinit. °C 1/1/91	Tfinal. °C 1/1/93	Hinit (MJ/m³)	Hinit (MJ/m²)	Hfinal (MJ/m³)	Hfinal (MJ/m²)	ΔH (MJ/m³)	ΔH (MJ/m²)
0.3	9.77	4.37	9.44		-1.24		-10.68	
0.5	11.49	5.71	12.84	2.23	1.41	0.02	-11.43	-2.21
1.0	14.98	8.92	19.74	8.15	7.76	2.29	-11.98	-5.85
1.1	15.34	9.59	20.46	2.01	9.08	0.84	-11.37	-1.17
1.6	18.82	12.85	27.34	11.95	15.52	6.15	-11.82	-5.80
2.6	22.44	16.07	34.50	30.92	21.91	18.71	-12.60	-12.21
4.6	24.11	17.76	37.81	72.31	25.25	47.15	-12.56	-25.16
9.6	37.54	30.87	64.38	255.46	51.18	191.07	-13.20	-64.39
14.6	42.35	33.24	73.89	345.68	55.86	267.61	-18.03	-78.07
19.6	40.97	32.01	71.16	362.64	53.44	273.27	-17.72	-89.37
29.6	31.18	34.30	51.79	614.79	57.96	557.00	6.16	-57.78
Total:			1706.1		1364.1		-342.0	
							%:	-22.3%

Cyclic annual variation in heat stored within the dump (MJ/m²):

ΔT	a	ΔH _c	ΔH _c %
12.5	0.168	117.8	7.7

Well #3**Average heat stored within the dump:**

Depth (m)	Tinit. °C 1/1/91	Tfinal. °C 1/1/93	Hinit (MJ/m³)	Hinit (MJ/m²)	Hfinal (MJ/m³)	Hfinal (MJ/m²)	ΔH (MJ/m³)	ΔH (MJ/m²)
0.3	7.01	1.19	3.98		-7.53		-11.51	
0.5	7.54	2.63	5.03	0.90	-4.68	-1.22	-9.71	-2.12
1.0	8.08	3.63	6.09	2.78	-2.71	-1.85	-8.80	-4.63
1.3	8.03	4.28	5.99	1.81	-1.42	-0.62	-7.41	-2.43
1.8	8.45	4.84	6.83	3.20	-0.32	-0.44	-7.15	-3.64
2.8	8.54	4.90	7.00	6.91	-0.21	-0.27	-7.21	-7.18
4.8	8.53	5.70	6.98	13.99	1.38	1.17	-5.61	-12.82
9.8	9.69	10.57	9.28	40.66	11.02	31.00	1.75	-9.65
14.8	11.37	13.83	12.60	54.70	17.46	71.21	4.86	16.51
19.8	14.27	13.63	18.34	77.36	17.08	86.35	-1.26	8.99
29.8	12.69	13.54	15.21	167.77	16.90	169.89	1.69	2.12
Total:			370.1		355.2		-14.8	
							%:	-4.1%

Cyclic annual variation in heat stored within the dump (MJ/m²):

ΔT	a	ΔH _c	ΔH _c %
14.9	0.163	192.3	53.7

Well #4**Average heat stored within the dump:**

Depth (m)	Tinit. °C 1/1/91	Tfinal °C 1/1/93	Hinit (MJ/m ³)	Hinit (MJ/m ²)	Hfinal (MJ/m ³)	Hfinal (MJ/m ²)	ΔH (MJ/m ³)	ΔH (MJ/m ²)
0.3	13.91	4.77	17.63		-0.46		-18.09	
0.5	17.20	5.56	24.14		4.18		-23.04	
1.0	24.85	8.88	39.27		15.85		-31.60	
1.6	28.56	11.28	46.61		25.76		-34.18	
2.1	34.30	14.19	57.97		26.14		-39.79	
3.1	44.29	19.38	77.73		67.85		-49.28	
5.1	50.86	30.50	90.73		168.46		-40.28	
10.1	51.91	42.18	92.81		458.84		-19.25	
15.1	49.75	37.44	88.53		453.35		-24.35	
20.1	45.36	40.58	79.85		420.95		-9.46	
30.1	34.43	35.77	58.22		690.36		2.65	
				Total: 2331.7		Total: 1765.3	Total: -566.5	
							%: -27.7%	

Cyclic annual variation in heat stored within the dump (MJ/m²):

ΔT	a	ΔH _c	ΔH %
12.2	0.221	133.4	6.5

Well #5**Average heat stored within the dump:**

Depth (m)	Tinit. °C 1/1/91	Tfinal °C 1/1/93	Hinit (MJ/m ³)	Hinit (MJ/m ²)	Hfinal (MJ/m ³)	Hfinal (MJ/m ²)	ΔH (MJ/m ³)	ΔH (MJ/m ²)
0.3	9.06	4.67	8.03		-0.65		-8.68	
0.5	10.79	6.07	11.45		1.95		-9.34	
1.0	13.28	9.29	16.38		6.96		-7.90	
1.5	15.88	10.62	21.52		9.48		-10.40	
2.0	19.89	12.11	29.46		12.75		-15.39	
3.0	26.17	16.32	41.88		35.67		-19.48	
5.0	35.14	23.32	59.63		101.51		-23.38	
10.0	40.70	35.98	70.63		325.64		-9.33	
15.0	47.81	43.91	84.70		388.31		-7.72	
17.8	49.03	44.28	87.11		240.53		-9.39	
				Total: 1122.8		Total: 897.0	Total: -225.8	
							%: -22.4%	

Cyclic annual variation in heat stored within the dump (MJ/m²):

ΔT	a	ΔH _c	ΔH %
13.4	0.239	139.8	13.9

Well #6**Average heat stored within the dump:**

Depth (m)	Tinit. °C 1/1/91	Tfinal °C 1/1/93	Hinit (MJ/m³)	Hinit (MJ/m²)	Hfinal (MJ/m³)	Hfinal (MJ/m²)	ΔH (MJ/m³)	ΔH (MJ/m²)
0.3	13.00	7.51	15.83		4.97		-10.85	
0.5	15.86	9.95	21.49		3.73		-11.70	
1.0	21.48	16.20	32.60		13.52		-10.45	
1.3	28.04	20.95	45.58		11.73		-14.02	
1.8	34.69	26.47	58.74		26.08		-16.27	
2.8	46.08	36.87	81.27		70.01		-18.22	
4.8	62.43	51.26	113.62		194.89		-22.09	
14.8	67.33	57.82	123.31		1184.66		-18.82	
19.8	65.68	59.55	120.05		608.41		-12.14	
29.8	44.12	44.86	77.39		987.22		1.46	
			Total:	3100.2		Total:	2688.3	Total:
								-411.9
							%:	-14.2%

Cyclic annual variation in heat stored within the dump (MJ/m²):

ΔT	a	ΔH _c	ΔH _c %
15.5	0.363	163.2	5.6

Note: Temperature at 9.8 m not included in the analysis.

E - Temperature data

Temperature data recorded during the monitoring period and used in this report (up to December 8, 1992) are presented next as tables and as figures showing the temperature measurements at each level against time.

Puits #1

Température (°C)

Jour zéro le: 1/1/91

Date	Jour	Profondeur du point de mesure (m)											
		0,3	0,5	1,0	2,0	2,5	3,5	5,5	10,5	15,5	20,5	25,5	
17/4/91	106	5,0	5,9	7,9	12,6	14,7	22,5	37,0	45,1	42,9	33,7	25,4	16,9
23/4/91	112	6,0	7,3	9,1	14,0	16,0	22,9	36,9	45,4	43,1	34,1	25,4	16,9
26/4/91	115	8,8	9,3	9,9	14,2	16,3	23,0	36,7	45,2	42,8	36,6	25,4	16,9
2/5/91	121	9,5	11,2	12,5	15,5	17,3	23,4	36,7	45,1	43,0	37,1	25,5	17,1
10/5/91	129	11,1	11,8	12,2	16,3	18,3	24,1	36,7	45,1	42,9	37,0	25,5	17,1
16/5/91	135	15,6	15,7	15,5	17,7	19,2	24,6	36,9	45,1	43,0	37,1	25,6	17,2
23/5/91	142	18,7	18,3	17,3	21,8	20,3	25,3	37,0	45,0	43,0	37,3	25,7	17,3
31/5/91	150	20,2	19,4	18,8	19,6	20,8	25,8	36,9	45,0	43,0	37,4	25,7	17,4
5/6/91	155	17,4	18,4	19,2	21,4	22,5	26,5	37,3	44,7	43,0	37,5	25,8	17,5
11/6/91	161	20,6	20,9	20,5	22,1	23,0	27,1	37,3	44,6	43,0	37,6	25,9	17,5
19/6/91	169	22,8	22,8	21,3	22,7	23,9	27,6	37,6	44,4	42,9	37,7	26,0	17,4
26/6/91	176	22,1	22,7	22,1	23,6	24,8	28,0	37,6	44,3	42,8	37,7	26,1	17,3
3/7/91	183	22,0	21,8	22,2	24,2	25,4	28,4	37,8	44,2	42,8	37,8	26,1	17,3
10/7/91	190	19,7	21,6	22,8	24,8	26,1	28,8	37,9	44,0	42,7	37,7	26,2	17,4
18/7/91	198	22,4	23,1	23,2	24,8	26,3	29,2	38,2	43,9	42,6	37,7	26,2	17,4
24/7/91	204	19,7	21,7	23,4	25,5	26,8	29,3	38,3	43,8	42,6	37,7	26,3	17,6
29/7/91	209	21,1	21,6	22,8	25,0	26,7	29,5	38,5	43,6	42,5	37,4	26,4	17,5
7/8/91	218	20,5	21,1	22,3	24,8	26,7	29,6	38,7	43,6	42,5	37,3	26,4	17,5
14/8/91	225	24,3	23,7	23,7	25,4	27,2	29,6	38,8	43,5	42,4	37,4	26,5	17,6
21/8/91	232	20,5	21,8	22,6	25,3	27,4	29,8	39,0	43,3	42,3	37,2	26,5	17,6
27/8/91	238	19,8	20,1	20,8	24,6	27,2	29,9	39,2	43,3	42,2	37,2	26,6	17,7
6/9/91	248	16,7	18,6	20,7	24,4	26,9	29,8	39,4	43,2	42,1	37,2	26,7	17,7
11/9/91	253	15,9	17,9	20,8	23,9	26,5	29,6	39,5	43,2	42,1	37,2	26,7	17,7
18/9/91	260	14,5	17,1	20,0	23,1	26,0	29,3	39,6	43,1	42,0	37,3	26,8	17,8
25/9/91	267	11,6	13,9	17,7	22,2	25,3	29,1	39,8	43,1	42,0	37,4	26,8	17,8
1/10/91	273	7,9	10,0	14,0	19,2	23,5	28,6	39,9	43,1	42,0	37,5	26,8	17,8
8/10/91	280	5,1	7,5	11,0	17,7	22,0	27,4	39,9	43,1	41,8	37,6	26,9	17,8
16/10/91	288	6,1	8,2	11,1	16,9	21,2	26,6	39,8	43,1	41,8	37,7	26,9	17,9
22/10/91	294	4,1	6,0	9,2	16,7	20,7	26,1	39,8	43,1	41,8	37,6	26,9	17,9
29/10/91	301	5,1	7,7	11,8	16,7	20,4	25,4	39,6	43,1	41,7	37,4	27,0	18,0
7/11/91	310	1,3	3,7	6,7	13,7	19,2	25,2	39,5	43,1	41,7	37,4	27,0	18,1
13/11/91	316	1,9	3,3	6,0	13,8	18,2	24,5	39,4	43,1	41,7	37,1	27,1	18,0
19/11/91	322	0,9	2,4	5,7	13,5	18,2	24,1	39,3	43,1	41,6	36,9	27,1	18,1
27/11/91	330	1,3	3,5	7,0	13,9	17,9	23,5	39,2	43,1	40,8	36,9	27,1	18,1
4/12/91	337	-3,8	-0,1	5,6	13,3	17,5	23,2	39,0	43,2	41,5	36,9	27,2	18,2
11/12/91	344	-0,3	0,9	3,9	12,1	16,8	23,0	38,8	43,2	41,5	36,8	27,2	18,2
18/12/91	351	-5,2	-1,1	3,4	11,2	16,2	22,4	38,7	43,2	41,5	36,7	27,2	18,2
24/12/91	357	-2,7	-0,4	2,9	11,2	15,9	22,0	38,5	43,2	41,4	36,7	27,3	18,2
31/12/91	364	-2,5	-0,4	2,2	10,4	15,5	21,8	38,3	43,2	41,4	36,6	27,3	18,3
8/1/92	372	-0,6	1,9	4,9	11,2	15,2	21,1	38,0	43,2	41,3	36,5	27,4	18,3
17/1/92	381	-2,1	1,0	5,5	11,1	15,6	21,1	37,7	43,2	41,4	36,5	27,4	18,3
22/1/92	386	-1,1	1,6	5,6	10,7	15,4	21,1	37,6	43,1	41,4	36,5	27,4	18,3
29/1/92	393	-1,1	0,6	4,3	10,7	15,4	20,9	37,2	43,1	41,3	36,4	27,4	18,4
5/2/92	400	0,4	2,2	5,3	10,7	15,0	20,5	37,2	43,1	41,2	36,4	27,5	18,4
13/2/92	408	-2,0	0,6	4,9	10,9	15,2	20,4	36,9	43,0	41,3	36,4	27,5	18,5
19/2/92	414	0,2	1,6	4,2	10,5	14,8	20,1	36,8	43,0	41,2	36,3	27,6	18,5
26/2/92	421	0,5	0,7	5,7	10,7	15,0	20,0	36,6	43,0	41,1	36,3	27,6	18,5
3/3/92	427	0,7	2,8	6,0	11,1	15,2	20,0	36,4	42,9	41,1	36,3	27,6	18,6
11/3/92	435	1,2	3,2	6,1	11,7	15,5	19,7	36,1	42,8	41,0	36,1	27,7	18,6
19/3/92	443	-2,3	-0,1	3,4	9,9	14,7	19,6	35,9	42,8	41,0	36,0	27,7	18,6
26/3/92	450	-0,5	0,1	2,8	9,1	13,7	18,8	35,7	42,7	40,9	35,9	27,7	18,6
2/4/92	457	-0,3	1,6	4,6	9,9	14,0	18,6	35,6	42,7	40,9	35,9	27,7	18,7

Puits #1

Température (°C)

Jour zéro le: 1/1/91

Date	jour	Profondeur du puits de mesure (m)											
		0,3	0,5	1,0	2,0	2,5	3,5	5,5	10,5	15,5	20,5	25,5	30,5
9/4/92	464	1,4	2,8	5,3	9,9	13,9	18,2	35,3	42,6	40,8	35,9	27,8	18,7
16/4/92	471	2,7	3,9	6,0	10,4	14,5	18,3	35,0	42,5	40,7	36,2	27,8	18,7
8/5/92	493	9,6	10,0	10,8	11,0	16,8	18,8	34,4	42,2	40,6	35,6		
15/5/92	500	10,7	11,5	13,6	15,0	17,7	19,0	34,4	42,1	40,7	35,8		
22/5/92	507	18,7	17,2	15,4	15,4	18,5	19,5	34,4	42,0	40,7	35,9		
28/5/92	513	13,7	14,0	15,1	16,7	19,5	20,0	34,5	42,0	40,6	35,9		
4/6/92	520	12,8	14,8	16,7	17,7	20,4	20,5	34,5	41,9	40,6	35,9		
10/6/92	526	14,5	15,6		18,4	21,1	21,0	34,7	41,8	40,5	35,8		
17/6/92	533	21,5	20,4		19,7	22,5	22,1	35,1	41,6	40,2	35,6	27,9	19,3
26/6/92	542	18,5	18,0	17,6	18,9	21,9	22,1	35,0	41,6	40,3	35,8		
2/7/92	548	16,4	17,3	18,8	20,0	22,7	22,3	35,2	41,5	40,2	35,8		
10/7/92	556	17,1	18,2	19,1	20,1	23,1	22,7	35,3	41,4	40,1	35,8		
15/7/92	561	17,9	19,2	19,6	20,6	23,5	22,8	35,4	41,4	40,1	35,8	28,1	19,2
22/7/92	568	14,9	16,9	19,7	21,4	24,2	23,2	35,6	41,3	40,0	35,8	28,2	19,3
30/7/92	576	14,2	16,4	18,9	21,1	24,1	23,4	35,7	41,2	39,8	35,7	28,2	19,3
6/8/92	583	19,3	18,1	19,0	20,9	24,1	23,6	35,9	41,1	39,8	35,7	28,2	19,3
12/8/92	589	15,7	17,0		21,4	24,5	23,7	36,0	41,1	39,7	35,6	28,3	19,4
18/8/92	595	19,2	19,8		21,4	24,6	23,9	36,2	41,0	39,5	35,5	28,2	19,5
27/8/92	604	15,9	18,1	20,1	21,4	24,6	23,9	36,2	41,0	39,6	35,5	28,3	19,4
4/9/92	612	13,6	15,3	17,3	19,9	23,8	24,0	36,4	40,9	39,5	35,5	28,3	19,5
10/9/92	618	14,0	14,7	16,7	19,7	23,6	23,8	36,4	40,9	39,4	35,5	28,4	19,5
17/9/92	625	16,1	16,1	16,7	18,7	22,8	23,5	36,5	40,9	39,3	35,4	28,4	19,5
24/9/92	632	8,3	10,6	13,8	18,4	22,5	23,3	36,5	40,7	39,3	35,4	28,4	19,5
30/9/92	638	6,9	10,0	14,2	17,8	21,9	23,1	36,6	40,8	39,2	35,3	28,5	19,6
8/10/92	646	9,4	11,0	13,4	17,1	21,6	22,7	36,7	40,8	39,2	35,3	28,5	19,6
14/10/92	652	5,8	8,6	12,8	16,9	21,4	22,5	36,7	40,8	39,1	35,3	28,5	19,6
21/10/92	659	3,1	5,0	8,6	14,7	19,9	22,1	36,6	40,9	39,1	35,2	28,5	19,7
28/10/92	666	2,9	4,8	8,0	13,2	18,5	21,4	36,6	40,9	39,0	35,2	28,5	19,7
5/11/92	674	3,4	4,8	7,3	12,8	18,0	20,7	36,5	40,8	39,0	35,0	28,6	19,8
12/11/92	681	2,3	3,9	7,0	11,9	17,4	20,3	36,4	40,9	39,0	35,0	28,6	19,8
20/11/92	689	-0,4	1,6	5,0	11,2	16,6	19,8	36,2	41,0	38,9	35,1	28,6	19,8
25/11/92	694	0,3	1,9	5,2	11,2	16,3	19,4	36,0	41,0	38,9	34,9	28,6	19,8
1/12/92	700	-0,3	1,7	5,1	10,5	16,0	19,0	35,8	41,0	38,8	34,8	28,6	19,8
8/12/92	707	-1,2	1,3	4,7	10,4	15,7	18,8	35,7	41,1	38,8	34,9	28,6	19,8

Puits #2

Température (°C)

Jour zéro le: 1/1/91

Date	jour	Profondeur du point de mesure (m)									
		0,3	0,5	1,0	1,1	1,5	2,6	4,6	9,6	14,6	19,6
10/2/91	40	-0,6	1,7	-0,4	8,2	11,7	16,0	13,7	29,2	34,5	34,5
12/2/91	42	-8,1	-2,2	6,7	7,0	13,7	18,0	18,3	33,3	40,0	38,5
22/2/91	52	-3,1	-0,4	4,0	6,4	11,7	16,0	18,5	34,5	40,0	40,0
27/3/91	85	0,0	0,0	4,0	6,7	11,3	14,6	16,5	33,3	40,0	38,5
9/4/91	98	4,7	6,8	9,0	8,9	9,8	11,5	14,7	32,8	39,2	39,3
17/4/91	106	4,3	4,9	6,9	7,3	9,6	13,4	15,7	33,1	39,5	39,3
23/4/91	112	4,9	5,6	6,9	7,8	10,2	13,7	16,0	33,2	39,8	39,5
26/4/91	115	8,0	8,1	8,0	8,8	10,7	13,8	16,3	33,1	39,5	39,2
2/5/91	121	9,2	10,6	12,0	12,5	13,4	15,2	17,9	33,5	39,5	39,3
10/5/91	129	10,5	10,9	11,1	11,6	13,5	16,4	18,4	33,4	39,5	39,2
16/5/91	135	15,7	15,9	15,5	15,7	16,1	17,4	18,8	33,6	39,4	39,2
23/5/91	142	19,0	18,5	17,3	17,4	17,1	18,4	19,8	33,9	39,3	39,2
31/5/91	150	17,7	18,4	17,9	18,0	18,8	19,9	20,1	34,1	39,4	39,1
5/6/91	155	16,8	17,6	18,6	19,0	20,0	21,1	21,2	34,7	39,4	39,0
11/6/91	161	20,9	21,4	20,9	22,0	21,1	21,6	23,0	35,0	39,3	38,9
19/6/91	169	22,6	22,7	21,3	21,4	21,6	22,7	23,7	35,3	39,1	38,8
26/6/91	176	22,6	23,5	23,1	23,3	23,2	23,7	24,4	35,6	38,9	38,8
3/7/91	183	22,6	22,2	22,7	23,0	23,9	25,1	24,7	35,9	39,1	38,6
10/7/91	190	19,2	21,2	23,1	23,6	25,0	26,3	26,3	36,3	39,0	38,5
18/7/91	198	23,1	23,3	24,7	25,1	25,6	26,5	26,8	36,5	38,9	38,4
24/7/91	204	20,4	22,5	25,1	25,4	26,6	27,6	28,3	36,9	38,9	38,3
29/7/91	209	21,1	21,4	23,2	23,7	25,9	28,0	27,8	37,0	38,8	38,2
7/8/91	218	20,4	20,7	22,7	23,2	25,5	27,9	28,5	37,8	39,1	38,1
14/8/91	225	24,6	24,1	24,6	24,9	26,0	27,7	28,9	37,7	39,2	38,0
21/8/91	232	19,8	21,1	23,0	23,5	26,0	28,3	29,1	38,0	39,4	37,9
27/8/91	238	20,0	20,6	22,1	22,9	25,5	28,3	30,2	38,1	39,4	37,8
6/9/91	248	16,7	18,6	21,7	22,3	25,4	28,5	29,7	38,5	39,4	37,7
11/9/91	253	15,5	17,5	21,7	22,3	25,4	28,8	29,8	38,6	39,5	37,6
18/9/91	260	14,5	17,2	22,0	22,1	25,5	28,9	30,3	38,6	39,5	37,6
25/9/91	267	11,2	13,1	18,9	18,8	23,4	26,9	30,2	38,4	39,6	37,5
1/10/91	273	6,9	8,8	14,7	14,6	20,9	27,1	29,6	38,3	39,5	37,5
8/10/91	280	5,4	8,4	14,6	15,6	20,7	25,2	27,7	38,1	39,6	37,4
16/10/91	288	6,0	8,5	13,7	14,5	19,6	23,6	26,5	37,7	39,7	37,3
22/10/91	294	5,4	8,1	14,4	14,5	20,3	24,4	26,0	37,4	39,7	37,3
29/10/91	301	6,4	8,8	14,9	15,0	20,0	23,3	25,5	37,1	39,8	37,2
7/11/91	310	2,2	5,7	13,6	13,5	20,1	25,7	27,9	36,7	39,7	37,2
13/11/91	316	3,7	6,4	13,6	13,7	20,3	25,0	26,7	36,6	39,5	37,1
19/11/91	322	2,5	4,4	11,2	11,8	18,3	23,8	24,7	36,3	39,6	37,1
27/11/91	330	2,8	5,6	11,8	12,1	17,8	22,5	23,8	36,1	39,5	37,0
4/12/91	337	-3,1	0,6	8,6	8,9	15,9	21,4	22,6	35,7	39,5	37,0
11/12/91	344	-0,7	0,4	6,5	7,5	13,9	20,3	21,4	35,2	39,2	36,9
18/12/91	351	-4,6	-0,2	7,2	8,3	14,5	19,3	21,2	34,7	39,3	36,9
24/12/91	357	-2,3	1,1	7,8	8,7	14,8	19,7	20,6	34,5	39,0	36,8
31/12/91	364	-1,2	1,7	8,0	8,8	14,3	18,5	19,9	34,3	39,0	36,8
8/1/92	372	-0,4	2,1	6,8	7,4	11,9	16,2	18,9	33,9	38,9	36,7
17/1/92	381	-4,2	-1,0	5,0	5,2	10,8	15,6	18,4	33,1	39,0	36,6
22/1/92	386	-4,2	-1,6	4,0	4,2	10,0	14,9	17,7	32,9	38,6	36,6
29/1/92	393	-3,4	-2,1	2,9	2,9	8,9	13,4	16,7	32,6	38,4	36,5
5/2/92	400	-2,3	-0,8	3,0	2,8	6,9	10,6	13,2	32,4	38,2	36,5
13/2/92	408	-5,3	-3,6	0,1	0,6	5,6	10,1	13,6	32,1	38,0	36,4
19/2/92	414	-2,0	-1,3	0,8	1,6	5,9	10,7	12,4	32,2	37,8	36,3
26/2/92	421	-2,6	-1,6	1,2	2,1	6,2	10,4	12,2	32,1	37,7	36,2
3/3/92	427	-3,7	-2,4	0,8	1,8	6,2	10,3	12,1	32,0	37,5	36,1
11/3/92	435	-3,3	-1,1	1,6	2,6	6,3	9,8	10,6	32,0	37,3	36,0
19/3/92	443	-5,3	-3,7	0,0	1,3	6,1	10,7	12,4	31,7	36,8	35,9
26/3/92	450	-2,0	-2,1	-0,3	1,0	5,6	10,1	11,9	31,8	36,3	35,7
2/4/92	457	-2,9	-1,7	0,8	1,9	5,6	9,6	11,7	31,7	36,1	35,6

Puits #2

Température (°C)

Jour zéro le: 1/1/91

Date	jour	Profondeur du point de mesure (m)										
		0.3	0.5	1.0	1.1	1.6	2.6	4.6	9.6	14.6	19.6	29.6
9/4/92	464	-0,8	-0,7	1,4	2,3	5,7	9,6	11,7	31,4	35,9	35,5	35,8
16/4/92	471	-0,6	-0,5	1,8	2,9	6,3	10,3	11,7	31,4	35,6	35,3	35,9
8/5/92	493	8,5	8,4	8,5	9,1	10,3	12,5	14,6	30,6	36,1	34,8	35,6
15/5/92	500	9,8	10,3	12,2	12,8	13,6	14,1	15,4	30,6	36,0	34,7	35,2
22/5/92	507	18,7	17,0	15,0	15,3	14,4	15,3	17,7	30,7	35,7	34,6	34,9
28/5/92	513	13,1	13,0	14,0	14,8	15,6	16,5	17,1	30,9	35,7	34,5	34,7
4/6/92	520	12,0	14,0	16,2	16,8	17,2	17,5	18,2	31,1	35,6	34,3	34,4
10/6/92	526	13,6	14,7	16,1	16,5	17,4	18,6	19,2	31,4	35,7		34,3
17/6/92	533	20,6	20,4	18,9	19,3	19,0	19,6	20,7	31,7	35,4	34,1	34,1
24/6/92	542	17,9	17,0	16,6	17,2	17,9	19,5	20,4	31,9	35,4	34,0	34,0
2/7/92	548	15,9	16,2	17,5	18,2	19,1	20,1	20,9	32,1	35,1	33,9	33,9
10/7/92	556	16,3	17,2	18,0	18,5	19,3	20,6	21,7	32,6	35,2	33,8	33,7
15/7/92	561	17,3	18,4	18,6	19,0	19,7	20,7	21,8	32,7	35,1	33,7	33,6
22/7/92	568	14,6	16,1	18,6	19,2	20,8	21,7	23,2	33,0	35,0	33,6	33,4
30/7/92	576	13,7	15,8	18,8	19,5	21,2	22,8	23,9	33,2	34,7	33,5	33,1
6/8/92	583	18,9	17,7	18,5	19,2	21,0	22,9	24,1	33,4	34,6	33,5	32,9
12/8/92	589				20,6	22,2	23,6	24,8	33,7	34,6	33,4	32,8
18/8/92	595	17,9	18,7	20,1	20,7	22,0	23,5	25,4	33,8	34,5	33,3	32,6
27/8/92	604	15,5	17,6	20,2	20,6	22,0	23,7	25,6	34,2	34,5	33,2	32,4
4/9/92	612	12,2	13,9	16,5	16,8	19,7	23,2	25,6	34,3	34,6	33,1	32,4
10/9/92	618	14,3	15,3	18,4	18,4	21,4	24,3	26,7	34,4	34,7	33,1	32,3
17/9/92	625	16,7	17,5	20,1	20,3	23,2	26,1	27,6	34,5	34,5	33,0	32,1
24/9/92	632	9,6	12,6	18,3	18,4	23,0	26,2	28,0	34,7	34,5	33,0	31,9
30/9/92	638	8,1	11,6	18,1	18,3	23,0	26,0	27,4	34,8	34,5	32,9	31,8
8/10/92	646	10,1	12,2	16,8	17,0	21,3	25,4	27,2	34,7	34,3	32,9	31,9
14/10/92	652	6,0	9,3	16,1	16,6	21,8	25,7	26,8	34,7	34,4	32,8	31,8
21/10/92	659	2,9	5,6	13,1	13,4	20,1	25,1	26,7	34,5	34,1	32,8	31,7
28/10/92	666	4,1	6,8	12,9	13,3	19,1	23,3	24,6	34,2	34,1	32,8	31,8
5/11/92	674	3,4	5,3	9,9	10,3	15,6	21,6	24,1	33,6	34,0	32,7	31,9
12/11/92	681	2,1	4,2	9,7	10,2	15,6	21,2	23,4	33,1	33,9	32,7	31,9
20/11/92	689	-0,4	2,3	8,7	9,6	15,3	19,7	21,6	32,8	33,6	32,7	32,0
25/11/92	694	0,5	2,7	8,4	9,0	14,3	18,9	20,5	32,5	33,5	32,7	32,1
1/12/92	700	-0,3	2,1	7,8	8,6	13,8	18,6	20,2	32,1	33,4	32,6	32,1
8/12/92	707	-2,0	1,0	6,9	7,6	13,1	17,5	19,0	31,7	33,1	32,6	32,2

Puits #3

Température (°C)

Jour zéro le: 1/1/91

Date	jour	Profondeur du point de mesure (m)									
		0,3	0,5	1,0	1,3	1,8	2,8	4,8	9,8	14,8	19,8
15/2/91	45	-10,4	-8,1	-3,9	1,2	1,7	3,8	6,7	9,9	11,7	13,7
22/2/91	52	-5,4	-4,1	-3,9	-3,1	-0,4	1,7	4,0	9,9	11,7	13,7
27/3/91	85	-2,2	-3,9	-3,9	-0,4	0,0	2,8	4,0	9,9	11,0	13,7
9/4/91	98	1,3	1,3	-0,2	-0,5	-0,3	0,0	2,4	8,7	10,7	13,5
17/4/91	106	1,4	0,9	0,1	-0,5	-0,4	0,9	2,7	8,6	11,0	13,2
23/4/91	112	2,1	1,7	0,3	-0,4	-0,3	0,9	2,8	8,6	11,2	13,2
26/4/91	115	5,5	4,4	1,2	0,1	-0,2	0,7	2,9	8,5	11,2	13,1
2/5/91	121	6,6	7,2	5,2	4,9	2,6	1,4	2,8	8,5	11,3	13,1
10/5/91	129	8,5	7,8	5,1	4,5	3,5	2,4	2,9	8,4	11,4	13,1
16/5/91	135	14,0	13,1	9,9	9,7	7,2	3,6	3,2	8,4	11,6	13,1
23/5/91	142	17,3	15,9	11,7	10,8	8,2	5,7	3,7	8,3	11,7	13,2
31/5/91	150	13,8	15,8	13,6	12,4	9,4	7,1	4,0	8,3	12,0	13,0
5/6/91	155	15,6	15,6	14,2	14,0	12,2	8,9	5,1	8,3	12,1	13,3
11/6/91	161	19,5	19,7	16,9	16,5	14,5	10,5	6,0	8,3	12,1	13,3
19/6/91	169	21,1	20,6	17,1	16,3	14,7	12,2	7,0	8,3	12,2	13,4
26/6/91	176	21,9	21,8	18,9	18,6	16,5	13,3	8,8	8,4	12,4	13,5
3/7/91	183	20,5	19,7	18,3	18,2	16,9	13,9	8,9	8,4	12,4	13,6
10/7/91	190	18,4	19,1	18,7	18,8	17,6	14,9	9,7	8,3	12,6	13,6
18/7/91	198	21,7	21,9	20,4	20,0	18,2	15,5	10,5	8,7	12,7	13,7
24/7/91	204	19,0	20,6	20,9	21,2	19,4	16,8	11,3	8,8	12,8	13,8
29/7/91	209	19,2	19,2	19,0	18,5	18,3	16,5	11,8	9,0	12,8	13,8
7/8/91	218	18,3	18,2	18,0	17,8	17,6	16,3	12,4	9,4	13,0	14,0
14/8/91	225	22,4	21,4	19,4	19,2	18,0	16,3	12,7	9,7	13,2	14,1
21/8/91	232	18,6	18,9	18,3	17,9	17,7	16,5	13,1	10,0	13,3	14,2
27/8/91	238	18,7	18,4	17,4	17,2	17,2	16,7	13,4	10,3	13,3	14,3
8/9/91	248	15,2	16,3	17,2	17,1	17,3	17,1	14,1	10,7	13,4	14,5
11/9/91	253	13,6	15,2	16,7	16,6	16,9	16,6	14,3	10,8	13,5	14,5
18/9/91	260	12,6	14,3	15,9	15,9	16,2	16,2	14,4	11,1	13,5	14,7
25/9/91	267	8,8	10,3	13,0	14,3	15,1	15,9	14,6	11,4	13,3	14,7
1/10/91	273	6,0	7,6	11,1	11,3	13,3	15,1	14,5	11,5	13,2	14,7
8/10/91	280	5,0	7,4	10,8	11,8	13,2	14,0	14,1	11,7	13,2	14,8
16/10/91	288	5,3	7,0	9,5	11,4	12,3	13,1	13,5	11,8	13,2	14,7
22/10/91	294	3,8	5,6	8,7	10,5	11,4	12,2	12,9	11,9	13,1	14,9
29/10/91	301	4,4	6,3	9,1	10,0	10,9	11,7	12,3	12,0	13,2	14,7
7/11/91	310	1,0	3,1	6,7	7,8	9,8	11,0	11,7	12,1	13,2	14,8
13/11/91	316	1,7	3,1	5,7	6,5	8,9	10,3	11,3	12,0	12,9	14,8
19/11/91	322	0,5	1,9	4,9	7,5	8,5	9,4	10,8	11,9	12,8	14,8
27/11/91	330	1,0	2,5	4,9	5,7	7,1	8,2	9,7	11,9	12,8	14,8
4/12/91	337	-5,5	-1,9	2,4	0,9	3,9	7,1	9,0	11,7	12,8	14,8
11/12/91	344	-2,7	-2,2	-0,3	0,3	3,3	6,1	8,4	11,4	12,3	14,8
18/12/91	351	-9,7	-6,5	-0,8	-1,4	2,4	5,6	7,5	11,2	12,2	14,8
24/12/91	357	-7,0	-4,5	-1,6	-0,1	2,4	4,1	6,7	11,0	11,9	14,7
31/12/91	364	-8,3	-6,0	-2,3	-0,1	1,5	3,2	5,8	10,8	11,6	14,7
8/1/92	372	-7,2	-4,3	-1,2	-1,1	-0,3	1,2	5,0	10,6	11,5	14,5
17/1/92	381	-13,5	-10,8	-5,2	-4,6	-1,2	0,7	4,3	10,5	11,6	14,4
22/1/92	386	-13,7	-11,7	-7,6	-6,5	-3,7	-1,4	3,9	10,4	11,6	14,4
29/1/92	393	-10,8	-11,0	-8,8	-8,4	-5,4	-3,6	3,2	10,4	11,4	14,2
5/2/92	400	-8,7	-8,2	-6,7	-5,6	-3,6	-2,5	2,5	10,3	11,4	14,2
13/2/92	408	-11,2	-10,1	-7,2	-7,2	-4,5	-3,5	2,1	10,2	11,7	14,0
19/2/92	414	-7,8	-7,6	-6,5	-5,8	-3,9	-2,9	1,8	10,0	11,6	13,9
26/2/92	421	-8,5	-7,9	-6,3	-6,1	-4,0	-2,9	1,6	9,9	11,6	13,8
3/3/92	427	-10,0	-9,4	-7,3	-7,5	-5,0	-3,5	1,4	9,9	11,7	13,7
11/3/92	435	-4,9	-4,4	-4,4	-4,5	-4,1	-2,9	1,1	9,7	11,5	13,7
19/3/92	443	-9,5	-8,6	-6,6	-6,7	-4,9	-3,6	1,0	9,6	12,2	13,6
26/3/92	450	-5,1	-6,4	-6,7	-6,4	-5,0	-3,6	0,9	9,4	12,4	13,5
2/4/92	457	-3,9	-3,4	-3,3	-3,5	-3,3	-2,8	0,8	9,3	12,4	13,5

Puits #3

Température (°C)

Jour zéro le: 1/1/91

Date	out	Profondeur du point de mesure (m)										
		0,3	0,5	1,0	1,3	1,8	2,8	4,8	9,8	14,8	19,8	29,8
9/4/92	464	-1,2	-0,9	-0,8	-1,8	-1,7	-1,6	0,8	9,1	12,1	13,5	13,3
16/4/92	471	-0,6	-0,7	-2,1	-1,5	-1,2	-0,9	1,0	9,2	12,7	13,4	13,3
8/5/92	493	6,1	4,9	1,7	2,9	0,6	0,2	1,6	8,8	13,2	12,9	13,5
15/5/92	500	7,2	7,5	7,0	6,9	4,7	3,0	2,0	8,8	13,4	12,9	13,4
22/5/92	507	17,0	15,0	10,3	15,0	9,3	5,4	2,6	8,8	13,4	12,9	13,4
28/5/92	513	11,3	11,0	10,2	11,1	9,1	6,7	3,5	8,8	13,6	12,9	13,4
4/6/92	520	11,5	12,5	12,1	11,6	10,2	7,5	4,6	8,9	13,7	13,0	13,4
10/6/92	526	12,3	13,0	12,4	11,6	10,6	8,3	5,2	9,0	13,0		13,4
17/6/92	533	19,2	18,1	14,8	15,8	12,8	10,2	6,2	9,2	13,9	13,1	13,4
26/6/92	542	16,3	15,2	13,2	12,6	11,8	10,4	7,2	9,4	14,0	13,2	13,4
2/7/92	548	14,2	14,4	14,0	13,6	12,8	10,8	7,7	9,5	14,1	13,3	13,4
10/7/92	556	15,2	15,6	14,5	14,2	13,3	11,4	8,3	9,6	14,2	13,4	13,4
15/7/92	561	16,4	16,6	15,0	13,9	13,1	11,7	8,7	9,7	14,2	13,5	13,4
22/7/92	568	12,8	14,2	15,1	14,8	14,3	12,5	9,2	9,9	14,3	13,6	13,4
30/7/92	576	12,9	14,5	15,5	14,9	14,9	13,5	9,8	10,0	14,3	13,6	13,4
6/8/92	583	16,8	15,5	15,1	16,2	14,9	13,7	10,4	10,2	14,3	13,7	13,4
12/8/92	589	12,9	14,5	16,0	15,4	15,1	13,8	10,8	10,3	14,4	13,8	13,4
18/8/92	595	17,0	17,2	16,2	16,3	15,1	14,1	11,1	10,5	14,4	13,9	13,4
27/8/92	604	16,2	15,9	16,3	15,6	15,1	14,3	11,6	10,8	14,5	14,0	13,4
4/9/92	612	11,3	12,3	13,2	13,6	13,9	13,9	12,0	11,1	14,7	14,0	13,3
10/9/92	618	12,4	12,7	13,6	13,1	13,4	13,6	12,2	11,2	14,6	14,1	13,3
17/9/92	625	14,7	14,3	13,8	13,8	13,5	13,4	12,3	11,4	14,6	14,2	13,3
24/9/92	632	7,1	9,3	12,0	12,5	13,0	13,4	12,4	11,5	14,6	14,2	13,3
30/9/92	638	5,8	8,3	11,4	12,2	12,8	13,0	12,4	11,6	12,4	14,2	13,3
8/10/92	646	7,5	8,5	9,7	10,3	11,9	12,4	12,3	11,8	14,5	14,2	13,3
14/10/92	652	4,7	6,8	9,7	10,3	11,6	12,1	12,1	11,9	14,4	14,3	13,2
21/10/92	659	1,2	3,0	6,4	9,5	10,7	11,5	11,9	12,0	14,2	14,3	13,3
28/10/92	666	1,8	3,5	6,4	9,2	10,3	10,9	11,4	12,0	14,1	14,3	13,3
5/11/92	674	1,9	3,0	5,1	7,7	9,0	9,8	10,7	12,0	13,9	14,3	13,3
12/11/92	681	1,2	2,6	4,8	6,7	7,5	8,2	9,9	12,0	13,7	14,3	13,3
20/11/92	689		0,2	2,9	4,2	6,6	7,6	9,0	11,8	13,3	14,3	13,3
25/11/92	694		0,0	2,3	2,3	4,6	6,9	8,6	11,7	13,3	14,3	13,3
1/12/92	700		-0,6	1,9	3,1	6,1	7,1	8,3	11,7	13,3	14,2	13,4
8/12/92	707		-2,0	1,3	0,0	4,4	6,3	7,8	11,1	13,1	14,2	13,4

Puits #4

Température (°C)

Jour zéro le: 1/1/91

Date	jour	Profondeur du point de mesure (m)									
		0,3	0,5	1,0	1,5	2,1	3,1	5,1	10,1	15,1	30,1
20/2/91	50	1,7	4,0	10,2	16,0	24,2	34,5	43,3	47,3	45,2	40,0
22/2/91	52	1,7	4,0	11,7	15,0	21,5	34,5	45,2	52,1	47,3	43,3
28/3/91	86	8,2	9,9	13,7	17,2	23,2	35,7	47,3	49,6	49,6	37,1
9/4/91	98	8,5	11,6	16,8	18,3	22,5	32,2	42,5	48,8	47,2	44,8
17/4/91	106	8,2	10,4	16,0	19,2	24,1	33,9	42,9	48,8	47,0	44,5
23/4/91	112	8,6	10,8	16,4	19,7	24,7	34,6	43,3	49,1	47,1	44,8
26/4/91	115	11,1	12,7	17,1	20,1	25,0	34,6	43,1	48,8	46,9	44,5
2/5/91	121	12,5	15,2	20,3	22,5	26,3	34,8	43,0	48,7	46,9	44,5
10/5/91	129	13,8	15,6	19,8	22,7	27,2	35,7	43,3	48,5	46,9	44,3
16/5/91	135	18,6	20,0	23,6	25,6	28,9	36,1	43,3	48,4	46,8	44,2
23/5/91	142	21,8	22,5	25,3	26,9	30,3	37,4	43,7	48,3	46,7	44,2
31/5/91	150	21,4	22,0	25,4	28,2	31,5	37,9	44,2	48,1	46,7	44,1
5/6/91	155	20,1	22,1	26,5	29,2	32,7	39,1	44,6	48,0	46,6	43,9
11/6/91	161	23,9	25,5	28,9	30,6	33,1	40,1	44,4	48,0	46,5	43,8
19/6/91	169	24,4	25,6	28,3	30,7	34,2	40,4	45,0	47,8	46,4	43,7
26/6/91	176	25,4	27,3	30,5	32,4	35,3	40,7	45,3	47,7	46,4	43,5
3/7/91	183	24,4	25,6	29,6	32,4	35,6	41,0	45,7	47,7	46,3	43,4
10/7/91	190	22,0	24,7	29,7	32,8	35,9	41,2	45,9	47,6	46,2	43,4
18/7/91	198	25,2	27,0	30,7	33,6	36,6	41,9	46,2	47,6	46,1	43,4
24/7/91	204	23,5	26,6	32,1	34,6	37,3	42,0	46,2	47,6	46,1	43,3
29/7/91	209	24,4	25,9	30,8	33,9	37,4	42,6	46,7	47,6	46,0	43,3
7/8/91	218	23,5	24,9	29,8	33,1	36,8	42,7	47,3	47,6	45,9	43,2
14/8/91	225	27,1	27,7	31,3	33,7	37,2	43,1	47,6	47,6	45,8	43,2
21/8/91	232	22,7	25,1	30,1	33,7	37,5	43,4	47,9	47,6	45,7	43,1
27/8/91	238	22,4	23,8	28,1	32,7	37,0	43,5	48,0	47,7	45,6	43,0
5/9/91	248	19,4	22,1	27,7	31,7	35,9	42,5	48,1	47,8	45,4	42,9
11/9/91	253	18,2	21,0	27,3	31,1	35,2	42,2	48,3	47,8	45,3	42,8
18/9/91	260	16,2	19,2	25,4	29,2	33,5	41,1	48,1	48,0	45,6	43,2
25/9/91	267	12,8	15,5	22,7	26,8	31,8	40,0	47,7	48,0	45,6	43,5
1/10/91	273	8,7	11,4	19,4	25,0	30,9	39,9	47,7	48,2	45,4	43,4
8/10/91	280	7,5	10,8	18,2	22,5	27,7	37,1	47,1	48,1	45,9	44,7
15/10/91	288	8,3	11,2	18,4	22,3	27,8	37,3	46,8	48,5	45,4	44,2
22/10/91	294	7,1	10,3	18,4	22,4	27,9	37,4	46,5	48,6	44,9	43,9
29/10/91	301	7,5	10,6	18,3	22,2	27,4	36,8	46,3	48,8	44,6	43,8
7/11/91	310	5,2	8,5	17,2	21,6	27,4	36,9	45,9	48,9	44,5	43,8
13/11/91	316	5,1	8,0	16,0	20,5	26,6	36,8	45,9	49,0	44,4	43,7
19/11/91	322	4,9	7,2	15,0	19,8	26,1	36,6	45,9	49,1	44,3	43,6
27/11/91	330	4,5	7,8	15,6	19,8	25,7	35,8	45,4	49,2	44,2	43,5
4/12/91	337	0,6	4,1	13,3	18,3	24,3	34,0	44,5	49,3	44,2	43,5
11/12/91	344	3,6	5,9	12,8	16,4	22,6	32,4	42,7	49,5	44,3	43,6
18/12/91	351	-2,1	2,1	11,8	15,6	21,2	30,2	42,2	49,6	44,6	43,8
24/12/91	357	-0,3	3,0	10,8	14,6	20,4	29,7	41,9	49,7	44,3	43,8
31/12/91	364	0,5	3,8	12,0	14,8	20,5	29,2	40,1	49,7	44,1	43,6
8/1/92	372	1,8	4,8	11,9	14,4	19,8	29,1	39,9	49,7	43,9	43,5
17/1/92	381	0,6	3,8	12,2	14,7	20,3	29,2	38,8	49,7	43,9	43,4
22/1/92	386	0,4	3,4	11,4	14,2	20,0	28,9	38,2	49,6	43,9	43,3
29/1/92	393	0,1	2,6	10,4	13,4	19,4	28,6	37,8	49,3	43,8	43,2
5/2/92	400	2,0	4,5	11,9	13,6	19,2	28,3	37,4	49,0	43,8	43,2
13/2/92	408	-1,1	1,8	9,9	12,9	18,6	27,6	37,0	48,6	43,7	43,1
19/2/92	414	1,4	3,6	10,2	12,4	17,8	26,7	36,5	48,3	43,7	43,0
26/2/92	421	1,0	3,2	9,6	12,1	17,2	25,6	35,8	47,9	43,7	43,0
3/3/92	427	0,2	2,5	8,8	11,5	16,6	24,9	35,6	47,5	43,6	42,8
13/3/92	437	-3,4	0,6	8,1	11,2	16,0	24,5	36,7	47,1	43,4	42,8
19/3/92	443	-2,9	-0,3	6,4	10,1	15,5	24,8	36,3	46,8	43,3	42,8
26/3/92	450	-0,4	-0,7	5,2	9,4	14,8	24,0	35,2	46,4	43,2	42,6
2/4/92	457	0,1	1,3	5,4	8,7	13,2	22,1	35,2	46,1	43,1	42,6

Puits #4

Température (°C)

Jour zéro le: 1/1/91

Date	jour	Profondeur du point de mesure (m)									
		0,3	0,5	1,0	1,6	2,1	3,1	5,1	10,1	15,1	30,1
9/4/92	464	1,2	2,3	6,1	9,1	13,3	22,1	35,6	45,8	42,9	42,8
16/4/92	471	2,4	3,5	7,3	9,8	14,0	22,5	35,1	45,5	42,8	42,9
8/5/92	493	9,5	9,7	11,6	13,2	16,2	22,6	33,6	44,1	42,5	43,2
15/5/92	500	10,4	11,6	14,9	16,3	18,2	23,0	33,6	44,2	42,2	42,9
22/5/92	507	18,7	17,4	17,3	17,4	19,2	23,8	33,4	44,3	42,0	42,8
28/5/92	513	14,0	14,3	17,1	18,7	20,6	24,4	33,4	44,2	41,7	42,7
4/6/92	520	13,8	15,8	19,3	20,5	22,0	25,5	34,0	44,1	41,6	42,5
10/6/92	526	15,1	16,5	19,4	20,9	22,7	26,2	34,4	44,0	41,4	42,6
17/6/92	533	21,7	21,2	22,0	22,7	24,2	27,5	35,1	43,9	41,2	42,5
24/6/92	542	18,4	17,9	19,7	21,4	22,6	28,3	35,9	43,8	40,9	42,2
2/7/92	548	16,8	17,6	20,6	22,7	24,7	28,5	36,3	43,7	40,8	42,1
10/7/92	556	17,6	18,5	20,7	22,7	24,9	28,8	36,5	43,6	40,5	42,0
15/7/92	561	18,2	19,3	21,2	23,0	25,1	29,0	36,7	43,6	40,4	41,9
22/7/92	568	15,6	17,3	21,2	23,9	25,9	29,3	36,9	43,6	40,2	41,7
30/7/92	576	15,7	17,7	21,6	24,2	26,4	30,0	37,5	43,5	40,0	41,6
6/8/92	583	19,4	18,5	21,1	23,6	26,1	30,1	37,6	43,4	39,7	41,4
12/8/92	589	16,0	17,6	22,0	24,6	26,6	30,3	37,8	43,3	39,6	41,3
18/8/92	595	19,6	20,3	22,5	24,5	26,7	30,4	37,6	43,3	39,4	41,2
27/8/92	604	16,7	18,6	22,0	24,4	26,7	30,6	38,1	43,2	39,2	41,0
4/9/92	612	13,4	14,8	18,4	21,7	25,0	29,9	38,0	42,8	39,0	41,2
10/9/92	618	14,7	15,3	18,8	21,8	24,7	29,5	37,7	42,8	38,9	41,1
17/9/92	625	16,7	16,8	19,0	21,5	24,2	29,1	37,3	42,9	38,7	40,9
24/9/92	632	9,4	11,7	16,9	20,6	23,8	28,6	37,3	42,6	38,5	41,1
30/9/92	638	8,1	10,8	16,4	20,0	23,2	28,2	37,0	42,7	38,2	40,9
8/10/92	646	9,7	11,0	14,9	18,3	21,9	27,6	36,8	42,7	37,9	40,7
14/10/92	652	6,7	9,0	14,3	18,1	21,6	27,2	36,2	42,6	37,8	40,5
21/10/92	659	2,9	4,6	10,2	15,0	19,4	26,0	35,7	42,5	37,6	40,4
28/10/92	666	3,4	5,0	9,8	13,9	18,2	24,9	35,1	42,5	37,3	40,2
5/11/92	674	2,9	3,8	7,5	11,8	16,4	23,9	35,3	42,3	37,2	40,0
12/11/92	681	2,3	3,5	7,4	11,1	15,3	22,7	33,8	42,5	36,9	39,7
20/11/92	689	0,8	2,0	6,3	9,7	13,7	20,4	32,6	42,2	36,7	39,5
25/11/92	694	0,4	1,4	5,4	8,9	12,8	19,7	32,2	42,2	36,4	39,4
1/12/92	700	-0,2	1,1	5,3	8,7	12,5	19,3	31,5	42,2	36,2	39,1
8/12/92	707	-0,5	0,8	5,2	8,6	12,4	19,1	30,9	42,2	36,0	38,9

Puits #5

Température (°C)

Jour zéro le: 1/1/91

Date	jour	Profondeur du point de mesure (m)									
		0.3	0.5	1.0	1.5	2.0	3.0	5.0	10.0	15.0	17.3
18/2/91	48	-6,8	-2,2	3,8	7,3	13,3	20,9	30,1	40,0	47,3	47,3
22/2/91	52	-3,9	-0,4	4,0	6,7	11,7	18,5	32,2	40,0	47,3	49,6
28/3/91	86	0,6	1,7	5,3	5,3	9,2	16,0	27,4	37,1	45,2	45,2
9/4/91	98	3,7	5,7	7,4	7,7	10,2	16,3	29,5	39,5	48,1	48,7
17/4/91	106	4,5	5,5	7,0	8,8	11,5	17,1	29,6	39,5	48,0	48,7
23/4/91	112	5,0	6,2	8,6	9,3	12,1	17,6	29,8	39,5	48,2	48,8
26/4/91	115	8,0	8,3	9,1	10,0	12,5	17,8	29,6	39,4	47,9	48,6
2/5/91	121	8,6	10,0	11,6	12,5	14,1	18,5	29,5	39,3	47,8	48,6
10/5/91	129	10,4	10,6	11,2	12,6	15,0	19,6	29,4	39,1	47,7	48,5
16/5/91	135	14,8	15,0	15,1	15,7	16,8	20,3	29,4	39,0	47,6	48,5
23/5/91	142	18,3	17,5	16,3	16,6	17,8	21,4	29,5	38,9	47,5	48,4
31/5/91	150	17,4	17,7	17,9	18,0	19,4	22,1	29,7	38,8	47,3	48,4
5/6/91	155	16,8	17,8	19,0	19,4	20,7	23,5	29,9	38,7	47,3	48,3
11/6/91	161	20,6	20,9	20,6	21,0	21,8	23,9	30,1	38,6	47,2	48,3
19/6/91	169	21,8	21,7	20,7	21,3	22,6	25,4	30,4	38,4	47,0	48,2
26/6/91	176	22,7	23,2	22,5	23,2	24,0	26,2	30,8	38,4	46,9	48,1
3/7/91	183	22,0	22,0	22,7	23,3	24,8	27,1	31,1	38,3	46,8	48,1
10/7/91	190	19,4	20,9	22,0	24,3	25,6	27,7	31,4	38,2	46,7	48,0
18/7/91	198	23,1	23,8	24,2	25,2	26,2	28,5	31,9	38,2	46,6	47,9
24/7/91	204	21,1	23,1	24,7	26,3	27,4	29,2	32,2	38,2	46,4	47,8
29/7/91	209	21,4	22,0	23,4	25,3	27,3	29,8	32,5	38,2	46,4	47,8
7/8/91	218	21,5	22,1	23,8	24,9	27,3	30,3	33,1	38,2	46,3	47,7
14/8/91	225	24,9	24,6	24,7	25,8	27,7	30,7	33,6	38,3	46,2	47,6
21/8/91	232	21,4	22,6	24,1	25,4	27,9	31,1	34,0	38,3	46,1	47,5
27/8/91	238	20,1	20,5	21,1	24,0	27,0	31,2	34,3	38,3	46,0	47,4
6/9/91	248	17,0	18,6	20,6	23,7	26,6	31,4	34,7	38,5	45,8	47,3
11/9/91	253	15,6	17,5	20,4	23,7	26,4	30,8	34,9	38,6	45,8	47,3
18/9/91	260	13,8	16,3	19,8	22,9	25,7	30,5	35,0	38,7	45,8	47,2
25/9/91	267	10,0	12,2	16,1	20,3	23,9	29,7	34,9	38,8	45,7	47,1
1/10/91	273	6,1	7,9	12,0	17,9	22,4	29,0	34,9	38,9	45,7	47,0
8/10/91	280	5,9	8,7	13,0	16,9	20,7	27,3	34,5	39,0	45,7	47,0
16/10/91	288	5,5	7,6	11,0	15,6	19,7	26,5	34,3	39,2	45,6	46,9
22/10/91	294	4,0	6,3	10,5	14,8	18,8	25,8	33,9	39,3	45,6	46,9
29/10/91	301	5,2	7,9	13,1	15,2	18,7	25,0	33,7	39,4	45,5	46,8
7/11/91	310	1,3	3,8	7,5	13,0	17,1	24,4	33,0	39,5	45,5	46,7
13/11/91	316	1,6	3,8	8,1	11,8	16,2	23,6	32,7	39,6	45,6	46,7
19/11/91	322	0,8	2,6	6,7	11,3	15,4	23,0	32,4	39,6	45,6	46,6
27/11/91	330	1,7	3,6	7,5	11,2	14,9	22,1	31,9	39,7	45,6	46,6
4/12/91	337	-5,3	-0,6	6,1	10,3	14,4	21,6	31,3	39,7	45,6	46,5
11/12/91	344	-1,5	-0,4	4,0	7,9	12,7	20,7	30,8	39,7	45,7	46,5
18/12/91	351	-7,0	-2,3	4,1	7,9	12,3	20,0	30,5	39,6	45,8	46,5
24/12/91	357	-3,3	0,1	4,8	6,7	11,4	19,4	30,0	39,6	45,8	46,4
31/12/91	364	-2,7	0,0	4,9	6,5	11,1	18,9	29,6	39,5	45,8	46,4
8/1/92	372	-1,9	1,2	5,9	6,9	11,1	18,5	29,2	39,5	45,8	46,4
17/1/92	381	-3,5	0,0	5,3	6,5	11,1	18,3	28,6	39,4	45,9	46,3
22/1/92	386	-4,9	-2,1	3,3	5,1	10,2	17,9	28,3	39,3	46,0	46,3
29/1/92	393	-4,0	-2,3	2,2	3,9	9,1	17,3	27,9	39,2	46,0	46,3
5/2/92	400	-2,3	-0,5	3,7	4,7	9,1	16,7	27,7	39,1	46,0	46,3
13/2/92	408	-3,9	-1,9	2,4	4,4	8,8	16,4	27,1	39,0	46,1	46,3
19/2/92	414	-1,8	-0,6	3,2	4,6	8,6	16,0	26,9	38,9	46,1	46,3
26/2/92	421	-1,6	-0,2	3,4	5,0	8,8	15,8	26,6	38,7	46,1	46,3
3/3/92	427	-2,7	-1,2	2,6	4,8	8,5	15,7	26,3	38,6	46,1	46,3
13/3/92	437	-2,2	0,4	4,4	5,6	9,0	15,6	26,3	38,5	46,1	46,3
19/3/92	443	-2,4	-0,5	3,0	5,2	8,8	15,6	26,0	38,3	46,1	46,3
26/3/92	450	-1,3	-0,5	3,3	5,3	8,8	15,5	25,9	38,2	46,1	46,3
2/4/92	457	-0,7	0,8	4,1	5,7	9,0	15,5	25,8	38,1	46,0	46,2

Puits #5

Température (°C)

Jour zéro le: 1/1/91

Date	jour	Profondeur du point de mesure (m)									
		0,3	0,5	1,0	1,5	2,0	3,0	5,0	10,0	15,0	17,0
9/4/92	464	0,0	1,2	4,1	6,3	9,5	15,9	26,1	38,1	46,0	46,2
16/4/92	471	-0,1	1,1	4,1	6,2	9,2	15,6	25,8	38,0	46,1	46,2
8/5/92	493	7,8	7,7	8,5	8,2	11,3	15,7	24,5	37,7	45,7	46,1
15/5/92	500	8,5	9,9	12,4	12,8	13,1	16,3	24,4	37,5	45,6	46,1
22/5/92	507	17,7	16,2	14,2	13,8	14,1	17,1	23,4	37,3	45,4	46,1
28/5/92	513	12,6	13,1	14,7	15,0	15,4	17,9	24,2	37,2	45,4	46,0
4/6/92	520	12,3	14,3	16,5	16,7	16,6	18,8	24,3	37,0	45,3	46,0
10/6/92	526	13,5	14,7	16,5	17,1	17,3	19,4	24,5	36,9	45,3	45,9
17/6/92	533	20,4	19,8	18,7	19,0	18,7	20,4	24,7	36,6	45,1	45,8
24/6/92	542	17,8	17,5	17,8	17,4	18,2	21,0	25,0	36,5	45,0	45,8
2/7/92	548	15,7	16,6	18,3	19,0	19,2	21,2	25,2	36,4	45,0	45,7
10/7/92	556	16,6	17,5	18,5	19,4	19,7	21,8	25,5	36,3	44,9	45,7
15/7/92	561	18,2	19,2	19,7	19,9	20,1	22,1	25,7	36,2	44,8	45,6
22/7/92	568	15,2	16,8	18,8	21,0	21,1	22,7	26,0	36,1	44,8	45,5
30/7/92	576	15,5	17,6	20,3	21,5	21,7	23,4	26,2	36,1	44,6	45,5
6/8/92	583	19,2	18,6	19,8	21,1	21,6	23,6	26,4	35,9	44,4	45,4
12/8/92	589	15,4	17,2	20,6	22,1	22,2	23,9	26,7	35,9	44,3	45,3
18/8/92	595	18,9	19,6	20,4	22,1	22,3	24,3	26,9	35,9	44,3	45,2
27/8/92	604	16,3	18,5	21,4	22,1	22,4	24,5	27,3	35,9	44,1	45,1
4/9/92	612	13,1	14,7	17,5	19,6	21,1	24,3	27,5	35,9	44,0	45,0
10/9/92	618	14,3	15,2	17,8	19,8	20,9	23,9	27,6	35,9	43,9	44,9
17/9/92	625	16,2	16,4	17,6	19,6	20,5	23,7	27,7	35,9	43,8	44,9
24/9/92	632	9,7	12,0	15,8	18,7	20,1	23,5	27,8	36,0	43,8	44,8
30/9/92	638	7,4	10,6	15,5	17,9	19,4	23,1	27,8	36,0	43,7	44,7
8/10/92	646	9,3	10,7	13,6	16,1	18,2	22,5	27,9	36,1	43,7	44,6
14/10/92	652	6,2	8,8	13,1	16,1	17,8	22,1	27,9	36,1	43,6	44,6
21/10/92	659	2,6	4,8	9,6	13,2	15,9	21,2	27,7	36,2	43,6	44,5
28/10/92	666	3,0	5,0	9,5	12,2	14,8	20,3	27,5	36,3	43,6	44,4
5/11/92	674	2,9	4,4	8,1	10,6	13,5	19,3	27,3	36,3	43,6	44,3
12/11/92	681	1,8	2,7	6,7	10,0	12,6	18,4	27,1	36,3	43,6	44,3
20/11/92	689	-0,2	1,9	6,3	9,1	11,7	17,3	26,5	36,4	43,6	44,2
25/11/92	694	-0,1	1,7	6,5	8,6	11,1	16,8	26,2	36,4	43,6	44,2
1/12/92	700	-0,5	1,6	5,8	8,3	10,8	16,4	25,9	36,4	43,6	44,1
8/12/92	707	-1,8	0,5	4,7	7,6	10,3	15,9	25,6	36,4	43,6	44,1

Puits #6

Température (°C)

Jour zéro le: 1/1/91

Date	Jour	Profondeur du point de mesure (m)										
		0,3	0,5	1,0	1,3	1,8	2,8	4,8	9,8	14,8	19,8	29,8
17/2/91	47	-0,6	1,7	9,9	21,5	29,2	40,0	52,3	58,1	61,8	61,8	43,3
22/2/91	52	1,7	5,3	11,7	21,5	29,2	41,6	54,9	58,1	61,8	58,1	43,3
28/3/91	86	9,2	10,6	14,6	20,0	28,3	38,5	58,1	61,8	66,2	66,2	43,3
9/4/91	98	10,4	13,7	18,9	23,4	28,8	39,4	57,6	61,9	66,1	64,3	44,0
17/4/91	106	9,4	12,5	17,7	24,8	31,9	40,7	59,0	62,3	65,7	64,0	43,9
23/4/91	112	9,9	12,3	17,8	24,6	30,8	41,4	58,5	62,6	66,7	64,8	44,2
26/4/91	115	12,5	14,2	18,5	25,3	31,4	41,8	58,4	62,1	66,1	64,2	44,0
2/5/91	121	14,6	17,5	22,7	26,8	32,3	42,2	58,5	61,9	65,8	64,3	44,1
10/5/91	129	15,0	16,9	21,3	26,7	32,8	42,9	58,6	61,9	66,0	64,3	44,1
16/5/91	135	20,2	21,9	25,9	29,7	34,9	43,5	58,6	62,1	66,0	64,3	44,1
23/5/91	142	22,7	24,0	27,1	31,4	36,0	44,2	58,5	62,1	65,9	64,3	44,2
31/5/91	150	21,9	23,6	27,4	31,7	36,2	44,3	58,7	62,1	66,0	64,3	44,2
5/6/91	155	21,2	23,5	27,8	31,8	36,9	45,2	58,8	62,2	66,0	64,3	44,2
11/6/91	161	25,1	26,9	29,5	33,9	37,9	46,2	59,0	62,1	65,5	64,0	44,1
19/6/91	169	25,9	27,1	29,6	34,9	39,5	47,4	59,5	62,1	65,4	63,9	44,0
26/6/91	176	26,6	28,6	31,8	36,6	40,8	47,9	59,7	62,1	65,3	63,9	44,1
3/7/91	183	25,1	26,6	30,5	36,4	41,1	48,6	60,1	62,0	65,3	63,7	44,0
10/7/91	190	23,6	26,4	31,2	37,1	41,6	49,2	60,2	61,9	65,2	63,7	44,1
18/7/91	198	26,5	28,6	32,5	37,5	41,8	49,9	60,3	61,6	65,0	63,7	44,1
24/7/91	204	24,6	27,9	33,1	38,9	42,9	50,5	60,4	61,4	64,9	63,2	44,0
29/7/91	209	24,5	26,4	31,0	38,5	43,1	50,8	60,5	61,4	64,8	63,1	44,0
7/8/91	218	23,7	25,7	30,3	36,7	41,7	49,7	60,5	61,2	64,8	63,2	44,1
14/8/91	225	27,3	28,4	31,8	37,7	42,1	50,0	60,5	61,1	64,8	63,2	44,2
21/8/91	232	23,3	25,5	30,1	37,6	42,4	50,5	60,6	61,0	64,6	63,1	44,1
27/8/91	238	23,4	25,0	29,4	35,2	40,5	49,9	60,6	60,5	64,4	63,1	44,2
6/9/91	248	20,5	23,2	28,4	35,0	40,4	49,3	60,6	60,4	64,0	63,2	44,3
11/9/91	253	19,3	22,5	28,2	33,7	38,8	47,8	60,0	60,2	64,2	63,4	44,4
18/9/91	260	17,8	21,2	27,0	31,8	37,2	46,8	59,7	59,8	63,9	63,4	44,5
25/9/91	267	13,6	16,7	23,2	28,9	35,0	45,7	59,6	59,3	63,5	63,4	44,5
1/10/91	273	9,7	12,6	19,8	25,7	33,0	44,9	59,5	59,0	63,3	63,4	44,5
8/10/91	280	9,3	12,9	19,7	25,5	31,8	43,3	59,0	58,9	63,1	63,4	44,5
16/10/91	288	9,3	12,3	18,6	23,9	30,6	42,9	58,8	58,4	63,0	63,4	44,5
22/10/91	294	7,8	11,0	17,7	23,4	30,2	42,4	58,7	58,1	62,8	63,4	44,6
29/10/91	301	8,2	11,5	18,1	23,5	29,9	41,7	58,6	57,8	62,8	63,4	44,6
7/11/91	310	4,9	8,6	15,9	21,8	28,9	41,6	58,5	57,2	62,2	63,4	44,6
13/11/91	316	5,3	8,0	14,8	21,6	28,9	41,6	58,4	57,0	62,5	63,3	44,6
19/11/91	322	4,9	7,5	14,6	22,2	28,8	41,3	58,2	56,6	62,4	63,3	44,6
27/11/91	330	4,9	8,3	15,6	22,1	28,6	40,9	58,0	56,3	62,4	63,3	44,6
4/12/91	337	0,3	4,2	12,7	18,5	26,4	40,1	58,1	55,9	62,4	63,3	44,6
11/12/91	344	1,1	3,7	10,7	17,6	25,4	39,6	57,9	55,4	62,3	63,2	44,6
18/12/91	351	-1,6	2,5	10,6	17,7	25,4	39,0	57,6	55,1	62,4	63,2	44,7
24/12/91	357	0,1	3,5	10,5	17,6	24,9	38,8	57,4	54,9	62,4	63,2	44,7
31/12/91	364	0,3	3,6	10,7	17,0	24,7	38,6	57,2	54,5	62,3	63,1	44,7
8/1/92	372	2,2	5,8	12,7	18,4	24,9	38,3	57,0	54,3	62,4	63,1	44,7
17/1/92	381	-3,8	0,7	9,7	15,9	24,2	38,3	57,1	53,6	62,3	63,0	44,7
22/1/92	386	-4,2	-0,5	7,9	14,7	23,4	38,3	57,0	53,2	62,3	63,0	44,7
29/1/92	393	-2,4	-0,5	7,4	14,2	22,8	37,8	56,7	52,6	62,2	62,9	44,7
5/2/92	400	-0,1	2,7	9,6	17,7	23,9	37,6	56,4	52,1	62,3	62,9	44,7
13/2/92	408	-3,6	-0,4	8,0	15,9	23,9	37,8	56,4	51,3	62,1	62,9	44,7
19/2/92	414	0,3	2,7	9,4	15,2	23,0	37,2	56,0	50,9	62,2	62,8	44,7
26/2/92	421	0,1	2,7	9,7	15,6	23,3	37,2	55,9	50,3	62,1	62,8	44,7
3/3/92	427	-1,3	1,4	8,9	15,5	23,5	37,5	55,9	49,7	62,1	62,8	44,7
13/3/92	437	-1,5	2,5	9,8	14,5	22,3	36,9	55,9	49,5	62,4	62,7	44,7
19/3/92	443	-2,1	0,9	8,4	14,2	22,2	36,4	55,6	49,0	62,3	62,6	44,7
26/3/92	450	-0,3	1,9	8,6	15,7	22,8	36,3	55,3	48,3	62,1	62,6	44,7
2/4/92	457	2,3	4,8	11,0	16,7	23,0	36,1	55,1	48,2	62,4	62,6	44,7

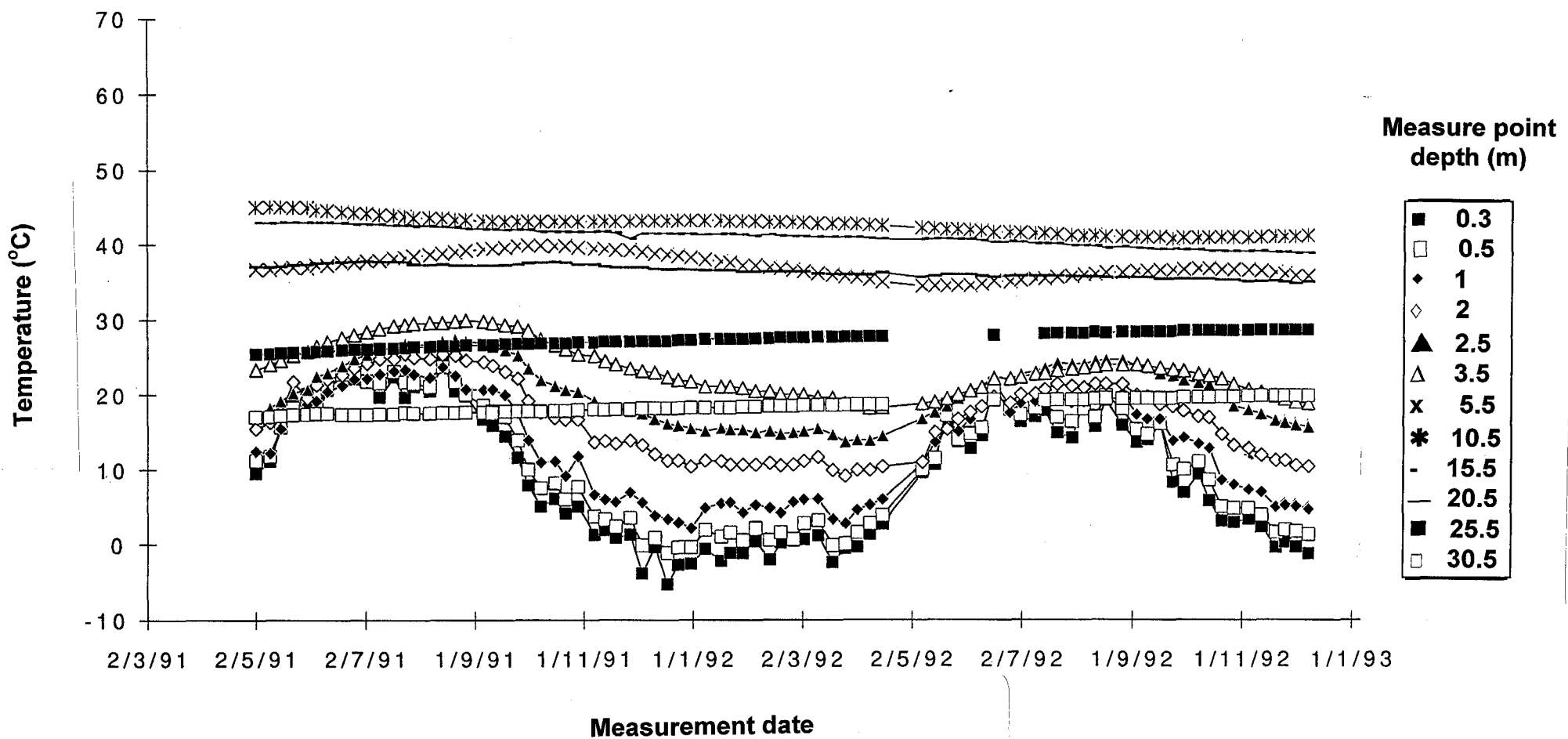
Puits #6

Température (°C)

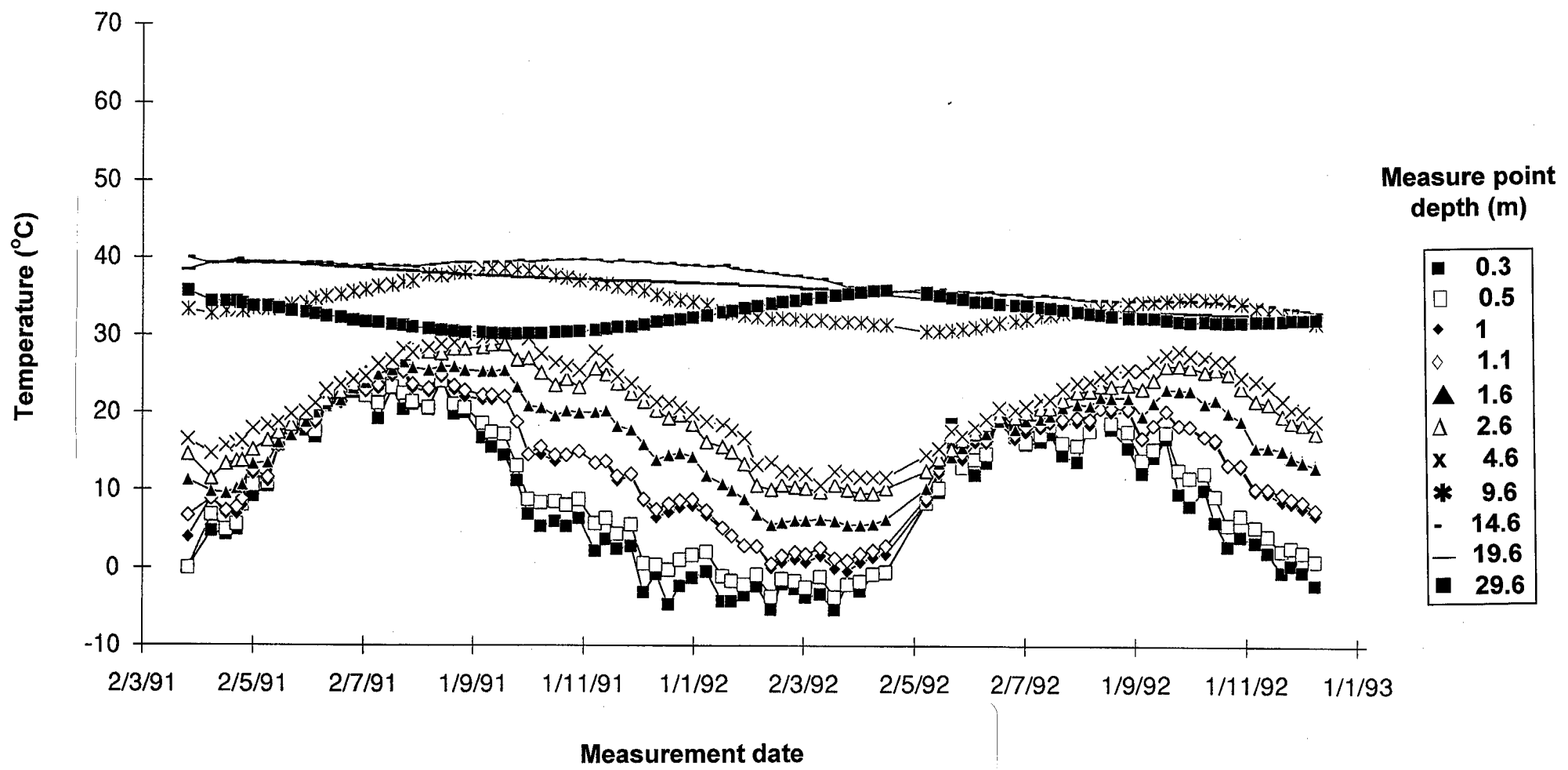
Jour zéro le: 1/1/91

Date	jour	Profondeur du point de mesure (m)									
		0,3	0,5	1,0	1,3	1,8	2,8	4,8	9,8	14,8	19,8
9/4/92	464	4,6	6,9	12,5	17,0	23,4	36,1	54,9	47,8	62,3	62,5
16/4/92	471	5,6	7,6	12,9	17,7	24,0	36,5	54,9	47,3	62,2	62,4
8/5/92	493	12,2	13,6	17,7	23,1	28,3	40,0	55,8	46,2	61,5	61,0
15/5/92	500	13,5	16,1	21,7	25,9	30,6	41,2	55,8	45,6	61,4	61,1
22/5/92	507	21,1	21,3	23,5	27,5	31,3	42,1	55,6	45,0	61,4	61,2
28/5/92	513	16,6	18,4	23,5	28,9	33,3	43,5	55,8	44,8	61,3	61,0
4/6/92	520	17,5	20,7	26,2	31,5	35,7	44,6	55,8	44,4	61,2	60,9
10/6/92	526	18,2	20,7	25,9	31,9	35,8	45,0	55,9	43,9	61,1	60,9
17/6/92	533	24,4	25,4	28,2	32,0	35,9	44,5	55,6	43,2	61,0	61,5
26/6/92	542	20,7	21,7	25,2	29,4	33,5	43,3	55,6	42,9	61,1	61,4
27/9/92	548	19,6	21,7	26,7	32,2	36,0	44,2	55,6	42,5	60,8	61,2
10/7/92	556	20,3	22,5	26,9	32,2	35,9	45,2	55,5	41,9	60,6	61,1
15/7/92	561	21,3	23,4	27,3	33,1	36,7	45,4	55,5	41,6	60,5	61,0
22/7/92	568	18,8	21,8	27,9	33,5	37,7	45,7	55,5	41,1	60,3	60,9
30/7/92	576	18,9	22,1	27,9	34,5	38,6	46,2	55,4	40,7	60,1	60,7
6/8/92	583	21,7	22,5	27,3	31,7	35,8	43,3	54,3	40,1	60,2	61,0
11/8/92	588				32,7	36,2	43,2	54,3	39,9	60,0	61,0
18/8/92	595	23,3	25,1	29,4	32,5	36,2	43,3	54,2	39,5	59,7	60,8
27/8/92	604	19,8	23,0	28,4	32,1	35,8	42,9	53,9	39,0	59,6	60,7
4/9/92	612	15,9	18,4	23,6	26,9	32,5	41,8	53,7	38,7	59,3	60,5
10/9/92	618	17,0	19,0	24,4	27,6	32,5	40,9	53,5	38,3	58,8	60,4
17/9/92	625	18,8	20,3	24,8	28,0	32,5	40,5	53,1	37,9	58,6	60,9
24/9/92	632	12,3	15,7	22,7	27,0	32,2	40,2	52,8	37,5	58,6	60,2
30/9/92	638	10,7	14,6	21,9	24,9	30,5	39,6	52,6	37,2	58,4	60,1
8/10/92	646	12,4	14,8	20,6	24,8	30,3	38,9	52,2	36,9	58,3	60,0
14/10/92	652	9,6	13,1	20,5	24,4	30,3	40,2	51,9	36,5	57,9	59,8
21/10/92	659	5,5	8,4	15,9	22,7	28,8	37,9	51,5	36,1	57,8	59,6
28/10/92	666	6,0	8,9	16,2	21,5	27,6	37,0	51,2	35,8	57,9	59,5
5/11/92	674	6,0	8,2	14,3	19,3	25,8	36,0	50,8	35,3	57,5	59,3
12/11/92	681	5,0	7,6	14,2	18,4	24,9	35,0	50,4	34,9	57,1	59,1
20/11/92	689	2,7	5,5	12,8	16,8	24,1	34,0	49,7	34,5	57,0	58,9
25/11/92	694	3,0	5,6	12,3	17,7	24,2	33,6	49,3	34,3	57,1	58,8
1/12/92	700	2,9	5,6	12,4	18,3	24,4	33,5	48,9	34,0	56,9	58,6
8/12/92	707	0,4	3,9	11,8	18,4	24,6	33,4	48,8	33,8	56,8	58,5

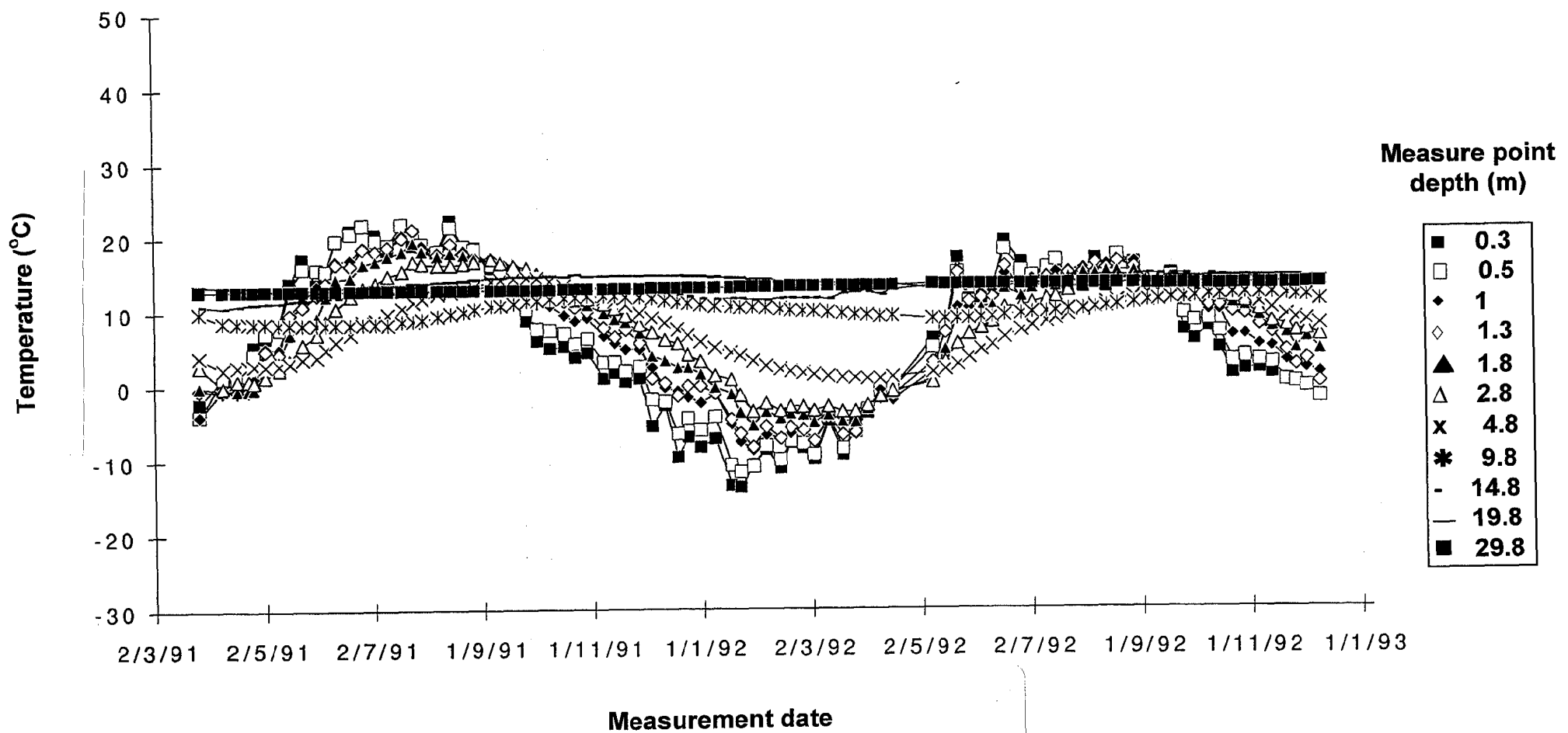
Température du puits #1



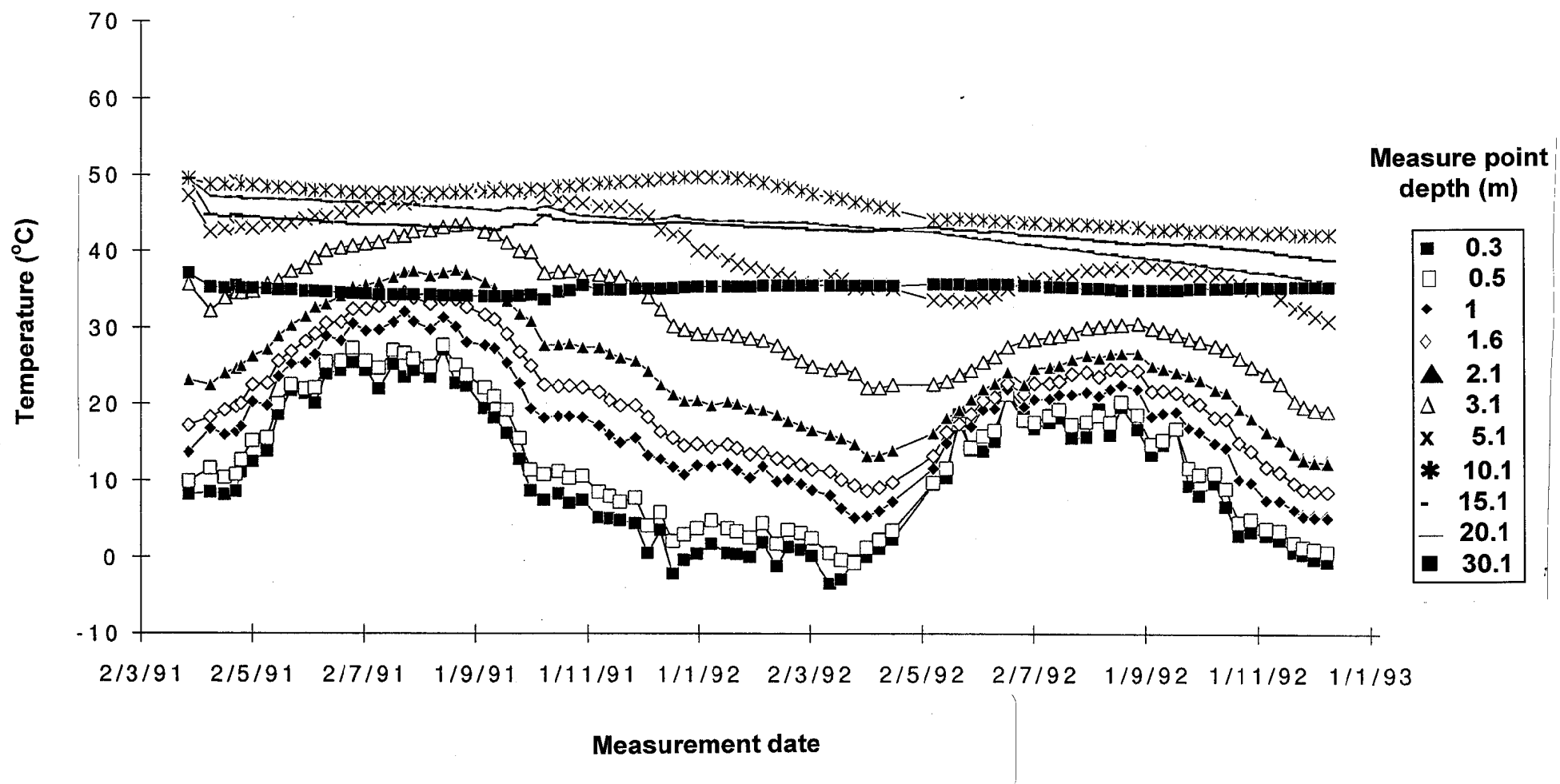
Température du puits #2



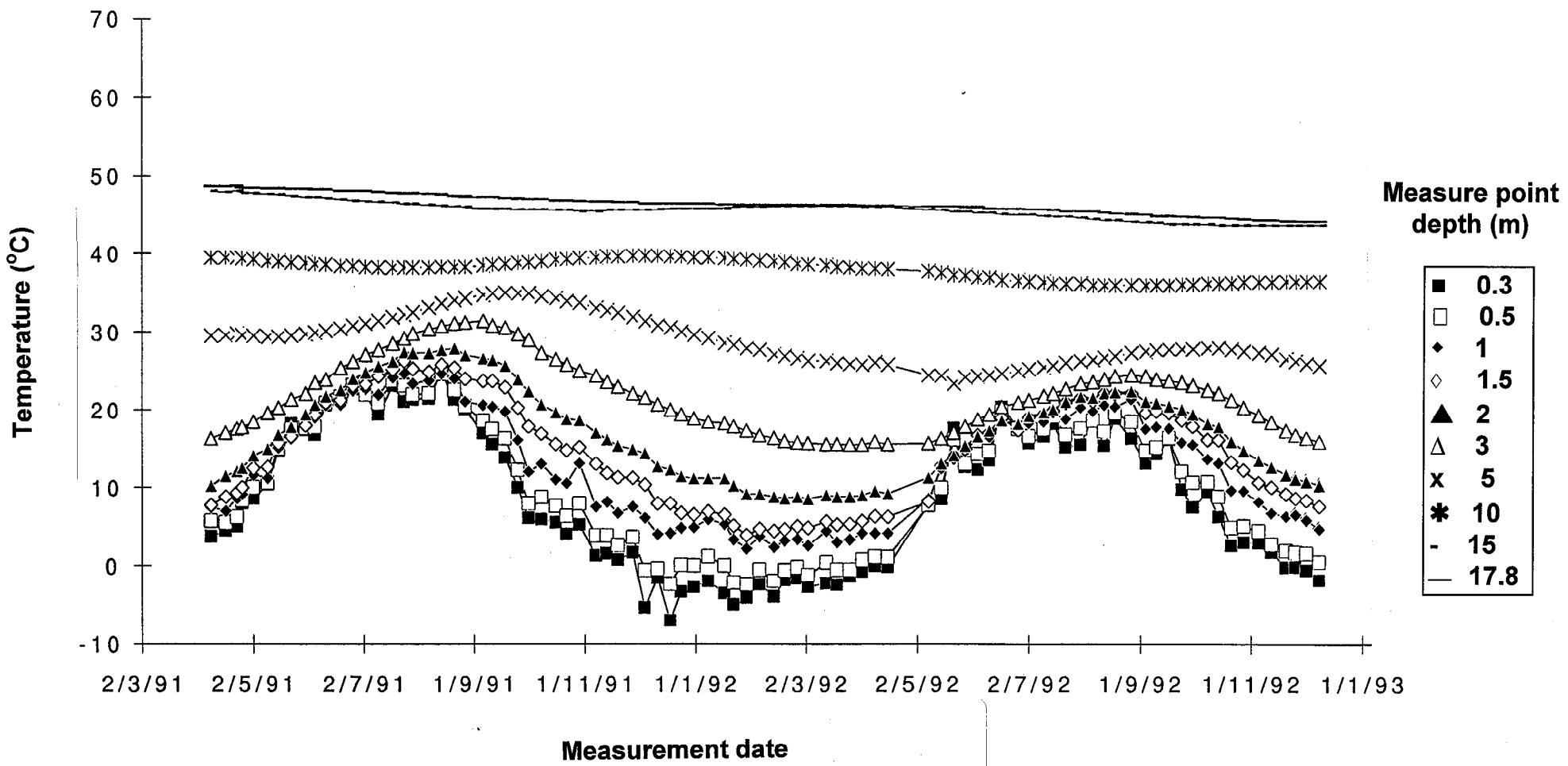
Température du puits #3



Température du puits #4



Température du puits #5



Température du puits #6

